Institut für Erd- und Umweltwissenschaften
Mathematisch-Naturwissenschaftliche Fakultät
Universität Potsdam

Quantification of total microbial biomass and metabolic activity in subsurface sediments

Kumulative Dissertation
zur Erlangung des akademischen Grades
"doctor rerum naturalium"
(Dr. rer. nat.)
in der Wissenschaftsdisziplin "Geomikrobiologie"

eingereicht an der
Mathematisch-Naturwissenschaftlichen Fakultät
der Universität Potsdam

von

Rishi Ram Adhikari

Potsdam, Juni 2013

Published online at the
Institutional Repository of the University of Potsdam:
URL http://opus.kobv.de/ubp/volltexte/2013/6777/
URN urn:nbn:de:kobv:517-opus-67773
http://nbn-resolving.de/urn:nbn:de:kobv:517-opus-67773

dedicated to my beloved brother Sandai †

Statement of original authorship

I, Rishi Ram Adhikari, hereby state that the work contained in this thesis has not previously been submitted for assesment, either in whole or in part, by either myself or any other person at either the Faculty of Mathematics and Natural Science at the University of Potsdam or at any other institution except where explicitly acknowledged.

To the best of my knowledge and belief, the thesis contains no material which has been previously published or written by another person except where due reference is made.

Hiermit erkläre ich, Rishi Ram Adhikari, dass diese Arbeit bisher von mir weder an der Mathematisch-Naturwissenschaftliche Fakultät der Universität Potsdam noch einer anderen wissenschaftlichen Einrichtung von Zwecke der Promotion eingereicht wurde.

Ferner erkläre ich, dass ich diese Arbeit selbständig verfasst und keine anderen als die darin angegebenen Quellen und Hilfsmittel benutzt habe.

Potsdam, June 2013

Acknowledgements

I am sincerely and immensely grateful to Dr. Jens Kallmeyer for providing me with the opportunity to conduct my PhD study under his direct supervision. This dissertation would not have been possible without his constructive and excellent guidance throughout my PhD. I would also like to thank my PhD supervisor Prof. Manfred Strecker for his support in scientific, bureaucratic and technical problems at all times.

I kindly thank the Federal Ministry of Education and Research (BMBF) for funding this project as part of the Forschungsverbundvorhaben GeoEn (Grant 03G0671A/B/C).

Special thanks are due to our Technician Axel Kitte for his availability to solve laboratory and technical issues at any time. I would also like to thank him for translating the Abstract of this thesis to German.

I would like to thank Prof. Steven D'Hondt from the University of Rhode Island for inviting me on the Equatorial Pacific Ocean Expedition and, together with Prof. Art Spivack, Prof. Rick Murray and Prof. David C. Smith, sparking my interest in subseafloor biosphere studies. I would also like to thank Dr. Fumio Inagaki from JAMSTEC, Japan for the wonderful time during the Mud Volcano Expedition onboard Chikyu and valuable discussions about microbial activity in subsurface sediments.
I would like to show my gratitude to Prof. Martin Trauth for providing me with an opportunity to get an introduction into the East African Rift System during the Volkswagen Summer Schools in 2010 and 2011 and also many thanks to Prof. Ralph Tiedemann, Dr. Christina Hertler and all participants for a memorable Kenya and Tanzania field visits. I would also like to thank the members of the Institute of Earth and Environmental Sciences, who were directly or indirectly involved helping this thesis coming to completion.

Many thanks to my colleagues from the Geomicrobiology Junior Group, Dr. Clemens Glombitza, Dr. Mashal Alawi, Dr. Beate Schneider, Julia Nickel, Sina Grewe, Patrick Sauer and Michael Lappé for fruitful discussions and helpful comments. A very special thank to "das Schönere Büro" colleagues Oliver Rach, Swenja Rosenwinkel, Sven Borchardt, Dr. Zuze Dulanya, Tobias Müller-Wrana and Clemens Witte for creating a productive and comfortable working environment at Golm.
Without blessings and supports from my parents, brothers, sister, and my family from Nepal and Germany, I would not have been where I am today. Last but not least many thanks to my wife Jenny for her love, patience and motivation at all times.

Abstract

Metabolically active microbial communities are present in a wide range of subsurface environments. Techniques like enumeration of microbial cells, activity measurements with radiotracer assays and the analysis of porewater constituents are currently being used to explore the subsurface biosphere, alongside with molecular biological analyses. However, many of these techniques reach their detection limits due to low microbial activity and abundance. Direct measurements of microbial turnover not just face issues of insufficient sensitivity, they only provide information about a single specific process but in sediments many different process can occur simultaneously. Therefore, the development of a new technique to measure total microbial activity would be a major improvement. A new tritium-based hydrogenase-enzyme assay appeared to be a promising tool to quantify total living biomass, even in low activity subsurface environments. In this PhD project total microbial biomass and microbial activity was quantified in different subsurface sediments using established techniques (cell enumeration and pore water geochemistry) as well as a new tritium-based hydrogenase enzyme assay.

By using a large database of our own cell enumeration data from equatorial Pacific and north Pacific sediments and published data it was shown that the global geographic distribution of subseafloor sedimentary microbes varies between sites by 5 to 6 orders of magnitude and correlates with the sedimentation rate and distance from land. Based on these correlations, global subseafloor biomass was estimated to be 4.1 petagram-C and ∼0.6% of Earth's total living biomass, which is significantly lower than previous estimates. Despite the massive reduction in biomass the subseafloor biosphere is still an important player in global biogeochemical cycles. To understand the relationship between microbial activity, abundance and organic matter flux into the sediment an expedition to the equatorial Pacific upwelling area and the north Pacific Gyre was carried out. Oxygen respiration rates in subseafloor sediments from the north Pacific Gyre, which are deposited at sedimentation rates of 1 mm per 1000 years, showed that microbial communities could survive for millions of years without fresh supply of organic carbon. Contrary to the north Pacific Gyre oxygen was completely depleted within the upper few millimeters to centimeters in sediments of the equatorial upwelling region due to a higher supply of organic matter and higher metabolic activity. So occurrence and variability of electron acceptors over depth and sites make the subsurface a complex environment for the quantification of total microbial activity.

Recent studies showed that electron acceptor processes, which were previously thought to thermodynamically exclude each other can occur simultaneously. So in many cases a simple measure of the total microbial activity would be a better and more robust solution than assays for several specific processes, for example sulfate reduction rates or methanogenesis. Enzyme or molecular assays provide a more general approach as they target key metabolic compounds. Since hydrogenase enzymes are ubiquitous in microbes, the recently developed tritium-based hydrogenase radiotracer assay is applied to quantify hydrogenase enzyme activity as a parameter of total living cell activity. Hydrogenase enzyme activity was measured in sediments from different locations (Lake Van, Barents Sea, Equatorial Pacific and Gulf of Mexico). In sediment samples that contained nitrate, we found the lowest cell specific enzyme activity around 10^{-5} nmol H_2 $cell^{-1}$ d^{-1}. With decreasing energy yield of the electron acceptor used, cell-specific hydrogenase activity increased and maximum values of up to 1 nmol H_2 $cell^{-1}$ d^{-1} were found in samples with methane concentrations of >10 ppm. Although hydrogenase activity cannot be converted directly into a turnover rate of a specific process, cell-specific activity factors can be used to identify specific metabolism and to quantify the metabolically active microbial population. In another study on sediments from the Nankai Trough microbial abundance and hydrogenase activity data show that both the habitat and the activity of subseafloor sedimentary microbial communities have been impacted by seismic activities. An increase in hydrogenase activity near the fault zone revealed that the microbial community was supplied with hydrogen as an energy source and that the microbes were specialized to hydrogen metabolism.

Zusammenfassung

Mikrobielle Gesellschaften und ihre aktiven Stoffwechselprozesse treten in einer Vielzahl von Sedimenten unterschiedlichster Herkunft auf. In der Erforschung dieser tiefen Biosphäre werden derzeit Techniken wie Zellzählungen, Aktivitätsmessungen mit Radiotracer-Versuchen und Analysen der Porenwasserzusammensetzung angewendet, darüber hinaus auch molekularbiologische Analysen. Viele dieser Methoden stoßen an ihre Nachweisgrenze, wenn Sedimente mit geringer Zelldichte und mikrobieller Aktivität untersucht werden. Bei der Untersuchung von Stoffwechselprozessen mit herkömmlichen Techniken kommt dazu, dass von mehreren Prozessen, die zeitgleich ablaufen können, jeweils nur einer erfasst wird. Deswegen wäre die Entwicklung einer neuartigen Messtechnik für die gesamte mikrobielle Aktivität ein wesentlicher Fortschritt für die Erforschung der tiefen Biosphäre. Ein vielversprechender Ansatz, um die gesamte lebende Biomasse auch in Proben mit geringer Aktivität zu bestimmen, ist eine Hydrogenase-Enzym-Versuchsanordnung mit Tritium als quantifizierbarer Messgröße. In dieser Doktorarbeit wurde die gesamte mikrobielle Biomasse und Aktivität von unterschiedlichen Sedimentproben einerseits mit herkömmlichen Methoden (Zellzählungen, Analyse der Porenwasserzusammensetzung) als auch mit einer neu entwickelten Hydrogenase-Enzym-Versuchsanordnung quantifiziert.

Mit einer großen Anzahl eigener Zellzählungsdaten von Sedimenten aus dem Äquatorialpazifik und dem Nordpazifik und ergänzenden publizierten Daten konnte gezeigt werden, dass Zellzahlen sich in ihrer globalen geographischen Verteilung je nach Bohrlokation um 5 bis 6 Größenordnungen unterscheiden. Dabei bestehen Korrelationen zur Sedimentationsrate und zur Entfernung zum Land, mit deren Hilfe sich die Gesamtbiomasse in Tiefseesedimenten zu 4,1 Petagramm-C abschätzen lässt. Das entspricht ∼0,6 % der Gesamtbiomasse der Erde und ist damit erheblich weniger als in früheren Schätzungen angegeben. Trotz der Korrektur auf diesen Wert spielt die Biomasse der tiefen Biosphäre weiterhin eine erhebliche Rolle in biogeochemischen Kreisläufen. Um die Zusammenhänge zwischen Aktivität der Mikroben, der Häufigkeit ihres Auftretens und Zustrom von organischem Material zu verstehen, wurde eine Expedition ins Auftriebsgebiet des Äquatorialpazifiks und zum nordpazifischen Wirbel durchgeführt. Daten der Sauerstoffaufnahme in Sedimenten des nordpazifischen Wirbels, die mit Sedimentationsraten von 1 mm pro 1000 Jahren abgelagert werden, zeigen, dass mikrobielle Gesellschaften über Millionen von Jahren ohne Zufuhr von frischem organischen Kohlenstoff überleben konnten. Im Gegensatz zum nordpazifischen Wirbel wird in Sedimenten des äquatorialpazifischen Auftriebsgebiets Sauerstoff bei höherer mikrobieller Aktivität und

Verfügbarkeit organischer Verbindungen oberflächennah in den ersten Milli- bis Zentimetern komplett umgesetzt. Auftreten und Variabilität von Elektronenakzeptoren nach Tiefe und Bohrlokation machen die tiefe Biosphäre zu einer komplexen Umgebung für die Quantifizierung der gesamten mikrobiellen Aktivität.

Aktuelle Studien zeigen das verschiedene Elektronenakzeptorprozesse gleichzeitig ablaufen können, obwohl man bisher davon ausgegangen war, dass diese sich thermodynamisch ausschließen. In vielen Fällen wäre also eine einfache Methode zur Messung der gesamten mikrobiellen Aktivität eine bessere und verlässlichere Lösung aktueller Analyseaufgaben als Messungen mehrerer Einzelprozesse wie beispielsweise Sulfatreduktion und Methanogenese. Enzym-oder Molekular-Versuchsanordnungen sind ein prozessumfassender Ansatz, weil hier Schlüsselkomponenten der Stoffwechselprozesse untersucht werden. Das Hydrogenase-Enzym ist eine solche Schlüsselkomponente und in Mikroben allgegenwärtig. Deshalb kann die Quantifizierung seiner Aktivität mit der neu entwickelten Hydrogenase-Enzym-Versuchsanordnung als Parameter für die gesamte mikrobielle Aktivität der lebenden Zellen verwendet werden. Hydrogenase-Aktivitäten wurden in Sedimenten unterschiedlicher Lokationen (Vansee, Barentssee, Äquatorialpazifik, und Golf von Mexico) gemessen. In Sedimentproben, die Nitrat enthielten, haben wir mit ca. 10^{-5} nmol H_2 $cell^{-1}$ d^{-1} die geringste zellspezifische Hydrogenase-Aktivität gefunden. Mit geringerem Energiegewinn des genutzten Elektronenakzeptors steigt die zellspezifische Hydrogenase-Aktivität. Maximalwerte von bis zu 1 nmol H_2 $cell^{-1}$ d^{-1} wurden in Sedimentproben mit $>$10 ppm Methankonzentration gefunden. Auch wenn die Hydrogenase-Aktivität nicht direkt in die Umsatzrate eines spezifischen Prozesses konvertierbar ist, können zellspezifische Aktivitätsfaktoren verwendet werden, um die metabolisch aktive Mikrobenpopulation zu quantifizieren. In einer weiteren Studie mit Sedimenten des Nankai-Grabens zeigen Daten der Zelldichte und der Hydrogenase-Aktivität einen Einfluss von seismischen Ereignissen auf Lebensraum und Aktivität der mikrobiellen Gesellschaften. Ein Anstieg der Hydrogenase-Aktivität nahe der Verwerfungszone machte deutlich, dass die mikrobiellen Gesellschaften mit Wasserstoff als Energiequelle versorgt wurden und dass die Mikroben auf einen Wasserstoff-Stoffwechsel spezialisiert waren.

List of Figures

List of Tables

Abbreviations

AO acridine orange 78

AODC acridine orange direct count 25

AOM anaerobic oxidation of methane 70

ATP adenosin 5'-triphosphate 99

CARD-FISH catalyzed reporter deposition- fluorescence *in situ* hybridization 51

CL core lipid

DAPI diamidinophenylindole 71

DCM dichloromethane 100

DNA deoxyribonuclic acid 90

DSAG Deep-Sea Archaeal Group 93

dsrA dissimilatory (bi)sulfite reductase 55

EDTA ethylenediaminetetraacetic acid xviii

GC-FID gas chromatography–flame ionization detector 102

GC gas chromatography 102

GDGT glycerol dialkyl glycerol tetraethers 94

GMT Generic Mapping Tools 29

HPLC-MS HPLC-mass spectrometry 101

HPLC high-performance liquid chromatography 101

ICDP International Continental Scientific Drilling Program 73

IODP Integrated Ocean Drilling Program 90

IPL intact polar lipid

mblf meter below lakefloor 79

mbsf meter below seafloor 90

MCG-1 Miscellaneous Crenarchaeaotic Group 1 93

MDL minimum detection limit 82

NADH nicotinamide adenine dinucleotide 63

ODP Ocean Drilling Program 26

PBS phosphate buffered saline 96

PCR polymerase chain reaction

RNA ribonuclic acid 13

rRNA ribosomal ribonuclic acid 89

SD standard deviation 21

SMTZ sulfate–methane–transition zone 70

SR sulfate reduction 70

SRB sulfate reducing bacteria 51

SRM sulfate reducing microbes 55

SRR sulfate reduction rates 55

TE Tris-ethylenediaminetetraacetic acid (EDTA)

TLE total lipid extract 100

TOC total organic carbon 74

Contents

1 Introduction

1.1 Scope of the thesis

This thesis deals with two important issues in subsurface sediment biosphere: (a) the quantification of microbial biomass and (b) the quantification of total microbial activity using a tritium–based hydrogenase enzyme assay. In the first part, microbial cells were enumerated in various sedimentary environments using the well–established cell extraction method of Kallmeyer et al. (2008). Furthermore, microbial cell sizes were measured to estimate total biomass, since total cellular carbon depends on microbial cell size, which varies greatly in different natural environments.

In the second part microbial activity is quantified. Conventionally, only a specific metabolic process (e.g. sulfate reduction, methanogenesis, etc.) is measured in order to quantify microbial activity in sediments. In cases where a single particular process is quantitatively important, it is often considered to be equivalent to a total metabolic activity. However, many of these methods have already reached their limit of detection at deep subsurface environments where microbial activity is extremely low. Furthermore, we know that microorganisms can live in complex syntrophic relationships (Boetius et al., 2000), so only a single metabolic activity does not truly represent overall microbial activity. In order to quantify total microbial activity, a tritium-based hydrogenase (H_2ase) enzyme assay was developed and applied at various environments without identifying specific metabolic process.

The following introduction gives an overview on microbial habitats, biomass, turnover rates and microbial total activity in various subsurface environments. This study will enhance our understanding about the poorly explored subsurface microbial biosphere.

1.2 General Background

1.2.1 Microbial habitats

Earth's atmosphere, lithosphere and hydrosphere are inhabited by microbes (Fig. 1.1). However, only the uppermost part of Earth's crust and the lowermost part of the atmosphere support microbial life, which include air, water, sediment or soil and rocks.

Microbial occurrence and relevance in the atmosphere have been investigated since the late nineteenth century (Miquel, 1883). Imshenetsky et al. (1978) have recovered living microbes

in an altitude of 48 to 77 km in the atmosphere. Although the atmosphere harbors viable vegetative cells and spores, it is debatable whether they are capable of sustained growth and multiplication due to lack of nutrients and moisture, and higher levels of radioactivity at high altitude (DeLeon-Rodriguez et al., 2013; Després et al., 2012). Furthermore, the residence time of these microbes in atmosphere is limited and eventually they fall back down to Earth. However the atmosphere plays a major role in transporting microbes from one place to another, thereby significantly impacting in microbial ecosystem (Ehrlich, 1998).

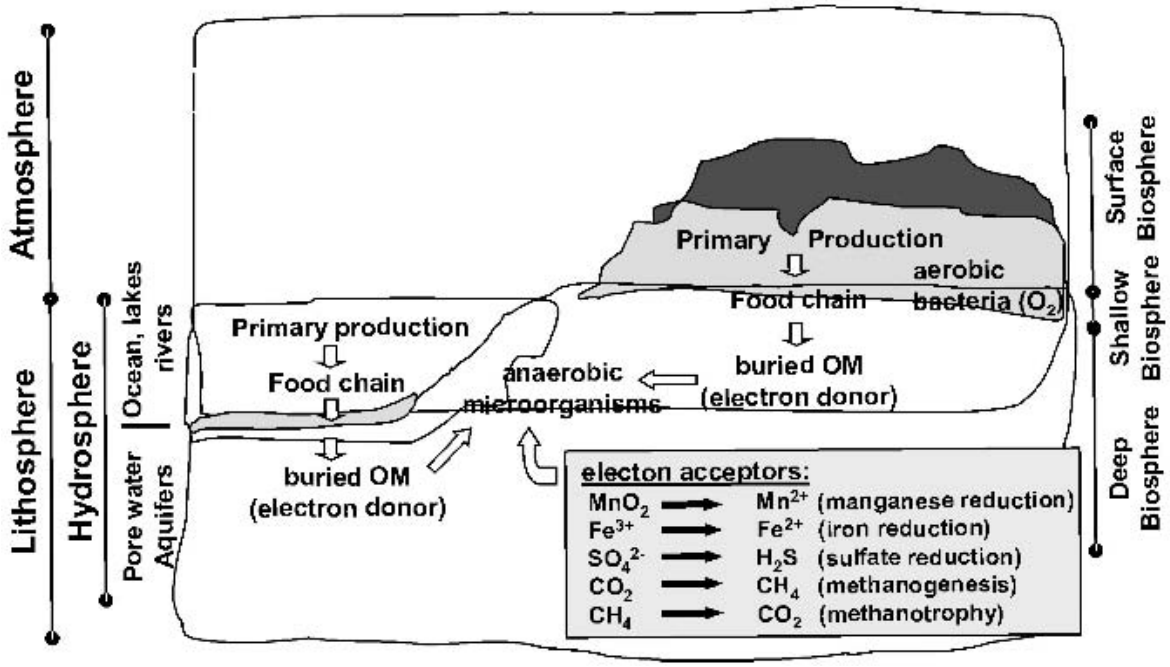

Figure 1.1: *Extension of the biosphere on Earth (Horsfield and Kieft, 2007)*

Unlike the atmosphere, the hydrosphere is completely inhabited by microbial life. Terrestrial and marine aquatic environments are full of microbes throughout water column from the surface to the greatest depths (Glud et al., 2013). The aquatic environment is a dynamic microbial habitat since active material exchange takes place with air at the water surface and with sediments at the bottom of the water column. A continuous supply of nutrients from the surface water towards underlying sediments is necessary for the survival of microbes in the subsurface (Russell and Cook, 1995).

Life is not only restricted in the uppermost exposed surface but also in the deep subsurface down to hundreds or even thousands of meters (Parkes et al., 1994; Roussel et al., 2008). Earth's subsurface can be divided into terrestrial and marine subsurface. These subsurface environments are drilled and explored explicitly for the exploitation of energy resources

and research purposes. International Continental Scientific Drilling Program (ICDP) and Integrated Ocean Drilling Program (IODP) are involved in terrestrial and subseafloor subsurface exploration for research purposes respectively. These two programs are providing samples to investigate subsurface biosphere, thereby understanding global biogeochemical cycles (Horsfield et al., 2006).

Terrestrial subsurface biosphere

The important role of living and active subsurface microorganisms in global biogeochemical cycles has been widely recognized in the last decades but most of the investigations were accomplished in subseafloor sediments (Inagaki et al., 2006; Parkes et al., 1994; D'Hondt et al., 2009; Hinrichs et al., 1999). Living microorganism are present in various terrestrial subsurface environments like in glaciers, ice–sheets, buried lakes, salt and deep gold mines, gas hydrates, oil reservoirs, hydrothermal vents, mud volcanoes, deep fractured rock etc (Horsfield and Kieft, 2007; Wagner et al., 2012).

Terrestrial habitats have been mostly explored by groundwater or some deep rock analysis (Breuker et al., 2011). Hoos and Schweisfurth (1982) analyzed microbial occurrence down to a sediment depth of 90 m in Lower Saxony, Germany. In 1987 Chapelle et al. discovered microbes in terrestrial coastal plain sediments of Maryland and in another study Colwell et al. (1997) found microbes in late Cretaceous rocks down to a depth of 2000 m. Fry et al. (2009) showed that microbes are present in a terrestrial drill core of 148 m length from a coal deposit in New Zealand. Microbes are capable of living almost everywhere in subsurface at wide range of temperature and pressure (Pedersen, 2006; Wagner et al., 2012). These studies suggest that the deep terrestrial subsurface biosphere is active everywhere and equally important for global biogeochemical cycles like subseafloor biosphere.

Subseafloor biosphere

The Oceans cover two third of Earth's surface and harbor a great variety of prokaryotic and eukaryotic cells. Similar to the water column, microorganisms are abundant in subseafloor sediments (Parkes et al., 2000). The study of subseafloor microbial life has been acknowledged in the scientific world due to its role in global biogeochemical cycles.

Before ZoBell and Johnson (1949) found "barophilic" bacteria in a marine mud sample from off Bermuda, it was not known that microbes could survive in subseafloor sediments (although Lipman, 1928, 1931, already mentioned the discovery of living microorganism in

ancient rocks). The study, in which pelagic sediments were investigated during a mid–Pacific Expedition to the Marshal Islands in 1950, proved that the microbial habitat indeed extends deeper down to few meters below seafloor (Morita, 1999). Parkes et al. (1994) showed that microbial life is not limited to few meters below the seafloor, rather several hundred meters.

To explore subsurface microbial habitats, it is possible to obtain samples for microbiological investigations from several hundred to thousand meters below the seafloor these days. The Japan Agency for Marine-Earth Science and Technology (JAMSTEC) has recently (2013) reported that the scientific deep sea drilling vessel Chikyu has set a new record by drilling down and obtaining rock samples from deeper than 2 kilometers below seafloor off Shimokita Peninsula of Japan in the northwest Pacific Ocean (IODP Expedition 337). The preliminary results show that microbial life is active at this depth.

1.2.2 Global subsurface microbial biomass

Not every subsurface microbial habitat is explored and fully investigated. However, we are aware that subsurface is the largest microbial habitat on Earth and constitutes large fraction of total living biomass on Earth (Kallmeyer et al., 2012).

Morita and ZoBell (1955) investigated microbial abundance in subseafloor sediments down to a few meters below seafloor for the first time. Since they could only culture microbes from the sediment samples down to a depth of 7.47 meter below seafloor (mbsf), they concluded that the end of marine biosphere were reached at this depth. The statement has been proven wrong by several subsequent studies. Using porewater analysis and radiotracer turnover experiments, for example, Whelan et al. (1985) identified microbial activity at a depth of 167 mbsf. Interestingly, they identified sulfate reduction, methanogenesis and fermentation along with methane production in deep sediments. These turnover rates in subsurface sediments are several orders of magnitude lower than in surface sediments (Hoehler and Jørgensen, 2013).

In their pioneering study for the quantification of global living biomass in subseafloor sediments, Parkes et al. (1994) enumerated microbial cells down to 518 mbsf. Based on these data Whitman et al. (1998) estimated that subsurface microbial biomass constitutes $1/3^{rd}$ of Earth's total living biomass. Since these data were mostly from highly productive coastal and upwelling areas, more data were needed for a more accurate estimation of total subsurface microbial biomass. Recently, total subseafloor sedimentary biomass was estimated using previously published cell count data from nutrient–rich sediments, and new data from extremely oligotrophic (south and north Pacific Gyre) environments (D'Hondt et al., 2009;

Kallmeyer et al., 2012). The new estimate reduced total living biomass to 10–45% of the previous estimate (Whitman et al., 1998; Kallmeyer et al., 2012).

Although the value is lowered significantly, subsurface biomass is still enormous and plays a major role in biogeochemical cycles (Jørgensen, 2012). However, due to complex behavior in microbial metabolism, it is still a major challenge to quantify microbial activity in subsurface environments to understand microbial role in global biogeochemical cycles.

1.2.3 Microbial activity in subsurface

Geochemical modeling as well as experimental data have shown that the rate of microbial activity in subsurface is several orders of magnitude lower than in the surface environments (Chapelle and Lovley, 1990; Phelps et al., 1994; Wang et al., 2008; Parkes et al., 2000). This means that the flux of energy and the availability of electron donors/acceptors are the limiting factors for microbial growth. The other factors like high pressure, and low/high temperatures could also be limiting factors for microbial metabolism. It is debatable whether these conditions are unfavorable for microbial growth or the microbes are well adapted for these environments (Hoehler and Jørgensen, 2013). In most subsurface environments the energy flux is so low that the microbes are forced to stop their growth and go for a survival strategy (Morita, 1999; Jørgensen, 2011). This is, however, a challenge for scientists to define: How low is low, or what is the difference between active, dormant and dead cells?

One of the most fundamental questions in subsurface research is how the microbial communities are supplied with energy and how they can utilize recalcitrant organic carbon (Jørgensen, 1982a,b). It is still unclear how these microbes live in such environments over a geologic time scale with such minimal energy availability. Subsurface microbes are very effective in obtaining energy from recalcitrant organic carbon, using multiple steps of metabolism by different types of microbes specialized for a certain metabolic step (Boetius et al., 2000). Under these circumstances, a quantitative study of microbial activity in the subsurface is only possible if the methods are sensitive enough and cover all metabolic processes at that environment.

Various methods are being used to quantify microbial activity, either considering specific metabolic process or total microbial activity. The most common methods that are used to quantify specific metabolic process in subsurface sediments are Fe/Mn reduction, sulfate reduction and methanogenesis (Oremland et al., 2000; Ferry, 1992; Hinrichs and Boetius, 2002; Ferdelman et al., 1997; Treude et al., 2005). So far only adenosin 5'-triphosphate (ATP)

measurement (Vuillemin et al., 2013) and H_2ase enzyme activity measurement (Schink et al., 1983; Soffientino et al., 2006) provide a measure of total microbial activity.

Froelich et al. (1979) showed the sequence of electron acceptors that are used by microbes to degrade organic matter in sediments. Microbes preferentially use electron acceptors that have the highest energy yield. Thermodynamically O_2 yields the most energy, followed by NO_3^-, Mn^{2+}, Fe^{2+}, SO_4^{2-}. Depending on the availability of a carbon source, electron acceptors may be consumed completely. In organic rich sediments, for example, O_2 is depleted usually within a few millimeters (Jørgensen, 1982a,b), whereas it can reach down to tens of meters below seafloor in highly oligotrophic regions like the North Pacific Gyre (Røy et al., 2012) or South Pacific Gyre (D'Hondt et al., 2009).

Apart from Ocean gyres, which cover ∼40% of the total Ocean surface, most of the subsurface sediments are anaerobic and sulfate reduction (SR) is the dominant carbon remineralization process (Jørgensen, 1982a,b). So in order to understand and quantify subsurface microbial activity in marine sediments, SR is one of the most important metabolic processes to measure. Sulfate reduction can be broadly divided into (1) organoclastic SR, where either hydrogen or low molecular weight substrates are used as electron donors (Jørgensen, 1982a,b; Martens and Berner, 1974), and (2) methanotrophic SR, where methane is oxidized (Martens and Berner, 1974). Current understanding of SR has been derived mostly from ^{35}S radiotracer experiments, which can detect sulfate reduction rates (SRR) in the nanomolar cm^{-3} d^{-1} range. However, this will provide us knowledge of only a specific process rather than overall microbial activity, although several specific metabolic processes may occur simultaneously (Wang et al., 2008). So a method to quantify total microbial activity in subsurface environments is a necessity. Among others, ATP (Vuillemin et al., 2013) and H_2ase enzyme activity (Soffientino et al., 2006) could be promising tools to measure total microbial activity in any environments (Adhikari and Kallmeyer, 2010).

ATP activity

ATP is a molecule that is produced only by living microorganisms, so ATP quantification has long been used to measure microbial activity in the subsurface (Tan and Rüger, 1989; Bird et al., 2001). However, methodological problems are great obstacles that need to be overcome in order to obtain reliable results in subsurface sediments. One of the major challenges of using ATP to quantify total microbial activity is to define a ratio between ATP and the amount of living biomass. Karl (1980) determined such a ratio but did not investigate the variability of

the ratio in different environments. However, if we focus only on deep sediments, the ATP per cell ratio would not be a big issue because the amount of living biomass does not vary much in deep subsurface (Kallmeyer et al., 2012) but we have to overcome other issues caused by low biomass and low activity. Due to low biomass and activity, a large sample size has to be processed to analyze ATP activity, which could be technically a big problem.

Vuillemin et al. (2013) have recently quantified microbial activity by ATP measurements in subsaline maar lake sediments. They measured in situ ATP activity in the sediments and compared it with total microbial population using diamidinophenylindole (DAPI) cell counts. A relatively similar trend of the ATP activity profile and cell counts shows that the method could be a valuable tool in sediment samples. They have analyzed samples with relatively high microbial cell abundance of ca. 10^8 cells g^{-1} sediment which is up to 5 orders of magnitude higher than in many deep subseafloor sediments (Kallmeyer et al., 2012). In the oligotrophic deep subsurface, microbial cell numbers as well as activity are extremely low and consequently ATP and total living biomass are also relatively low.

In environmental samples the carbon content in a microbial cell varies between 7 to 31 fg, which is 10 to 50 times lower than in cultured cells (Fagerbakke et al., 1996). When we calculate the cellular ATP content in deep subsurface sediments, we come to an ATP concentration in the range of femtomole per cm^3 sediment (see Adhikari and Kallmeyer, 2010, for calculation), whereas commercially available ATP assay kits measure ATP in the picomole per cm^3 range, so these kits would have reached their limit of detection. As a general trend, microbial cell counts decrease logarithmically with depth, which means as we go deeper into the sediment, the amount of ATP decreases drastically (Martens, 2001). Commercially available ATP kits measure the intensity of the luminescence produced during the reaction between luciferase and ATP, which can easily be interfered by the sediment matrix, especially when the amount of ATP is extremely low. In order to extract enough ATP, a large sample volume is needed, which makes sample processing technically difficult.

Hydrogen metabolism and hydrogenase enzyme

Hydrogen, which can be exchanged efficiently between different microbes and is easily available in every environment, is a valuable energy source in the microbial world (Barz et al., 2010; Hinrichs et al., 2006; Hoehler et al., 1998, 2001; Lin et al., 2005b). Due to its strong control on the thermodynamics of redox–based metabolism, molecular hydrogen significantly influences microbial ecosystems in the subsurface (Hoehler et al., 2002). Furthermore, in most natural

ecosystems, H_2 partial pressure is very low (about 70 nmol L^{-1}) but the hydrogen turnover rate is rather rapid, for example 3-5 nmol L^{-1} s^{-1} in sediments of the methanogenic zone (Hoehler et al., 1994). This rapid hydrogen turnover rate causes drastic fluctuation in partial pressure, making difficult to measure accurate hydrogen concentration to understand hydrogen metabolism in the subsurface.

In any natural environments, hydrogen is necessary for cellular metabolism, where it is either produced or consumed. For example hydrogen, which is produced by fermentation processes, is utilized by nearby hydrogen–consuming microbes. The hydrogen–consuming microbes help to reduce the partial pressure of hydrogen in this environment, which creates thermodynamically favorable conditions for further degradation of organic matter and ultimately gaining more energy per mole of carbon (Hoehler et al., 2002). This hydrogen utilization is only possible with the help of the catalytic property of the microbial H_2ase enzymes.

About 35–50% of all intracellular enzymes contain transition metal ions in their active site for biological catalysis (Cammack et al., 2001). An important class of such metalloenzymes are the H_2ase enzymes, which were first described by (Stephenson and Stickland, 1931). Hydrogenase is a family of exclusively intracellular enzymes expressed by almost all microorganisms, mostly prokaryotes, but also eukaryotes like algae, protozoa, and fungi (Vignais et al., 2001).

According to the type of metal on the active site, hydrogenases are classified into three classes:

- Ni–Fe hydrogenases are the largest and the best characterized group of hydrogenases, containing a Ni–Fe active site (Albracht, 1994). Most Ni–Fe hydrogenases catalyze the cleavage of molecular hydrogen into protons and electrons i.e. a hydrogen consumption reaction (Fig. 1.2A).

- Fe–Fe hydrogenases contain an iron-iron active site and are mainly responsible to catalyze the reaction to produce hydrogen molecules for maintaining a proton gradient inside the microbial cell (Adams et al., 1990, Fig. 1.2B).

- Fe–S cluster hydrogenases have been found in some methanogenic archaea and were initially considered to be metal–free enzymes and were later renamed as Fe–only H_2ase (Lyon et al., 2004; Thauer et al., 1996, Fig. 1.2C).

Different hydrogenases have different functions in cellular metabolism. According to their central functions, hydrogenases can be distinguished into: (1) hydrogen uptake H_2ase, (2)

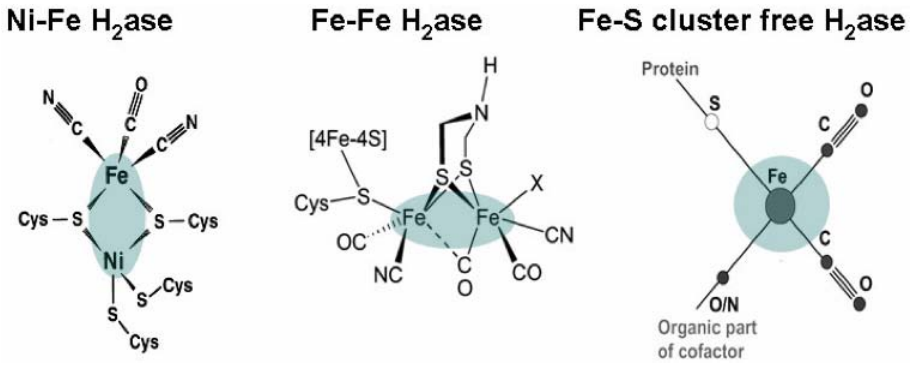

Figure 1.2: *Types of hydrogenases (After Cammack et al., 2001): (A) Ni–Fe H_2ase, (B) Fe–Fe H_2ase and (C) Fe–S cluster free H_2ase*

hydrogen production H_2ase and (3) hydrogen–sensing H_2ase (Vignais et al., 2001). Along with the interconversion of molecular H_2 into protons and electrons or vice versa ($H_2 \rightleftharpoons 2H^+ + 2e^-$; Krasna and Rittenberg, 1956) the enzyme catalyzes the isotopic exchange reaction between water and deuterium/tritium (HD+ $H_2O \rightleftharpoons$ HDO + H_2; Adams et al., 1990; Schink et al., 1983).

The property of H_2ase enzymes to catalyze an isotope exchange reaction between hydrogen and tritiated water has been focused in this study to quantify microbial activity in sediment. The quantification of H_2ase enzyme activity to understand microbial activity has been done in several studies mainly in pure cell culture or in organic carbon–rich sediments (Schink et al., 1983; Soffientino et al., 2006). Recently Nunoura et al. (2009) have measured H_2ase activity in deep subsurface (down to 600 mbsf) sediments with low cell numbers (ca. 10^4 cells g^{-1} sediment) in the Brazos–Trinity Basin and the Mars–Ursa Basin on the Gulf of Mexico (IODP Expedition 308).

Since the enzyme is ubiquitous in microbes of any environment, and catalyzes reactions to produce/consume electrons and protons depending on the microbial need, the enzyme activity could give us a total microbial activity in any environment, regardless of which specific metabolic process is present. Some of the advantages of this method are: (1) it is not necessary to identify a specific metabolic process, (2) the technique quantifies total microbial activity, (3) the method could be applied to any natural environment, and (4) the method could be used in extremely oligotrophic deep subsurface environments.

In this dissertation, along with total microbial cell abundances, total microbial activity is quantified in various environments using a tritium–based H_2ase enzyme assay.

Objectives

The main aims of my PhD project are:

1. Quantification of microbial population in subsurface sediments and understanding their role in global biogeochemical cycles (Chapters 2 and 3),

2. Comparison of various methods that are currently applied to quantify subsurface microbial activity to identify their strengths and limitations (Chapter 4), and

3. Development of a sensitive method to quantify subsurface microbial activity in such environments, where current techniques have reached their limit of detection (Chapter 5 and 6).

To fulfill the aims, intense scientific collaboration with international experts from the University of Rhode Island, the University of Aarhus, the GeoForschungsZentrum Potsdam (GFZ), and the JAMSTEC Japan was carried out.

1.3 Outline of the Thesis

This is a cumulative thesis, which consists of seven chapters. Out of these seven chapters, five chapters are in the form of manuscripts. The Chapters 2, 3 and 4 are already published in international peer–reviewed scientific journals while Chapters 5 and 6 will be submitted soon.

Chapter 1: Introduction

This chapter provides the scope and the aims of the thesis. It also presents a brief introduction to the subsurface sedimentary biosphere, microbial turnover rates and microbial activity in subsurface environments.

Chapter 2: Global distribution of microbial abundance and biomass in subseafloor sediment

J. Kallmeyer, R. Pockalny, R. R. Adhikari, D. C. Smith and S. D'Hondt

PNAS (2012), Vol. 109 (40), 16213-16216

In Chapter 2, the global geographic distribution of subseafloor sedimentary microbes was evaluated. Based on published and our own cell count data, global microbial subseafloor sedimentary biomass was recalculated. We showed that the total global subseafloor biomass is $2/3^{rd}$ smaller than previously estimated.

As a co-author I have performed total microbial cell counts during a R/V Knorr Expedition to the equatorial in January-March 2009. I, myself, have produced data that are represented by the red dots and blue dots in Fig. 2.1. More data are shown in Figs. 2.4 and 2.5 in the supplementary material. I have carried out the first actual deep subsurface cell size measurements reported in the scientific literature and presented these data in Fig. 2.7 in the supplementary material. In their commentary regarding biomass estimation and cell size, Hinrichs and Inagaki (2012) in Science magazine wrote: "... Kallmeyer et al. (2012) use the lowest value to date, but they back up their choice convincingly with statistical data on the size distribution of indigenous cells ... "

Chapter 3: Aerobic microbial respiration in 86–million–year–old deep–sea red clay

H. Røy, J. Kallmeyer, R. R. Adhikari, R. Pockalny, B. B. Jørgensen and S. D'Hondt

Science (2012), Vol. 336 (6083), 922-925

In Chapter 3, we show that microbial communities can subsist at tens of meters below seafloor in marine sediments without fresh supply of organic matter for millions of years under extreme energy limitation. The penetration of O_2 down to the depth of >30 m in north Pacific gyre sediment shows that the microbial community size is determined by the rate of carbon flux, which is controlled by sedimentation rate.

As a co-author I have performed total microbial cell counts for all locations used in this study. The data were used for the quantification of specific microbial respiration. The data represented by the open circles in Fig. 3.2B were measured by myself. The whole paper is mainly concerned with cell specific respiration i.e. the cell counts data and the oxygen data are the main datasets used in this manuscript.

Chapter 4: Detection and quantification of microbial activity in the subsurface

R. R. Adhikari and J. Kallmeyer

Chemie der Erde-Geochemistry (2010), Vol. 70 (3), 135-143

Chapter 4 provides a review of currently available techniques for the quantification of microbial turnover processes in subsurface environments. Here we have discussed strengths and limitations of these techniques for the exploration of subsurface environments. In this chapter, we mention that an enzyme assay could be a promising tool to quantify total microbial activity for a better understanding of the subsurface biosphere.

I have carried out literature research and wrote the manuscript with the assistance of my PhD supervisor.

Chapter 5: Distribution and activity of hydrogenase enzymes in subsurface sediments

R. R. Adhikari, J. Nickel, C. Glombitza, A. Spivack, S. D'Hondt and J. Kallmeyer

will be submitted to Limnology and Oceanography (2013)

We applied a highly sensitive tritium-hydrogenase enzyme assay for the quantification of total microbial activity to several subsurface sediments from different regions. We have also

compared these enzyme activity data with specific turnover rates and total cell numbers. Our results showed a very similar per cell rate of H_2ase activity in all sediments, which is a strong proof that the enzyme assay could be used as a *catch-all* parameter to quantify subsurface microbial activity.

I have analyzed all samples for H_2ase measurements and produced data of cell counts and enzyme activity. I have prepared the first draft and write the manuscript. Julia Nickel and Clemens Glombitza provided sulfate data from Barents Sea and Lake Van sediments, respectively. Art Spivack provided geochemical data from the equatorial Pacific sediments. Steven D'Hondt was PI of the EQP Expedition and helped in interpretation of the results. My PhD supervisor Jens Kallmeyer designed the research, helped with the interpretation of the results along with the preparation of final version of the manuscript.

Chapter 6: Impact of seismogenic fault activities on deep subseafloor life

F. Inagaki, Y. Morono, J. S. Lipp, Y. Takano, R. R. Adhikari, A. H. Kaksonen, T. Terada, Y. Chikaraishi, T. Futagami, J. Kallmeyer and K.-U. Hinrichs

will be submitted to PLoS ONE (2013)

In Chapter 6, various parameters, like lipids, deoxyribonuclic acid (DNA), ribonuclic acid (RNA) analyses and H_2ase enzyme activity were analyzed to understand microbial activity in a tectonically active zone. Our enzyme activity data nicely fit into these analyses, showing a great potential of the method for the quantification of total microbial activity in deep subsurface environment.

To this large project funded by JAMSTEC and IODP, I have contributed by measuring H_2ase activity and provided the text block of my analysis and results. Along with cell counts data, H_2ase is one of the most important parameter to understand microbial activity in such deep subsurface where a continuous energy is supplied due to the subduction of oceanic plates.

Chapter 7: Conclusions and outlook

This chapter summarizes the main conclusions of the results and provides an outlook for future work.

2 Global distribution of subseafloor sedimentary biomass

The global geographic distribution of subseafloor sedimentary microbes and the cause(s) of that distribution are largely unexplored. Here, we show that total microbial cell abundance in subseafloor sediment varies between sites by ca. five orders of magnitude. This variation is strongly correlated with mean sedimentation rate and distance from land. Based on these correlations, we estimate global subseafloor sedimentary microbial abundance to be 2.9×10^{29} cells [corresponding to 4.1 petagram (Pg) C and ~0.6% of Earth's total living biomass]. This estimate of subseafloor sedimentary microbial abundance is roughly equal to previous estimates of total microbial abundance in seawater and total microbial abundance in soil. It is much lower than previous estimates of subseafloor sedimentary microbial abundance. In consequence, we estimate Earth's total number of microbes and total living biomass to be, respectively, 50–78% and 10–45% lower than previous estimates.

Introduction

Bacteria and archaea drive many fundamental processes in marine sediment, including oxidation of organic matter, production of methane and other hydrocarbons, and removal of sulfate from the ocean (D'Hondt et al., 2004; Hinrichs et al., 2006; Jørgensen, 1982b). Previous studies of subseafloor sediment from ocean margins and the eastern equatorial Pacific Ocean reported high abundances of microbial cells (D'Hondt et al., 2004). RNA studies indicate that many of these cells are active (Schippers et al., 2005), have a diverse community composition (D'Hondt et al., 2009; Inagaki et al., 2006), and exhibit high diversity in their anaerobic metabolic activity (D'Hondt et al., 2009). Cell counts from these environments generally show little variation between sites (D'Hondt et al., 2004; Parkes et al., 2000) and decrease logarithmically with sediment depth, although there can be sharp peaks of high cell densities in zones of anaerobic methane-oxidation (D'Hondt et al., 2004; Parkes et al., 2005).

In 1998, Whitman et al. (1998) estimated subseafloor sedimentary microbial abundance to be 35.5×10^{29} cells, comprising 55–86% of Earth's prokaryotic biomass and 27–33% of Earth's living biomass. For their estimates, they assumed the average relationship of cell concentration to depth in six Pacific sites to characterize sedimentary microbial concentrations throughout the world ocean. Based on quantifications of intact phospholipid biomarkers from 15 Pacific Ocean sites and 1 Black Sea site, Lipp et al. (2008) subsequently estimated microbial abundance in subseafloor sediment to be 5×10^{30} cells.

Previously published cell counts are generally from ocean margins and the eastern equatorial Pacific Ocean. Recent counts from the South Pacific Gyre (D'Hondt et al., 2009) and the North Pacific Gyre are several orders of magnitude lower and show a more rapid decrease with depth (Fig. 2.1A). In these regions, dissolved oxygen penetrates deeply into the sediment and microbial activity is generally aerobic (D'Hondt et al., 2009; Røy et al., 2012). Metabolic activity per cell is extremely low among the anaerobes of both ocean margins and upwelling regions (D'Hondt et al., 2002) and the aerobes of the open-ocean gyres (D'Hondt et al., 2009; Røy et al., 2012).

The differences between cell counts from ocean margins and upwelling areas and cell counts from oceanic gyres raise three questions. First, how does the abundance of microbes in subseafloor sediment vary throughout the world ocean? Second, what property or properties are likely to control that variation? Third, how does this variation affect estimates of total subseafloor sedimentary biomass and Earth's total biomass?

Materials and Methods

To address these questions, we compiled our cell counts from the South Pacific Gyre (D'Hondt et al., 2009), the North Pacific Gyre, and the eastern equatorial Pacific Ocean with previously published counts from ocean margins and the equatorial Pacific Ocean (Fig. 2.1B). We limited this compilation to sites with cell counts both above and below 1 mbsf. To compare the data from different sites, we parameterized the cell distribution at each site by plotting cell abundance against subseafloor sediment depth for each site and then calculating a best-fit maximum likelihood estimate of a power-law function by minimizing the mean squared error (details provided in Supporting Information) using nontransformed data.

Of the 57 total sites, 34 exhibited a characteristic decrease in cell concentration with correlation coefficients exceeding 0.5 for power-law maximum likelihood regressions. The 23 sites omitted from the study had regression values less than 0.5 due to noisy or erratic cell concentration trends. These noisier data are often explainable by anomalous depositional settings or local geological anomalies [e.g., in the Nankai Trough (Moore et al., 2001), where cell concentration increases at greater depth due to in situ thermogenic generation of microbial substrates (Horsfield et al., 2006); in the Mediterranean Sea, where organic-rich sapropel layers cause elevated cell abundances in certain depth intervals and brine incursions occur at greater depths (Cragg et al., 1998, 1999); at the base of continental margins, where mass wasting events alter sediment accumulation rates (Cragg, 1995)]. These sites with anomalous

cell distributions were omitted from further calculations. For each of the 34 sites analyzed further, we determined two parameters: (i) cell concentration at 1 mbsf (variable b) and (ii) rate of decrease in cell counts with depth (variable m) (details are provided in Supporting Information).

Table 2.1: *Percentage of variance for (i) cell count at 1 mbsf (b) and (ii) rate of cell count decrease with depth (m) explained by various parameters*

Variable	Cell count at 1 mbsf (b)	Rate of decrease with sediment depth (m)
Mean sedimentation rate	72	42
Distance from land	58	56
Sea-surface chlorophyll	22	4
Gross primary production	29	9
Water depth	38	15
Sea-surface temperature	10	13
Sedimentation rate and water depth	72	45
Sedimentation rate and distance from land	85	62

Data sources are provided in Supporting Information

To test possible causes of geographic variation in subseafloor sedimentary cell abundance, we then calculated the correlations of b and m to several oceanographic parameters that vary strongly between ocean margins and midocean gyres (Table 2.1). Of these individual parameters, mean sedimentation rate is most highly correlated with both b and m. The combination of mean sedimentation rate and distance from land (distance from landmasses greater than 105 km^2) explains an even higher percentage of the variance in both b and m (Table 2.1). The residuals are normally distributed, and our sites span the broad range of sedimentation rate/distance combinations that occur in the world ocean (Fig. 2.2). Principal component analyses indicate that the addition of any of the remaining variables does not increase the explanation of variance in either b or m.

Results

These correlations are consistent with a strong influence of organic matter burial rate on subseafloor sedimentary cell abundance. Burial of organic matter from the surface world is generally inferred to be the primary source of electron donors for microbes in most subseafloor sediment (D'Hondt et al., 2004; Jørgensen et al., 2000). The rate of organic matter oxidation in subseafloor sediment has been described as declining with age according to a power-law function (Middelburg, 1989) or logarithmically (Rothman and Forney, 2007). Correlation

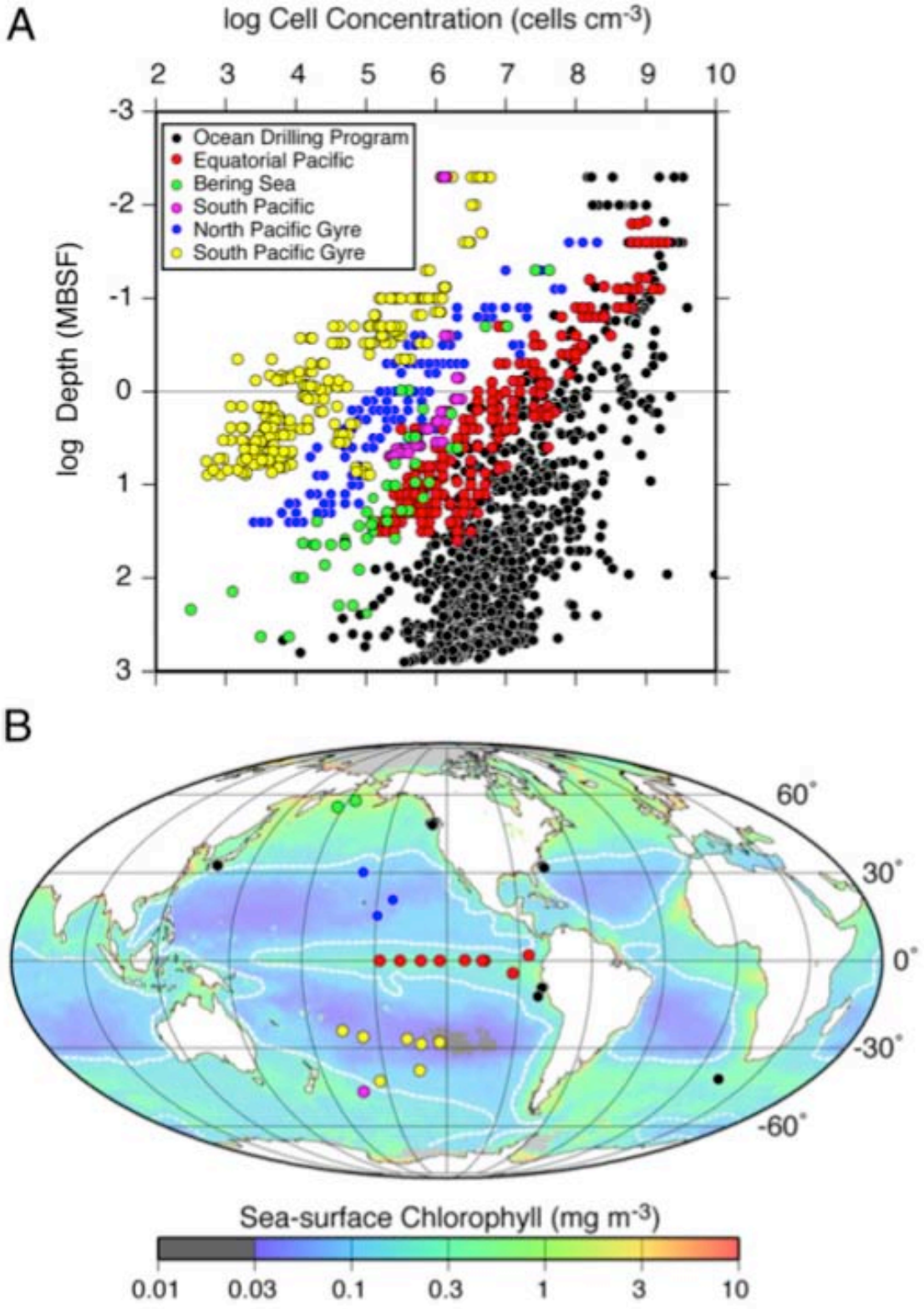

Figure 2.1: *Subseafloor sedimentary cell counts used for this study. (A) Counted cell concentration vs. depth (mbsf) for the sites used in this study. (B) Site locations overlain on a map of time-averaged sea surface chlorophyll-a (Takai et al., 2008).*

between concentration of intact phospholipids (a proxy for microbial biomass) and total organic carbon content in subseafloor sediment shows a clear relationship between subseafloor microbial biomass and buried organic matter (Lipp et al., 2008), indicating that the availability of electron donors, with organic matter being the quantitatively most important one, strongly controls microbial activity and abundance.

Factors that affect organic burial rate include the productivity of the overlying ocean, water depth, the flux of organic matter from land, and sedimentation rate (Berger and Wefer, 1990; Jahnke, 1996). Some of these parameters influence organic burial rate directly (mean sedimentation rate), whereas others influence it indirectly, by influencing organic flux to the seafloor (water depth), marine productivity (sea-surface chlorophyll, sea-surface temperature,

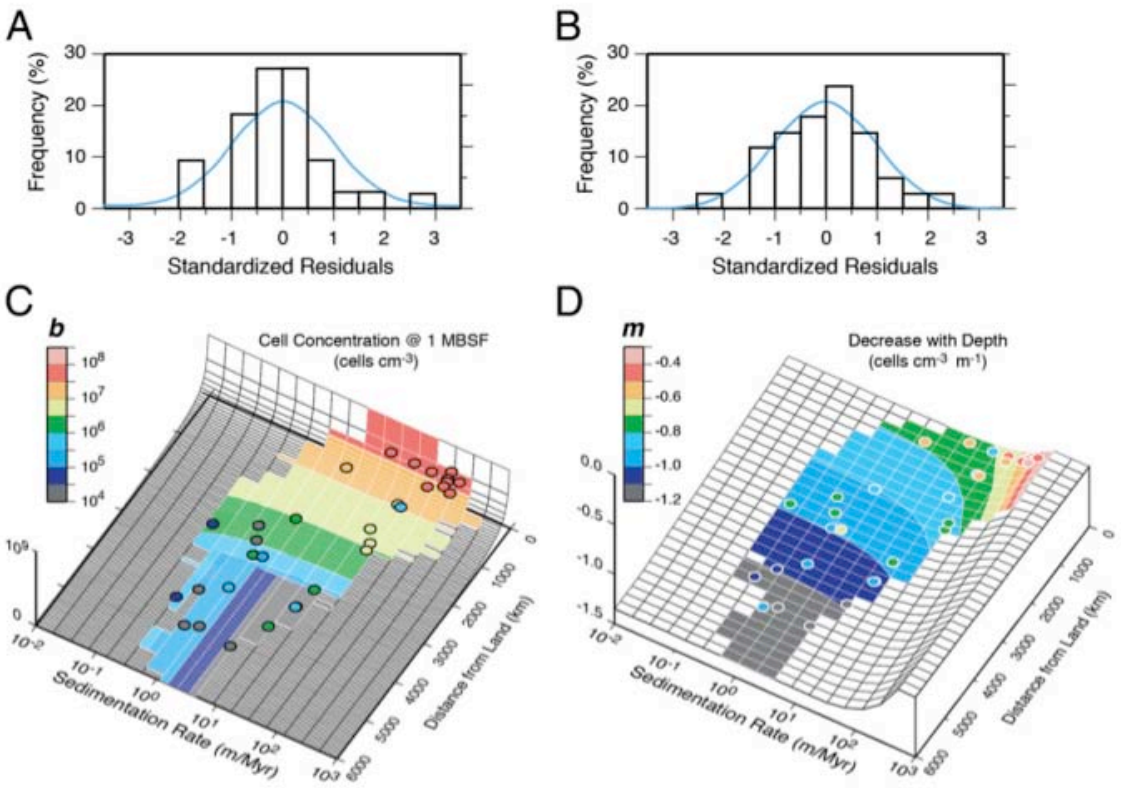

Figure 2.2: *Distributions of cell abundance at 1 mbsf (b) and the power-law rate of decrease of cell abundance with depth (m) relative to sedimentation rate and distance from land. (A) Distribution of residuals for b. (B) Distribution of residuals for m. The histograms show the distributions of the actual residuals. The blue lines are the probability density functions for normal distributions with the appropriate SDs. (C) Distribution of b vs. sedimentation rate and distance from land. (D) Distribution of m vs. sedimentation rate and distance from land. Colored fields in C and D mark the actual range of combinations of sedimentation rate and distance from land in the world ocean. Note that data used for this model (shown as dots in C and D) occur throughout this range of actual combinations. Dot colors indicate actual values of b and m for each site.*

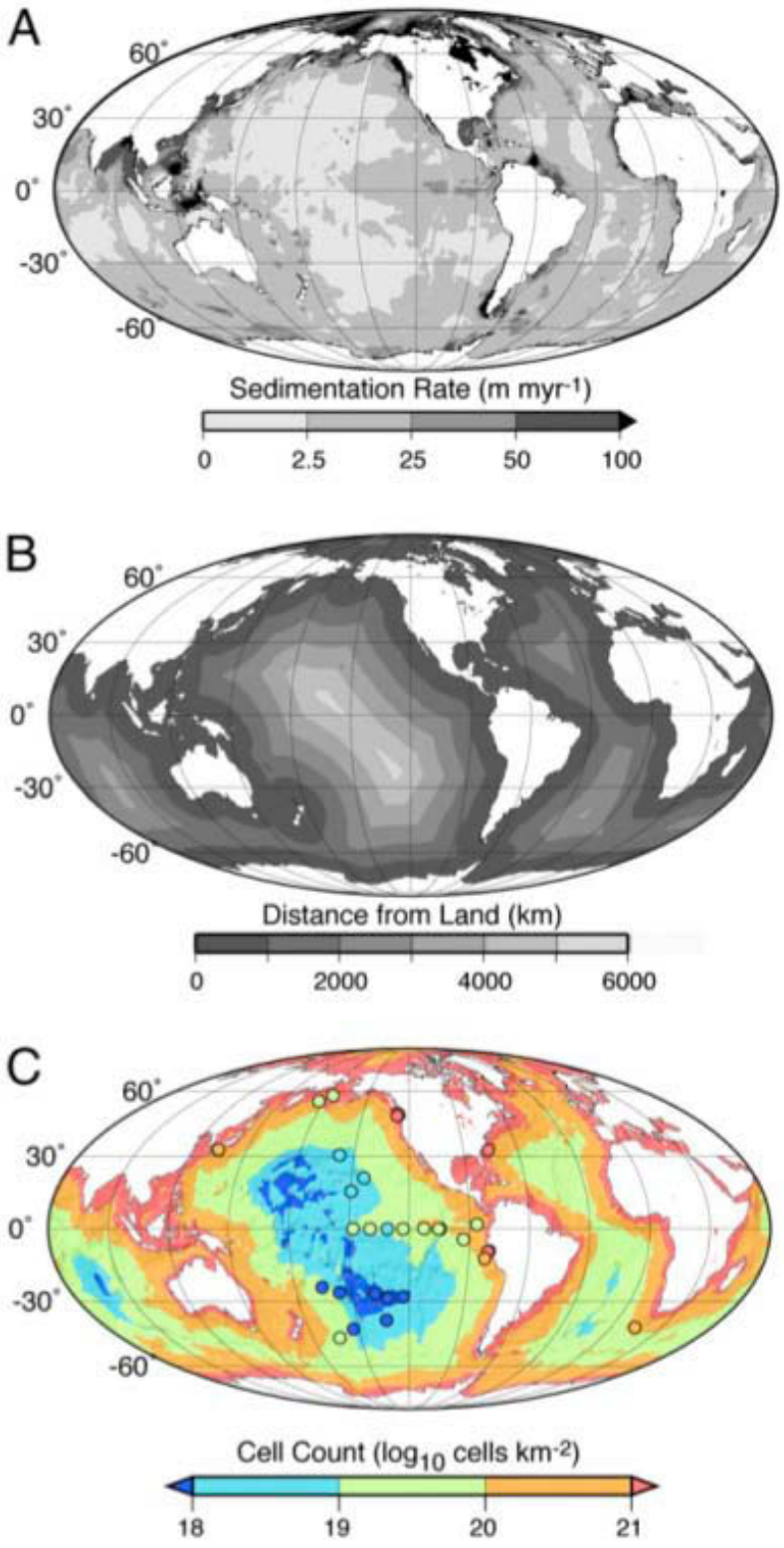

Figure 2.3: *Global distribution of subseafloor sedimentary cell abundance. (A) Geographic distribution of sedimentation rate (Laske and Masters, 1997). (B) Geographic distribution of distance from shore (Wessel and Smith, 1998). (C) Geographic distribution of integrated number of cells (derived from b, m, and sediment thickness). Dot colors indicate numbers of cells calculated for actual sites (*$\log_{10}$ *cells* km^{-2}*).*

and gross primary production), or flux of organic matter from land. Organic burial rates have been estimated from many of these properties for most of the world ocean (Jahnke, 1996; Seiter et al., 2005). Other potential electron donors include reduced metal [e.g., Fe(II), Mn(II)] and H_2 from water radiolysis. However, in the anoxic sediment that constitutes the vast majority of sediment in near-shore regions and open-ocean upwelling systems, sulfate is the predominant external electron acceptor (D'Hondt et al., 2002); consequently, thermodynamic considerations preclude use of reduced metal as a predominant electron donor (D'Hondt et al., 2004). H_2 from water radiolysis appears likely to be a significant electron donor only in sediment that contains extremely little organic matter, such as the sediment of midocean gyres (Blair et al., 2007; D'Hondt et al., 2009).

To build a global map of subseafloor sedimentary cell abundance, we used global maps of mean sedimentation rate and distance from land (Fig. 2.3 A and B) to create global maps of the distributions of b and m (Supporting Information). These distributions of b and m were then combined with global distributions of marine sediment thickness (Divins, 2008) to integrate cell abundance over the entire sediment column in each 1° by 1° grid of the world ocean (Fig. 2.3C). The maximum sediment thickness used in this calculation for any grid was 4,000 m; this depth is the approximate average depth of the 122°C isotherm, the upper temperature limit for presently known microbial life (Takai et al., 2008), assuming an average geothermal gradient of ∼30°C km^{-1}. If the known temperature limit to life rises, this maximum depth will have little effect on global maps of subseafloor cell distributions, because 97% (by volume) of marine sediment is shallower than 4,000 mbsf.

Because cell concentration varies by as much as four orders of magnitude at any given depth and sediment thickness varies by two to three orders of magnitude throughout the ocean, total cell number integrated over the entire sedimentary column varies by ca. five orders of magnitude between sites (Fig. 2.3C). Depth-integrated cell abundance is highest at continental margins and lowest in midocean gyres.

Integrating over the world's ocean area, we estimate the total number of cells in subseafloor sediment to be 2.9×10^{29} cells. A bootstrap exercise to check our analytical solution yielded a median value of 3.3×10^{29} cells, with the first standard deviations (SDs) at 1.2×10^{29} and 8.0×10^{29} cells (see Supporting Information for details).

The geographic distribution of subseafloor sedimentary cells varies greatly from continental margins to the open ocean. Although the world's ocean shelves (water depth <150 m) cover only ∼7% of the total oceanic area, they harbor 33% of the total cells in subseafloor sediment.

In comparison, the oligotrophic (<0.14 mg m^{-3} of chlorophyll-a) oceanic gyres cover about 42% of the world ocean and contain 10% of the total cells.

Discussion

Our estimate of total cell abundance in subseafloor sediment (2.9×10^{29}) is 92% lower than the previous standard estimate (35.5×10^{29}) (Whitman et al., 1998)(9). It is also ∼70% lower than other estimates of around 10×10^{29} (Lipp et al., 2008; Parkes et al., 2000). The reasons for this difference are twofold. First, our database is more geographically diverse than those of the previous studies. In particular, our database includes gyre areas with extremely low cell abundances. Second, like the most recent study (Lipp et al., 2008) but unlike the previous studies (Parkes et al., 2000; Whitman et al., 1998), we used estimates of actual sediment thickness throughout the world ocean derived from geophysical data (Divins, 2008; Laske and Masters, 1997).

Comparison of our subseafloor sedimentary estimate to previous estimates of microbial abundance in other environments should be treated with caution because uncertainties on the estimates for other environments are either not quantified or extremely large. This said, our results suggest that the number of subsurface prokaryotes may roughly approximate the total number of prokaryotes in surface environments. Our estimate of total microbial abundance in subseafloor sediment (2.9×10^{29}) is roughly equal to the estimates of Whitman et al. (1998) for the total number of prokaryotes in seawater (1.2×10^{29}) and in soil (2.6×10^{29}). It also approximates their lower bound estimate for total microbial abundance in the terrestrial subsurface (2.5×10^{29}; their upper bound is 25×10^{29}).

Our more recent estimate of subseafloor sedimentary cell abundance significantly decreases the estimate of Earth's total prokaryote population. Combining our subseafloor sedimentary estimate with the estimates of Whitman et al. (1998) for prokaryote numbers in seawater, soil, and the terrestrial subsurface decreases the estimated number of Earth's total number of prokaryotes by 50–78% (from 41.8–64.3×10^{29} cells to 9.2–31.7×10^{29} cells).

Conversion of total cell abundance to total microbial biomass requires an estimate of carbon content per cell, which, in turn, depends on cell volume and the amount of carbon per cell. Microbial cell volume varies by many orders of magnitude (Schulz and Jorgensen, 2001); however, as a general rule, cells react to nutrient limitation by size reduction (Velimirov, 2001). Organic matter becomes increasingly recalcitrant with depth (Jørgensen, 1982b); therefore,

microbial cells in deep subseafloor environments have to adapt to low availability of organic electron donors and organic nutrients. It is thus reasonable to assume that cells will be rather on the small side of the size spectrum, which has profound implications when converting cellular abundance into biomass.

The absolute lower limit for cell size is determined by the minimum amount of macromolecules (e.g., DNA, RNA, ribosomes, proteins) necessary to maintain functionality. Based on the molecular size of a minimum set of these macromolecules (Himmelreich et al., 1996), the calculated minimum cellular volume would be in the range of 0.014–0.06 μm^3; for a spherical cell, this would translate into a diameter of 0.3–0.5 µm. As a general trend, cells with diameters and volumes below 0.2 µm and 0.05 μm^3, respectively, are predominantly rod-shaped (Velimirov, 2001) because of a higher surface-to-volume ratio compared with spherical cells. Because there is a minimum set of macromolecules that any cell needs for functioning and survival, small cells tend to have a higher C content per cell volume than larger cells (Romanova and Sazhin, 2010).

There are no previously published studies of actual cell size distributions in deep subseafloor sediment. Preliminary flow cytometry studies on subseafloor samples and our own observations suggest cell widths and lengths in the range of 0.25–0.7 µm and 0.2–2.1 µm, respectively (see Supporting Information for details). Other studies assumed average spherical cell diameters of 0.5 µm (Lipp et al., 2008) or volumes of 0.21 μm^3 (Parkes et al., 1994) for calculating subseafloor biomass. Assuming that the majority of subseafloor cells have a diameter of 0.25–0.7 µm and cell shapes vary between spherical and short rods, cell volumes range from 0.008 to 0.718 μm^3, with an average of 0.042 μm^3. Using an allometric model (Simon and Azam, 1989) that acknowledges the higher C content of smaller cells (Romanova and Sazhin, 2010), the carbon content per cell would be ∼14 fg C $cell^{-1}$ with minimum and maximum estimates of 5 and 75 fg C $cell^{-1}$, respectively, which is rather to the low end of previously used values: 18 fg C $cell^{-1}$ (Lipp et al., 2008), 65.1 fg C $cell^{-1}$ (Parkes et al., 1994), and 86 fg C $cell^{-1}$ (Whitman et al., 1998).

Based on our estimates of total subseafloor sedimentary cell abundance and cellular carbon content, our calculation of subseafloor microbial biomass amounts to 4.1 petagram (Pg), with minimum and maximum estimates of 1.5–22 Pg C, respectively. This estimate is significantly lower than the previous estimate of 303 Pg C of Whitman et al. (1998) and somewhat lower than the estimates of 90 Pg of Lipp et al. (2008) and 60 Pg of Parkes et al. (1994).

This result significantly decreases the estimate of Earth's total living biomass. Using

published estimates (Whitman et al., 1998) for the total carbon content of plants and non-subseafloor prokaryotes, Earth's total (plant + prokaryote) biomass is reduced from 915 to 1,108 Pg C down to 614 to 827 Pg C (average = 713 Pg C). Subseafloor sedimentary biomass comprises only 0.18–3.6% (average = 0.6%) of the total.

Acknowledgements

The authors thank the crews and shipboard scientific parties of our RV Roger Revelle cruise to the South Pacific Gyre (Knox-02RR) and our RV Knorr cruise (195-III) to the equatorial Pacific Ocean and North Pacific Gyre. We also thank the co-chiefs, science party, and crew of Integrated Ocean Drilling Program Expedition 323 to the Bering Sea, especially Emily A. Walsh, Heather Schrum, Nils Risgaard-Petersen, and Laura Wehrmann, for taking cell count samples. We thank Jeremy Collie for advice regarding data analysis. J.K. and R.R.A. are supported through the Forschungsverbund GeoEnergie by the German Federal Ministry of Education and Research. Expeditions Knox02-RR and Knorr 195-III were funded, respectively, by the Ocean Drilling Program and Biological Oceanography Program of the US National Science Foundation (Grants OCE-0527167 and OCE-0752336). R.P., D.C.S., and S.D. were funded by National Science Foundation Grants OCE-0527167, OCE-0752336, and OCE-0939564. This is contribution 136 of the Center for Dark Energy Biosphere Investigations.

Supporting Information

Cell Counts

For each cell enumeration (D'Hondt et al., 2009; Kallmeyer et al., 2009), we took 2-cm^3 samples from the center of a freshly cut core end using a sterile cutoff 3-cm^3 syringe. We carried out cell counts according to the method of Kallmeyer et al. (2008). We extruded the 2-cm^3 sediment plug into a sterile 15-mL centrifuge tube containing 8 mL of 2.5% (wt/vol) NaCl solution with 2% (vol/vol) formalin as a fixative and then thoroughly shook the tube to form a homogenous suspension. In cases where cell densities were high enough ($>10^5$ cells cm^{-3}), we made direct cell counts by staining this slurry with SYBR Green I, placing a small aliquot of the slurry directly on a 0.2-µm pore size filter and enumerating manually under a fluorescence microscope (Noble and Fuhrman, 1998). Counts obtained with SYBR Green I have been found to be indistinguishable from acridine orange direct counts (AODCs) (Morono et al., 2009). All Ocean Drilling Program cell counts were AODCs (Parkes et al., 2000). Also, studies on aquatic cells show no difference between counts with SYBR Green I and SYBR Gold (Shibata et al., 2006).

Independent of the stain used, direct counting has a minimum detection limit (MDL) around 10^5 cells cm^{-3} (Kallmeyer, 2011). For samples with lower cell abundances, we found it necessary to detach and separate the cells from the mineral matrix using a cell extraction protocol (Kallmeyer et al., 2008). Most counts at the South and North Pacific Gyre sites were of extracted cells because gyre cell abundances drop below the direct count MDL within decimeters to meters below the seafloor; for the same reason, a few counts of the deepest equatorial Pacific sediment were also of cell extracts. Because total counts using the cell extraction technique include cells from volumes of sediment that are 100- to 500-fold larger than can be used for direct counts, the MDL decreases to 10^3 cells cm^{-3} for samples processed using cell extraction. We quantified the efficiency of cell extraction by performing direct cell counts without extraction on a few samples from the upper few meters of sediment at each gyre site. Fig. 2.4 gives an example of the difference between extracted (blue) and nonextracted (red) cell counts. In many cases, they fall within 1 SD of each other. We used the extraction method only when cell abundances were too low to be counted by direct counting (fewer than $\sim 10^5$ cells cm^{-3}). The error introduced to our global biomass estimate by loss of cells due to cell separation is small, because the sites for which cell separation was used (mainly the ocean gyres) only account for a small fraction of the total counts. Also, due to the higher number

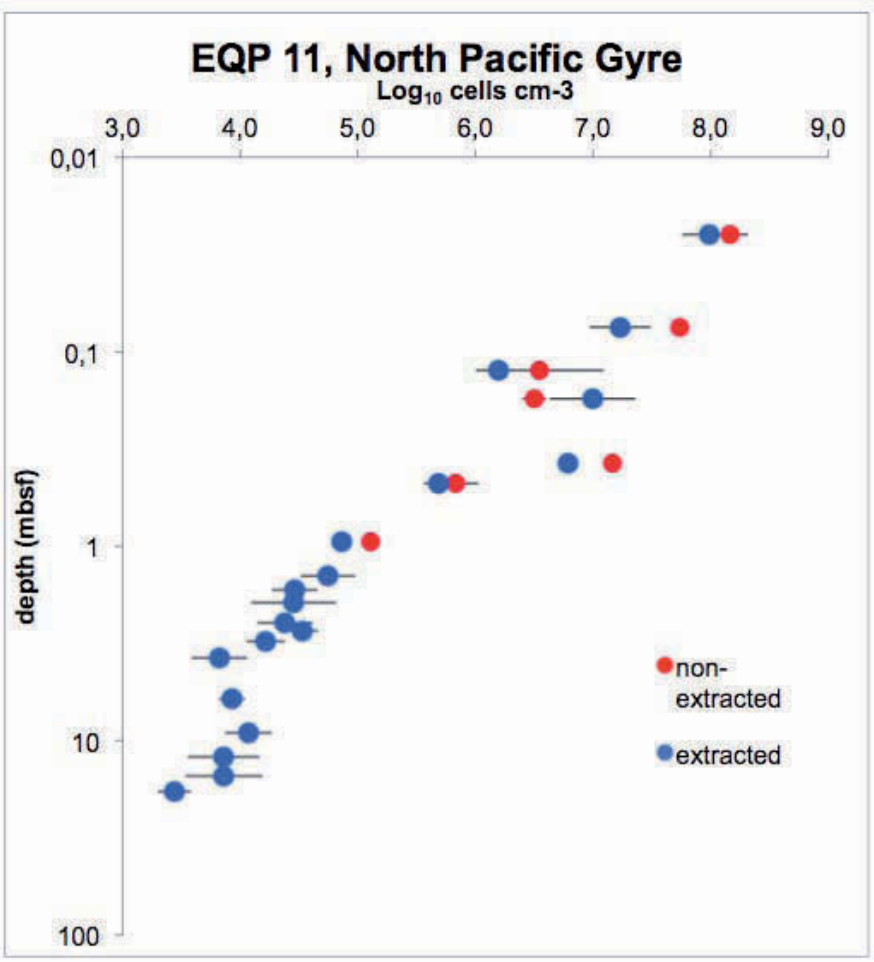

Figure 2.4: *Comparison of cell counts done on cell extracts (blue dots) and direct counts without extraction (red dots). The error bars are 1 SD. Because the minimum detection limit for direct counting is around 10^5 cells cm^{-3}, the comparison could only be carried out in the upper part of the core.*

of cells counted, the results from the cell extraction are much more tightly constrained than direct counts from the same sample.

For our nonseparated direct counts, we used the same procedure to account for cells covered by sediment particles that was used for all Ocean Drilling Program (ODP) direct counts (Cragg et al., 1990). There are more elaborate techniques to account for covered cells (reviewed in Fry, 1998), but to keep our data fully comparable with previous ODP data, we decided to use the same technique.

Consideration of Cell Sizes for Calculation of Microbial Biomass

To the extent that cells in subseafloor sediment tend to be on the small end of the size spectrum, there is a theoretical chance for cells to pass through the filter. The minimum number of macromolecules (e.g., DNA, RNA, ribosomes, proteins) necessary to maintain functionality

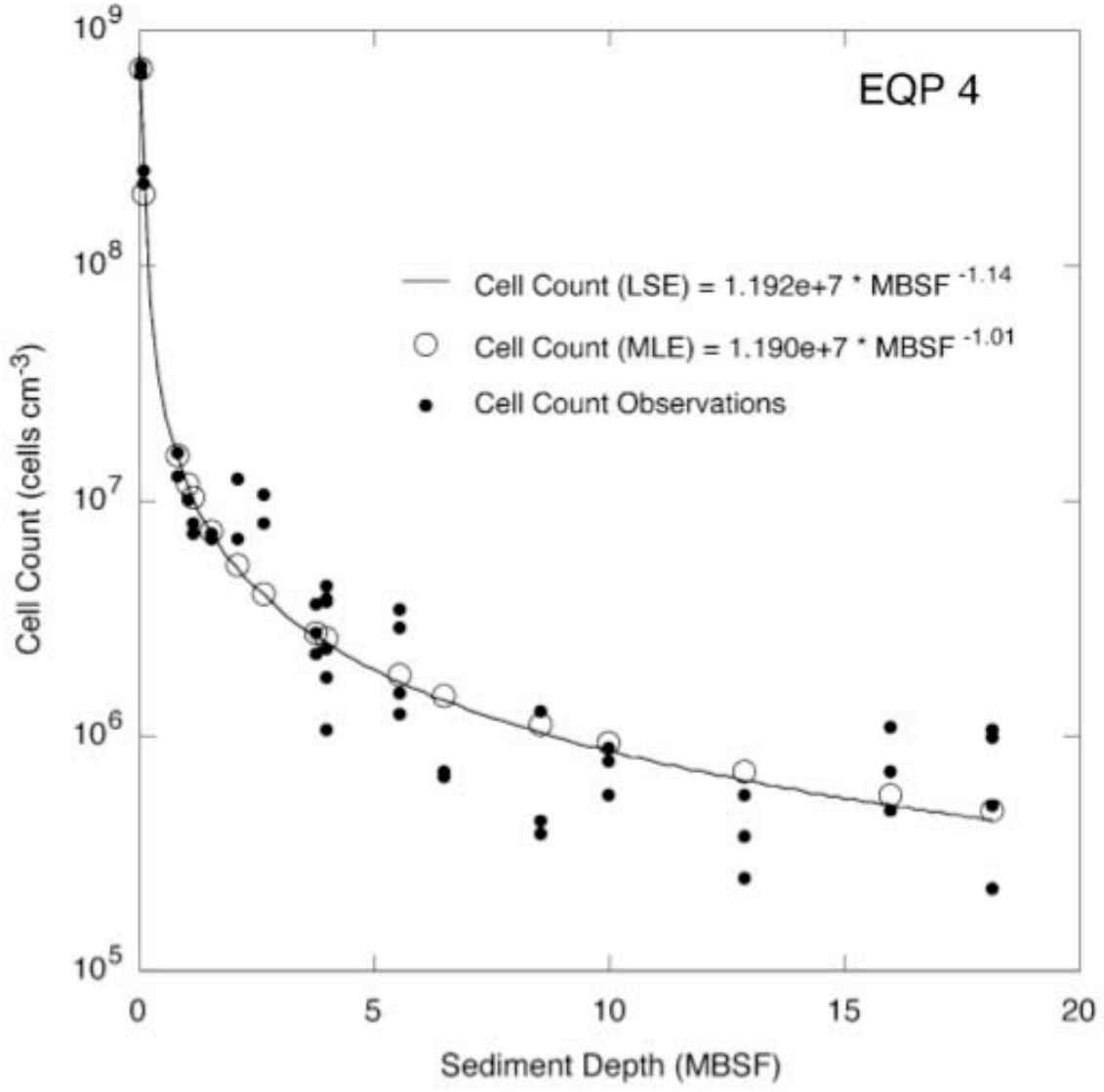

Figure 2.5: *Example of depth vs. cell concentration plot for a single site (EQP-4). Depth is plotted on the x axis, and cell abundance is plotted on the y axis. Actual cell counts are shown as filled circles. The conventional least-squares error best-fit power law function (R^2=0.93) is shown as a solid line. The corresponding estimates of cell abundance calculated with the maximum likelihood estimator method that minimizes the mean-square error are shown as open circles. Cell counts are plotted on a logarithmic scale for visual clarity; the calculations were performed on non transformed data.*

(Himmelreich et al., 1996) results in a calculated minimum cellular volume in the range of 0.06–0.6 µm^3, translating into a diameter of 0.48–1µm when assuming a spherical cell. The spirochetes contain some extremely thin filamentous species with cell diameters of about 0.1–0.15 µm but they reach at least 5–6 µm in length (Staley, 1999). As a general trend, cells with diameters and volumes below 0.2 µm and 0.05 µm^3, respectively, are predominantly rod-shaped (Velimirov, 2001) because of a higher surface-to-volume ratio relative to spherical cells. Studies of viral abundance in seawater and marine sediment show that there is a distinct

size gap between viruses and microbial cells rather than a continuous size spectrum (e.g., Noble and Fuhrman, 1998). This indicates that there is a certain minimum size for cells to remain functional. The biogenic origin of even smaller (few 10s of nanometers in diameter) microbe-like structures (e.g., McKay et al., 1996) has so far not been confirmed.

Only up to 20% of the cells in a sediment sample are motile; the remaining cells are attached to sediment particles of various sizes (Fenchel, 2008). For cell counts performed on sediment slurries, it is rather unlikely that all motile cells are smaller than 0.2 µm; therefore, only a small fraction of the total population has the potential to pass through the filter due to their small size. Assuming the minimum width of a cell to be 0.1 µm and 0.18 µm for filamentous and spherical cells, respectively, it appears unlikely that a major fraction of the attached cells would attach themselves to particles that are small enough for the cells to remain small enough to pass through the filter despite being still attached.

For cell counts performed on cell extracts, where the cells were first detached from the particles and then separated by density centrifugation, all cells are freely floating in solution, and should therefore be treated as "motile" Although there is some loss of cells due to the separation procedure (Shibata et al., 2006), this loss is unlikely to be due to cells becoming smaller than 0.2 µm due to loss of attached sediment particles because the separation-related cell loss does not increase with sediment depth, as would be expected if cells become smaller with depth due to nutrient limitation. In fact, Schippers et al. (2005) reported the opposite, with cell numbers obtained from counts on separated and nonseparated samples converging with increasing sediment depth and lower cell abundances.

Track-etched polycarbonate filters, which have been used for the vast majority of cell counts, may have some larger pores caused by fusion of multiple smaller ones (Stockner et al., 1990). Since the introduction of aluminum oxide membranes with a much more even distribution of pore sizes (Weinbauer et al., 1998), there have not been any reports of counting differences caused by the use of different filters.

Given the above information, it seems unlikely that a significant fraction of the total population passes uncounted through the filter, although it is impossible to rule out the possibility that some extremely small cells pass the filter. Considering the facts that (i) cell counts vary with depth over several orders of magnitude and (ii) accuracy for many counts is on the order of half an order of magnitude, this relatively small potential error can be neglected.

In addition to our own cell count data (D'Hondt et al., 2009; Kallmeyer et al., 2009), we compiled literature data of subseafloor sedimentary cell counts. In cases where data were only available as graphs, they were digitized using the program Graph digitizer V1.6 (freeware). We used only data from publications in which cell abundances were determined by counting of the cells with fluorescent stains, usually acridine orange (AO), DAPI, or SYBR Green I. To ensure data consistency, we did not include cell abundances estimated using other methods, such as most probable number counts or phospholipid concentrations. The site locations and sources of the data are listed in Table 2.2.

Cell Count Trends

We identified trends in cell count variability by plotting cell abundance (cells per cubic centimeter) as a function of sediment depth (mbsf). These calculations were performed on nontransformed data. A best-fit power-law curve was generated with a maximum likelihood estimator method by minimizing the mean-squared error between estimated and actual and best-fit values (Fig. 2.5). The best-fit estimate of cell abundance at 1 mbsf is identified as b, and the power-law rate of decrease of cell abundance with depth is identified as m. For easier graphical representation of the data, cell counts are plotted on a logarithmic scale.

Correlation with Global Environmental Parameters

We identified several environmental parameters (Table 2.3) as possible factors that could explain geographic trends of high and low cell abundances. Because one of our ultimate goals is to understand the global distribution of subseafloor sedimentary cell abundance, we focused on environmental parameters with global extent and continuous grid-scale geographic resolution of at least 0.67° by 0.67°. We used linear regressions and principal component analyses to identify the environmental parameter(s) that most closely correlate with cell counts.

Our regression analysis began with obtaining appropriate values for each environmental parameter at each cell count location. We obtained values of some parameters (e.g., water depth) at ODP sites from ODP initial reports (Davis et al., 1992, 1997; D'Hondt et al., 2003; Flood et al., 1995; Gersonde et al., 1999; Moore et al., 2001; Paull et al., 1996; Phillips et al., 1987; Taylor et al., 1999; Westbrook et al., 1994) or from our own shipboard data. For most variables, however, we estimated the parameters using available grids (Table 2.3) and the "grdtrack" function from the Generic Mapping Tools (GMT) software package (Müller et al.,

2008). An initial principal component analysis with these parameters indicated that two to three components are required to explain the total variance in b and m.

We conducted both single- and multicomponent linear regressions. The results of single-component linear regressions indicated that distance from land and sedimentation rate are the primary components required to explain b and m. Our analysis also indicated that size of the landmass used to calculate distance from land is an important variable. By using an order-of-magnitude approach, we identified the best correlation when considering only landmasses with a surface area >105 km^2 (i.e., Iceland). The single-component linear regression correlation coefficients for b are 0.72 for sedimentation rate and 0.58 for distance from land. The comparable correlation coefficients for m are 0.42 for sedimentation rate and 0.56 for distance from land.

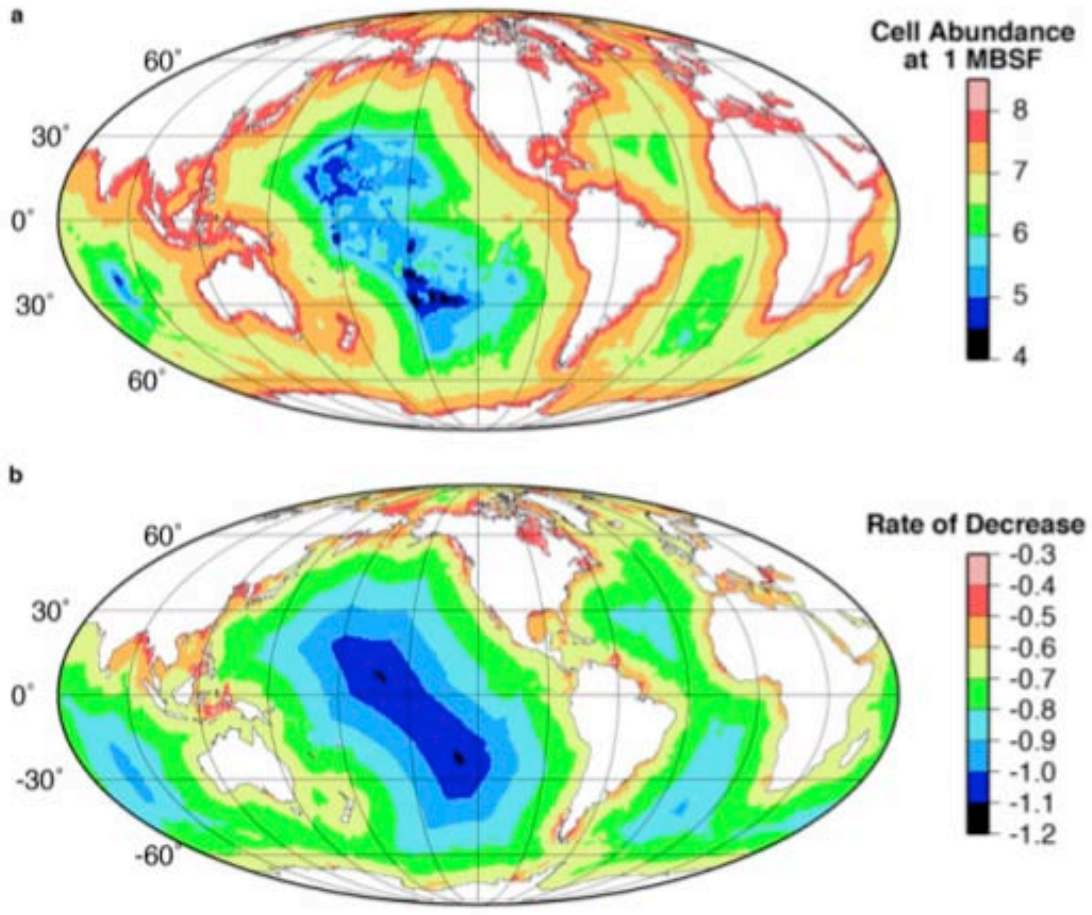

Figure 2.6: *(a) Global plots of cell count in* $\log_{10}$ *cells* cm^{-3} *at a depth of 1 m (b) and (b) power-law rate of decrease of cell count with sediment depth (m).*

The multicomponent linear regressions with a critical P value of 0.05 also identified distance from land and log of the sedimentation rate as the two most significant environmental parameters for b ($r^2 = 0.85$) and m ($r^2 = 0.62$). The corresponding equations for the best-fit surfaces are shown in Eqs. 2.1 and 2.2:

$$b = -7.44 \times 10^6 + 2.24 \times 10^5 \cdot R + 9.41 \times 10^8 \cdot D^{1/\epsilon} \quad (2.1)$$

$$m = -0.65 + 0.002 \cdot R - 8.75 \times 10^{-5} \cdot D \quad (2.2)$$

R is sedimentation rate in Myr^{-1}, D is distance from land in kilometers, and ϵ is the exponent (e.g., -1.651) of the best-fit curve used to transform distance from shore exponentially.

We calculated a variance inflation factor of 2.14 for the distance from land and sedimentation rate parameters used in our study. This value is well below conservative critical values (e.g., 2.5), indicating that our correlations are not exaggerated due to the collinearity of these parameters.

Calculation of Global Distribution

We generated global maps of cell count at a depth of 1 m (b) and rate of decrease of cell count with sediment depth (m) (Fig. 2.5 using Eqs. 2.1 and 2.2 in conjunction with global grids of distance from land and sedimentation rate Fig. 2.3). We created the global distance from land grid with the World Vector Shoreline database available as part of the GMT software package (Müller et al., 2008). For landmasses larger than 105 km^2, we calculated the great circle closest distance to land for any location in the ocean with a resolution of 0.5° by 0.5°. We created the global sedimentation rate map by merging sediment thickness grids (Divins, 2008; Laske and Masters, 1997) and dividing by the basement age grid (Müller et al., 2008).

Depth-Integrated Cell Counts

We quantified distributions of subseafloor sedimentary cell abundance (Fig. 2.3) by using the global maps of b and m (Fig. 2.6) and integrating the cell abundance as a function of sediment thickness.

Eq. 2.3 describes the exponential relationship between depth below seafloor (X, in meters) and cell count (Y, in cells per cubic centimeter):

$$Y = bX^m \tag{2.3}$$

To determine the number of cells in a given sediment column (surface area in square centimeters) with a thickness Z (in meters), it is necessary to find the integral of Eq. 2.3 and integrate from Z_1 to Z_2, where $Z_1 < Z_2$:

$$Y = \int_{Z_1}^{Z_2} bX^m \tag{2.4}$$

The result is a simple integral for m $\neq$ -1, but it must rewritten as a natural log

for m = -1

$$Y = \frac{b}{m+1}(Z_2^{m+1} - Z_1^{m+1}) \quad \text{for m} \neq \text{-1} \tag{2.5}$$

$$Y = b[\ln(Z_2) - \ln(Z_1)] \quad \text{for m} = 1 \tag{2.6}$$

where Z_1 and Z_2 are sediment depth in meters.

Ideally, Z_1 would be 0 mbsf (i.e., seafloor surface). However, when m is in the range of -0.9 to -1.1, the resulting integrations yield anomalous results because of the asymptotic nature of the slopes at depths less than 0.1 mbsf. Also, the upper 0.1 mbsf of sediment is usually mixed by bioturbation and has rather uniform properties. Therefore, our preferred value of Z_1 is 0.1 mbsf. This minimum depth limit of 0.1 mbsf allows for direct comparison with previous estimates of subseafloor cell abundance and biomass (Lipp et al., 2008; Whitman et al., 1998).

For Z_2, we used the sediment thickness grid created by merging the two databases (Divins, 2008; Laske and Masters, 1997). We limited cell abundance calculations to a maximum sediment thickness of 4,000 m, which is the predicted mean subseafloor depth of the 122°C isotherm and temperature limit for microbial life (Takai et al., 2008), assuming a geothermal gradient of 30°C km^{-1}. The regions for which sediment thickness data are not available are

primarily coastal regions; consequently, we assumed a sediment thickness of 4,000 m for regions that lack sediment thickness data because sediment tends to be thick along coasts.

Global Compilation

This global map of subseafloor cell abundance covers 99% of the total ocean surface area, with only 1% not determined due to grid resolution (grids that included both land and sea were not included in the map). Because this remaining 1% was located adjacent to land, we estimated its cell inventory by assuming (i) sediment and sedimentary cells occur to 4,000 mbsf and (ii) b and m values characteristic of near-shore environments. Because near-shore sediment is not always 4,000 m or more in thickness, the result may be a high estimate of cell abundance for these coastal grids.

We quantified total subseafloor sedimentary cell abundance by spatially integrating (summing) all the cell abundance estimates from the entire ocean surface area with the "grdvolume" function available with the GMT software package (Wessel and Smith, 1998). Because cell counts of extracted cells may be slightly lower than direct counts, we assessed the sensitivity of our total abundance estimate by making the extreme assumption that actual cell abundances at our gyre sites are an order of magnitude higher than our gyre cell counts (including both extracted counts and direct counts); gyre cell abundances are so low that this assumption changes the estimate of global cell abundance only slightly, from 2.9×10^{29} cells to 3.2×10^{29} cells.

We quantified the upper and lower bounds of our total abundance estimate (2.9×10^{29}) with a bootstrap method, which randomly sampled the probability density functions derived from the best-fit residuals (Fig. 2.2). We added the sampled residual values to the respective slope and intercept grids and calculated cell abundance with the same procedure as that described above. This process was repeated 1,000 times, and the resulting cell counts were used to determine various quantiles: 5%, 16%, 50%, 84%, and 95%. These quantiles effectively represent the median (50%), the upper and lower bounds of the first SD (16% and 84%), and the upper and lower bounds of second SD (5% and 95%).

Biomass Estimates

A wide range of factors for converting cell volume to cellular carbon content has been published (reviewed in Bölter et al., 2002). Published conversion factors vary ca. 100-fold (14–1,610 fg C μm^3); however, these factors are based on both pure cultures and environmental samples

from a wide variety of environments, and these studies report a 600-fold range of cell volumes (0.026–15.8 μm^3) from environment to environment. The relatively weak relationship between cell volume and carbon content also becomes obvious in a plot of ln(fg C $cell^{-1}$) vs. ln(V[μm^3]), which exhibits a correlation coefficient (r^2) of only 0.533 (Romanova and Sazhin, 2010). The relationship between cell volume and carbon content is known to be affected by the individual cell growth condition, fixation, and staining method, as well as by the technique used to determine carbon content. Because there is a minimum set of macromolecules that any cell needs for functioning and survival, small cells tend to have a higher C content than larger cells (Romanova and Sazhin, 2010).

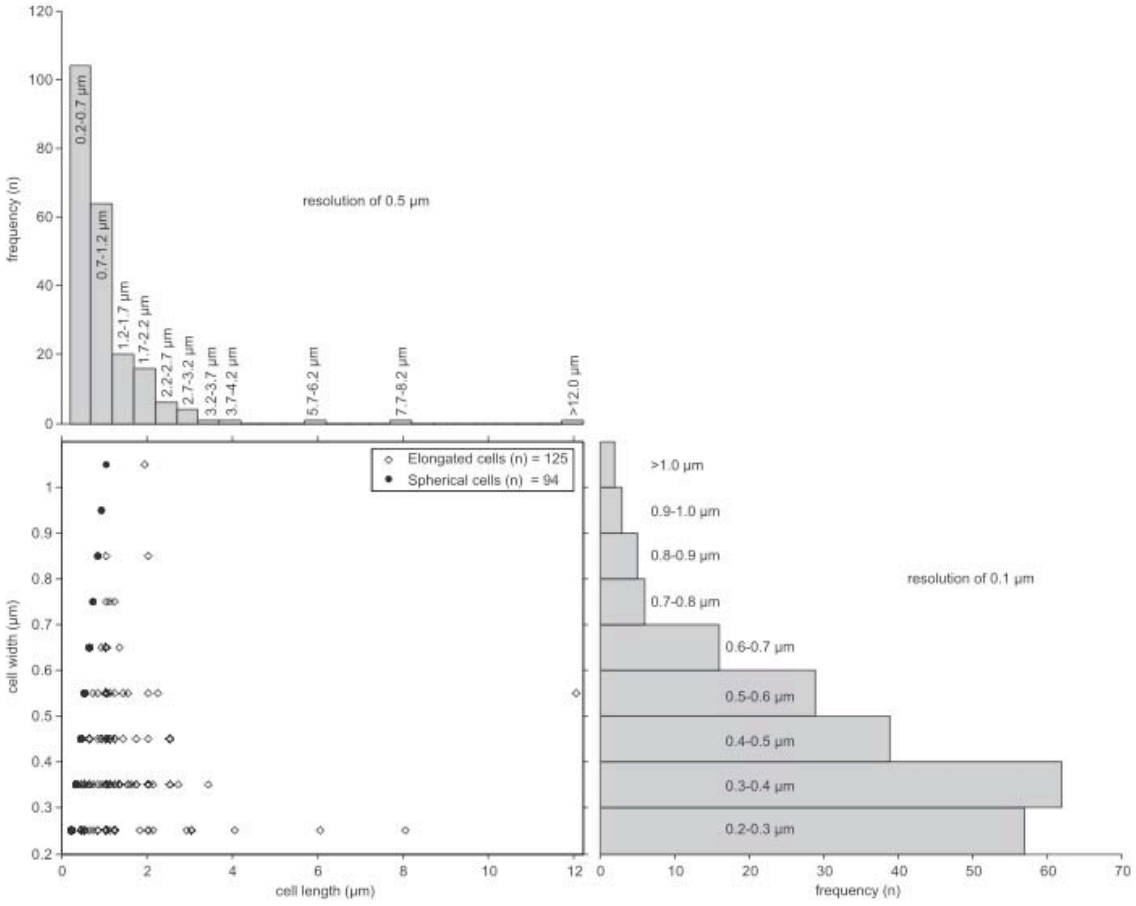

Figure 2.7: *Cell sizes in subseafloor sediment samples. Cell width and length indicate the shortest and longest dimensions of a cell, respectively.*

So far, there is no comprehensive study of the actual distribution of cell size in deep subseafloor sediment. Our cell size determinations of subseafloor samples suggest that about half of the cells are more or less spherical and the rest are mainly short rods with a length-to-width ratio between 2 and 3. About 95% of the measured cell sizes were in the range of

0.25–0.7 µm in width and 0.2–2.1 µm in length (Fig. 2.7). Other studies assumed an average spherical cell size of 0.5 µm (Lipp et al., 2008).

Our calculation of subseafloor biomass is based on the following assumptions:

i) Cell diameters range from 0.25 to 0.7 µm, and cell shapes are either spherical or slightly elongated, with a maximum length-to-width ratio of 3 (i.e., the largest cell would be a 0.7-µm- wide and 2.1-µm-long rod, and the smallest one would be a 0.25-µm-diameter sphere). The median cell would be a 0.3-µm- wide and 0.7-µm-long rod. Thus, cell volumes would range from 0.008 to 0.718 μm^3, with an average of 0.042 μm^3.

ii) Using an allometric model (Simon and Azam, 1989) that acknowledges the higher C content of smaller cells (Romanova and Sazhin, 2010), the carbon content per cell would range from 5 to 75 fg C $cell^{-1}$ with an average of 14 fg C $cell^{-1}$.

Using other published conversion factors derived from natural samples (Bölter et al., 2002), cellular carbon contents may be as low as 0.882 fg $cell^{-1}$ or as high as 517 fg $cell^{-1}$; still, they fall within less than an order of magnitude of our calculations.

Table 2.2: *List of all sites used for the calculation*

Site/hole	Latitude	Longitude	Location	Source
146/888	48°10'N	126°40'W	Cascadia Margin	Cragg et al., 1995[1]
146/889	48°42'N	126°52'W	Cascadia Margin	Cragg et al., 1995[1]
164/995	31°48'N	75°31'W	Blake Ridge	Wellsbury et al., 2000[2]
164/996	32°30'N	76°11'W	Blake Ridge	Wellsbury et al., 2000[2]
168/1,026	47°46'N	127°46'W	Juan de Fuca Ridge	Mather and Parkes, 2000[3]
177/1,088	41°8'S	13°34'E	Southern Ocean	Wellsbury et al., 2001[4]
190/1,176	32°35'N	134°40'E	Nankai Trough	Moore et al., 2001[5]
190/1,178	32°44'N	134°29'E	Nankai Trough	Moore et al., 2001[5]
201/1,227	8°59'S	79°57'W	Peru Margin	D'Hondt et al., 2003[5]
201/1,230	9°7'S	80°35'W	Peru Margin	D'Hondt et al., 2003[5]
201/1,231	12°1'S	81°54'W	Peru Margin	D'Hondt et al., 2003[5]
SPG1	23°51'S	165°38'W	South Pacific Gyre	D'Hondt et al., 2009[6]
SPG2	26°03'S	156°53'W	South Pacific Gyre	D'Hondt et al., 2009[6]
SPG4	26°29'S	137°56'W	South Pacific Gyre	D'Hondt et al., 2009[6]
SPG5	28°26'S	131°23'W	South Pacific Gyre	D'Hondt et al., 2009[6]
SPG6	27°55'S	123°09'W	South Pacific Gyre	D'Hondt et al., 2009[6]
SPG9	38°03'S	133°05'W	South Pacific Gyre	D'Hondt et al., 2009[6]
SPG10	39°18'S	139°48'W	South Pacific Gyre	D'Hondt et al., 2009[6]
SPG11	41°51'S	153°06'W	South Pacific Gyre	D'Hondt et al., 2009[6]
SPG12	45°57'S	163°11'W	South Pacific Gyre	D'Hondt et al., 2009[6]
EQP-01	1°48'N	86°11'W	Pacific Equatorial Upwelling	Kallmeyer et al., 2009[7]
EQP-02	4°14'S	92°57'W	Pacific Equatorial Upwelling	Kallmeyer et al., 2009[7]
EQP-03	0°2'S	105°25'W	Pacific Equatorial Upwelling	Kallmeyer et al., 2009[7]
EQP-03a	0°2'S	105°25'W	Pacific Equatorial Upwelling	Kallmeyer et al., 2009[7]
EQP-05	0°4'N	123°01'W	Pacific Equatorial Upwelling	Kallmeyer et al., 2009[7]
EQP-06	0°2'N	130°53'W	Pacific Equatorial Upwelling	Kallmeyer et al., 2009[7]
EQP-06a	0°4'N	130°46'W	Pacific Equatorial Upwelling	Kallmeyer et al., 2009[7]
EQP-08	0°0'N	147°47'W	Pacific Equatorial Upwelling	Kallmeyer et al., 2009[7]
EQP-09	15°7'N	149°29'W	North Pacific Gyre	Kallmeyer et al., 2009[7]
EQP-10	20°41'N	143°21'W	North Pacific Gyre	Kallmeyer et al., 2009[7]
EQP-11	30°21'N	157°52'W	North Pacific Gyre	Kallmeyer et al., 2009[7]
1342	54°50'N	176°55'W	Bering Sea	This study
1343	57°33'N	175°49'W	Bering Sea	This study

[1]Cragg BA, et al. (1995) The impact of fluid and gas venting on bacterial populations and processes in sediments from the Cascadia Margin Accretionary System (Sites 888–892) and the geochemical consequences. Proceedings of the Ocean Drilling Program–Scientific Results, eds Carson B, Westbrook GK, Musgrave RJ, Suess E (Ocean Drilling Program, College Station, TX), Vol 146, pp 399–413.

[2]Wellsbury P, Goodman K, Cragg BA, Parkes RJ (2000) The geomicrobiology of deep marine sediments from Blake Ridge containing methane hydrate (Sites 994, 995, and 997). Proceedings of the Ocean Drilling Program–Scientific Results, eds Paull CK, Matsumoto R, Wallace PJ, Dillon WP (Ocean Drilling Program, College Station, TX), Vol 164, pp 379–391.

[3]Mather I, Parkes RJ (2000) Bacterial profiles in sediments of the eastern flank of the Juan de Fuca Ridge, Sites 1026 and 1027. Proceedings of the Ocean Drilling Program–Scientific Results, eds Fisher AT, Davis EE, Escutia C (Ocean Drilling Program, College Station, TX), Vol 168, pp 161–165.

[4]Wellsbury P, Mather I, Parkes RJ (2001) Bacterial abundances and pore water acetate concentrations in sediments of the Southern Ocean (Sites 1088 and 1093). Proceedings of the Ocean Drilling Program–Scientific Results, eds Gersonde R, Hodell DA, Blum P (Ocean Drilling Program, College Station, TX), Vol 177.

[5]Moore GF, Taira A, Klaus A eds (2001) Proceedings of the Ocean Drilling Program–Initial Reports (Ocean Drilling Program, College Station, TX), Vol 190.

[6]D'Hondt S, et al. (2009) Subseafloor sedimentary life in the South Pacific Gyre. Proc Natl Acad Sci USA 106:11651–11656.

[7]Kallmeyer J, Pockalny RA, D'Hondt SL, Adhikari RR (2009) A new estimate of total microbial subseafloor biomass. Eos, Transactions, American Geophysical Union 90(52)(Suppl): B23C–0381 (abstr).

Table 2.3: *List of databases used for the parameters tested for correlation with cell abundance at 1 mbsf and rate of decrease of cell abundance with depth*

Parameter	Database
Chlorophyll-a	Multiyear (1998–2003) average from SeaWiFS[1]
Gross primary production	Multiyear (2002–2011) median from Eppley VGPM[2]
Sea-surface temperature	AVHRR Pathfinder SST data[3]
Basement age	Drill site information[4−13] or global basement age grids[14]
Mean sedimentation rate	Sedimentation thickness[15,16] divided by basement age[14]
Distance from land	DMA coastline for landmasses with surface area >105 km^2 [17]

AVHRR, advanced very high resolution radiometer; DMA, Defense Mapping Agency; SST, sea surface temperature; SeaWiFS, sea-viewing wide field of view sensor, VGPM, vertically generalized production model.

[1]Gregg WW, Casey NW, McClain CR (2005) Recent trends in global ocean chlorophyll. Geophys Res Lett, 10.1029/2004gl021808.

[2]Behrenfeld MJ, Falkowski PG (1997) Photosynthetic rates derived from satellite-based chlorophyll concentration. Limnol Oceanogr 42(1):1–20.

[3]Casey KS, Brandon TB, Cornillon P, Evans P (2010) The past, present and future of the AVHRR Pathfinder SST Program. Oceanography from Space: Revisited, eds Barale V, Gower JFR, Alberotanza L (Springer).

[4]Davis EE, Mottl MJ, Fisher AT eds (1992) Proceedings of the Ocean Drilling Program–Initial Reports (Ocean Drilling Program, College Station, TX), Vol 139.

[5]Westbrook GK, Carson B, Musgrave RJ eds (1994) Proceedings of the Ocean Drilling Program–Initial Reports (Pt 1) (Ocean Drilling Program, College Station, TX), Vol 146.

[6]Flood RD, Piper DJW, Klaus A eds (1995) Proceedings of the Ocean Drilling Program–Initial Reports (Ocean Drilling Program, College Station, TX), Vol 155.

[7]Paull CK, Matsumoto R, Wallace PJ eds (1996) Proceedings of the Ocean Drilling Program–Initial Reports (Ocean Drilling Program, College Station, TX), Vol 164.

[8]Davis EE, Fisher AT, Firth JV eds (1997) Proceedings of the Ocean Drilling Program–Initial Reports (Ocean Drilling Program, College Station, TX), Vol 168.

[9]Taylor B, Huchon P, Klaus A eds (1999) Proceedings of the Ocean Drilling Program–Initial Reports (Ocean Drilling Program, College Station, TX), Vol 180.

[10]Gersonde R, Hodell DA, Blum P eds (1999) Proceedings of the Ocean Drilling Program–Initial Reports (Ocean Drilling Program, College Station, TX), Vol 177.

[11]Phillips GN, Myers RE, Palmer JA (1987) Problems with the placer model for Witwatersrand gold. Geology 15:1027–1030.

[12]Moore GF, Taira A, Klaus A eds (2001) Proceedings of the Ocean Drilling Program–Initial Reports (Ocean Drilling Program, College Station, TX), Vol 190.

[13]D'Hondt SL, Jørgensen BB, Miller DJ eds (2003) Controls on Microbial Communities in Deeply Buried Sediments, Eastern Equatorial Pacific and Peru Margin Sites 1225-1231 (Ocean Drilling Program, College Station, TX), Vol 201, p 81.

[14]Müller RD, Sdrolias M, Gaina C, Roest WR (2008) Age, spreading rates, and spreading asymmetry of the world's ocean crust. Geochemistry Geophysics Geosystems 9(4), Q04006.

[15]Laske G, Masters G (1997) A global digital map of sediment thickness. Eos, Transactions, American Geophysical Union 78(46) (Suppl): S41E-1 (abstr).

[16]Divins DL (2008) NGDC Total Sediment Thickness of the World's Oceans and Marginal Seas (National Oceanic and Atmospheric Administration).

[17]Wessel P, Smith WHF (1998) New, improved version of the Generic Mapping Tools released. Eos, Transactions, American Geophysical Union 79:579.

3 Aerobic microbial respiration in 86-million-year-old deep-sea red clay

Microbial communities can subsist at depth in marine sediments without fresh supply of organic matter for millions of years. At threshold sedimentation rates of 1 millimeter per 1000 years, the low rates of microbial community metabolism in the North Pacific Gyre allow sediments to remain oxygenated tens of meters below the sea floor. We found that the oxygen respiration rates dropped from 10 micromoles of O_2 liter^{-1} year^{-1} near the sediment-water interface to 0.001 micromoles of O_2 liter^{-1} year^{-1} at 30-meter depth within 86 million-year-old sediment. The cell-specific respiration rate decreased with depth but stabilized at around 10^{-3} femtomoles of O_2 cell^{-1} day^{-1} 10 meters below the seafloor. This result indicated that the community size is controlled by the rate of carbon oxidation and thereby by the low available energy flux.

The discovery of living microbial communities in deeply buried marine sediments (Parkes et al., 1994; Schippers et al., 2005) has spurred interest in life under extreme energy limitation (Jørgensen and D'Hondt, 2006). The subtropical gyres are the most oligotrophic regions of the oceans. Primary productivity in the surface waters of the gyres is low, yet within the same order of magnitude as the surrounding open ocean (Fig. 3.1). Oxygen penetrates many meters into the seabed below the gyres, which indicates extremely low rates of microbial community respiration (D'Hondt et al., 2009; Fischer et al., 2009) in contrast to the rest of the seabed (Fischer et al., 2009), where in general oxygen penetration is limited to millimeters to decimeters depth, according to a square root function of the organic matter flux (Cai and Sayles, 1996; Rasmussen and Jørgensen, 1992; Wenzhöfer et al., 2001; Wenzhöfer and Glud, 2002).

On R/V Knorr voyage 195, we collected sediment cores up to 28 m along the equator and into the North Pacific Gyre and measured the oxygen distribution throughout the retrieved cores by using needle-shaped optical O_2 sensors (PreSens Precision Sensing GmbH, Regensburg, Germany) (Fig. 3.1). Along the equator, from the Galapagos (site 3) and 4700 km westward into the Pacific Ocean (site 8), the oxygen flux across the sediment-water interface decreased moderately from 60 to 45 mmol m^{-2} year^{-1}, whereas the oxygen penetration depth increased from 6 to 9.5 cm (Fig. 3.1 and Table 3.1). The trend in oxygen flux followed the trend in primary production in the surface water. The increase in oxygen penetration depth in the sediment along the equator is less pronounced than the decrease in oxygen flux, which is

expected from the general relation between oxygen flux and oxygen penetration (Jahnke and Jackson, 1987). From the equator (site 8) and into the North Pacific Gyre (site 11), the primary productivity decreased by 50%, but the oxygen penetration depth increased from 9 cm to greater than 30 m. Such a large change in oxygen penetration cannot be explained by less productivity in the gyre nor by the increase in water depth (Antia et al., 2001).

The volumetric oxygen consumption rates down the length of the core were modeled at high resolution from the deep oxygen profiles we obtained. In the model, we calculated carbon mineralization as the product of the measured particulate organic carbon concentration at each depth (C_{org}) and an initially unknown and depth-dependent reactivity (k) of the C_{org}.

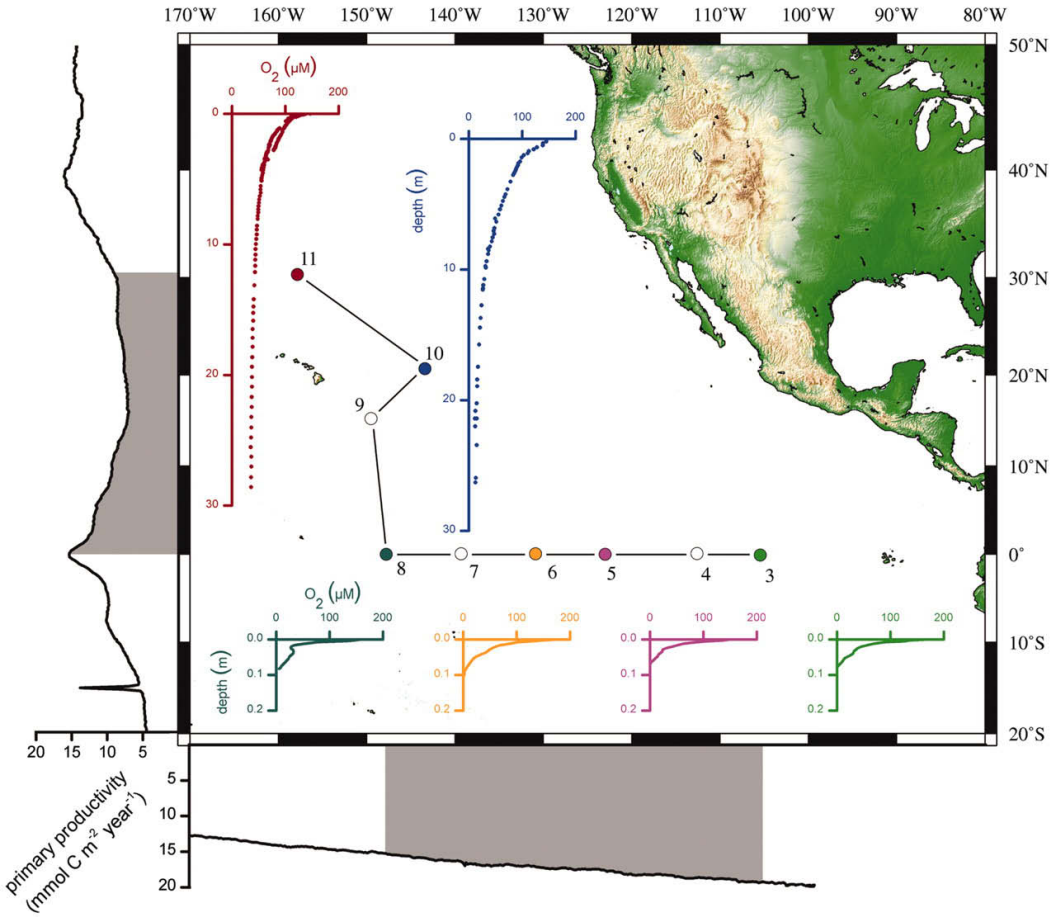

Figure 3.1: *Cruise track, sampling sites, and primary production along the cruise track. The primary production was estimated from Sea-WiFs remote-sensing data converted into integrated primary productivity averaged over 10 years by the Institute of Marine and Coastal Sciences Ocean Primary Productivity Team (Rutgers, State University of New Jersey) using the algorithms from (Behrenfeld and Falkowski, 1997). The shaded areas mark the data along the actual cruise track. The inserted graphs show the oxygen distribution in the sediment at the sampled sites. Sites 4 and 7 on the equator followed the trend in the other equatorial sites and are omitted for clarity only. At site 9 we retrieved only 4 m of core, but the profile was similar to sites 10 and 11. By site 11, we reoccupied the GPC-33 site that has been studied in great detail (e.g., Kyte et al., 1993).*

For simplicity, we assume a 1:1 molar ratio between carbon oxidation and O_2 consumption. We further assumed that k decreases monotonically with time (t), and that the decrease can be described by a power law function (Middelburg, 1989):

$$k = A \times (t + t_0)^B \tag{3.1}$$

The mass balance of oxygen throughout the core, taking into account molecular diffusion and oxygen consumption, was solved using the software Comsol Multiphysics. Measured depth-dependent values for porosity, molecular diffusion coefficient (D_m), and C_{org} were fed into the model as smoothed tabulated files and interpolated to fit the modeling grid. Parameters in Eq. 3.1 were varied to find the best fit to the measured deep oxygen profiles, resulting in the volumetric oxygen consumption rate along the length of the core and the relation between carbon age and oxidation rate. This approach had two advantages relative to calculating the reaction rate for oxygen only from profile curvature within discrete intervals (Berg et al., 1998). First, we avoided lumping high rates in the upper part of an interval with lower rates in the lower part, because this invariably leads to underestimation of the rates at the top of the interval. This is critical near the sediment surface, where the rates changed rapidly. Second, the relation between carbon reactivity and age can be used to predict how burial velocity influences the depth distribution of oxygen consumption and thus oxygen distribution (see below).

The deep oxygen profiles in the North Pacific Gyre were modeled well by assuming that the degradability of organic matter in the sediment follows a simple power law function of carbon age (Fig. 3.2A). Oxygen penetration depth in the seabed beneath the North Pacific Gyre is more than 30 m. In the Atlantic gyres, with a similar organic carbon flux to the deep seafloor, oxygen penetrates only to 0.2 to 0.5 m in the sediment (Wenzhöfer and Glud, 2002). The difference is a result of the low sedimentation rate in the North Pacific Gyre, where 90% of the organic matter mineralization in the 100-m deep oxic sediment at site 11 takes place in the top 6 cm. Carbon burial from the upper bioturbated zone into the deeper sediment is extremely slow, and the material is therefore highly refractory at depth. The fraction of total carbon mineralization that takes place below 1 m is about 1%.

The effect of low sedimentation rates on oxygen distribution was shown by using a numerical model similar to the one used to quantify oxygen consumption rates. Instead of feeding the

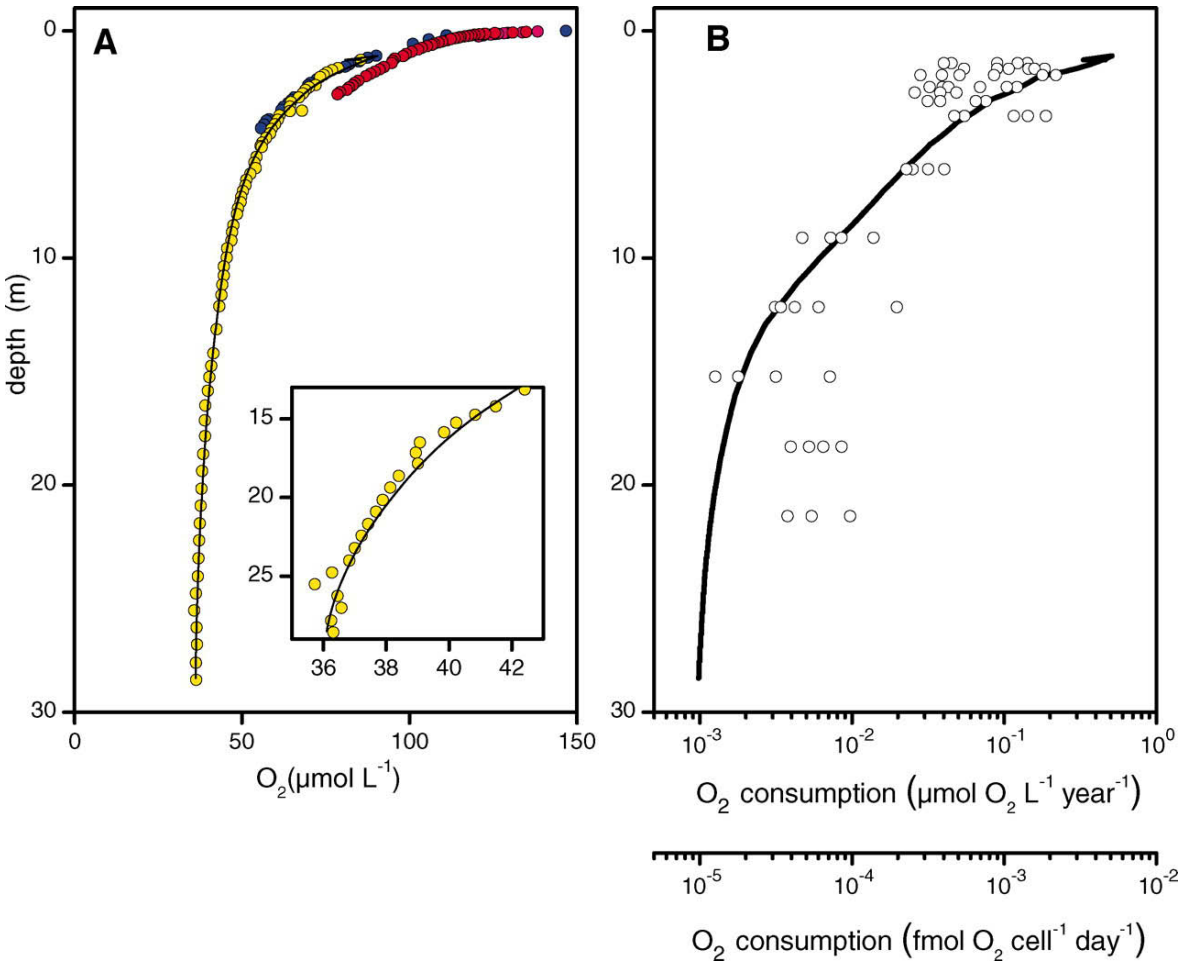

Figure 3.2: *Oxygen distribution in the seabed below the North Pacific Gyre at site 11. (A) Data originate from three independent sediment cores. The curve illustrates the fit used to calculate volume-specific oxygen consumption rates. (Inset) Data and fit for lower part of core. (B) Curve is the modeled volumetric oxygen consumption rates. Open circles are the cell-specific oxygen consumption rates obtained by dividing the volumetric oxygen consumption rate by cell counts.*

measured carbon concentration profile into the model, we imposed a flux of carbon to the sediment surface. Burial was implemented as a downward advective term. Carbon and oxygen consumption were implemented by Eq. 3.1 with the fit parameters determined from site 11. We then varied the burial rate and calculated steady-state oxygen profiles (Fig. 3.3).

The shape of the theoretical oxygen distributions are close to those observed in the North Pacific Gyre (Fig. 3.3). All modeled profiles have the same oxygen gradient, that is, total oxygen flux, at the sediment-water interface because the scenarios are modeled with the same carbon input and because practically all the carbon is mineralized. At decreasing sedimentation rates, oxygen penetrates deeper because relatively less mineralization happens far below the surface. A shorter distance of diffusion between the sediment surface and the depth of mineralization caused less overall depletion of oxygen, although the total depth-integrated

oxygen consumption was the same. A sudden shift in oxygen penetration, from dm range to the full depth of the sediment, occurs in a relatively narrow range of sedimentation rates of 1 to 5 mm per 1000 years. The sedimentation rate at site 11 has been stable at about 0.2 mm per 1000 years for the past 70 million years, with a moderate increase occurring during the most recent 2.5 million years (Kyte et al., 1993).

The total sediment thickness at the core sites in the North Pacific Gyre is 88 to 100 m (Divins, 2009). Extrapolation of the oxygen gradient at the bottom of the cores suggests that the entire sediment column is oxic, at least at site 11. The fully oxic sediment column excludes

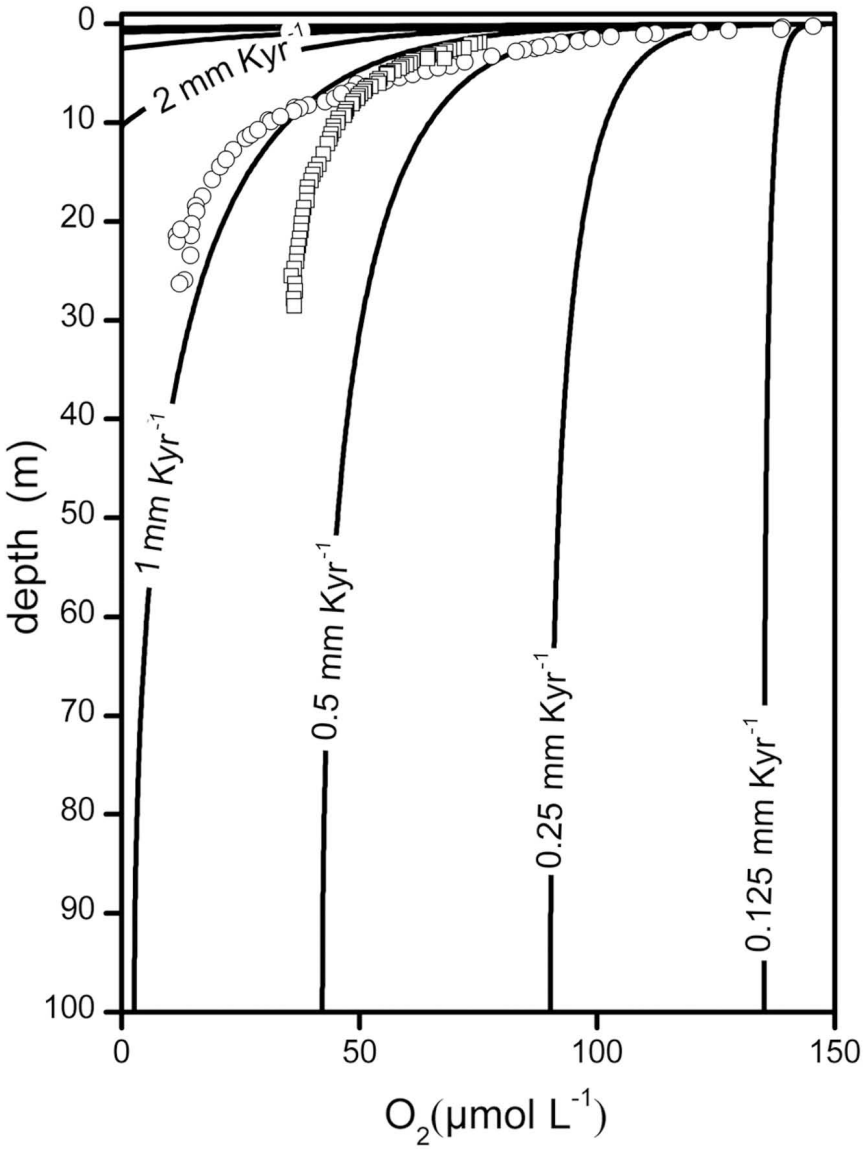

Figure 3.3: *Oxygen profiles modeled from a constant influx of organic material but varying sediment accumulation rates. All profiles represent the same oxygen uptake rate at the sediment surface. Symbols show measured oxygen profiles from site 9 (circles) and site 11 (squares).*

anaerobic metabolic pathways that normally dominate subsurface mineralization of organic matter in the seabed. This provides a unique opportunity to quantify carbon mineralization rates as a function of sediment age across a long time span. Both traditional nonparametric modeling of oxygen consumption rates from profile curvature (Berg et al., 1998) and the applied power law model yielded volumetric oxygen consumption rates that decreased from 10 mmol O_2 liter^{-1} year^{-1} at a depth of 0.5 m below the sediment-water interface to 0.001 mmol O_2 liter^{-1} year^{-1} in sediment older than 66 million years, that is, buried below 20 to 30 m at site 11 (Kyte and Wasson, 1986) (Fig. 3.2B).

The fit to a simple power law model (Fig. 3.2A) gave an exponent of –1.7, in contrast with an exponent of –1 reported by (Middelburg, 1989). Other continuously decreasing functions could have been used to describe the trend in the data, for example, a reactive continuum model that assumes exponential depletion of multiple hypothetical pools of complex organic matter (Berner, 1980; Boudreau and Ruddick, 1991). That approach is comparable to ours because a power law can be expressed as a sum of many exponential functions. We prefer the power law for its simplicity and because a model based on changing chemical properties of dead organic matter agreed well with the chemical alterations that occurred during aging and maturation.

The number of prokaryotic cells in the surface sediment of the North Pacific Gyre was 10^8 cells cm^{-3}. The cell counts decreased along the length of the core to 10^3 cells cm^{-3} at 20 m below the sea floor. Below that depth, the cell density was too low to enumerate by fluorescence microscope counting even after cell extraction (Kallmeyer et al., 2008). The cell density decreased relatively less down along the core than the volumetric oxygen consumption rate. The mean oxygen consumption rate per cell therefore decreased with increasing sediment depth and age (Fig. 3.2B). The per-cell respiration rate appeared to stabilize at around 10^{-3} fmol cell^{-1} day^{-1}. This overlaps with the range of cell-specific sulfate reduction rates in coastal subsurface sediments (Holmkvist et al., 2011; Ravenschlag et al., 2000), but it is 3 orders of magnitude below the cell-specific respiration rate of anaerobic heterotrophs in pure culture (Knoblauch et al., 1999) and below the respiration rate devoted to maintenance in the slowest-growing chemostat cultures (van Bodegom, 2007). Thus, life in the subsurface is probably more similar to cultures in long-term stationary state (Finkel, 2006) than to growing cultures. The higher cell-specific respiration rates reported previously from deeply oxygenated sediments in the South Pacific Gyre (D'Hondt et al., 2009) are not comparable because those

are average rates for the entire sediment column and are skewed upward by relatively high rates of metabolism at the sediment-water interface.

The similarity in mean metabolic rate per cell between sites with very different mineralization rates and different terminal electron acceptors suggests that these microbial communities may be living at the minimum energy flux needed for prokaryotic cells to subsist and that the total available energy flux ultimately controls the microbial community size in the deep biosphere.

Acknowledgments

The assistance from E. Caporelli, B. Costello, and E. Benway at Woods Hole Oceanographic Institution (WHOI) was crucial for our participation in the R/V Knorr cruise. We thank B. Gribsholt, the shipboard science party, the WHOI long-coring team, and the crew of the R/V Knorr for cooperation at sea. Net primary production data were provided by R. O'Malley from Oregon State University (`www.science.oregonstate.edu/ocean.productivity/index.php`). Our study was funded by the Danish National Research Foundation, the German Max Planck Society, Aarhus University, the German Federal Ministry of Research and Education via the GeoEnergie Project, and the US NSF (OCE grant 0752336 and the NSF-funded C-DEBI Science and Technology Center). This is C-DEBI publication number 130.

Supplementary Materials

Materials and Methods

Sediment cores were collected during the RV Knorr Cruise 195 Leg 3 in the Equatorial Pacific from January to February 2009. We used a multi-corer to retrieve ∼0.3 m long undisturbed cores across the sediment water interface, a light gravity corer for 3-6 m long cores, and a large piston corer (Woods Hole Oceanographic Institution) for penetration down to 30 m. The oxygen distribution at the sediment-water interface down to 0.12 m was measured top-down in cores retrieved by the multi-corer. The sealed cores were placed at 2°C immediately after recovery. Prior to oxygen measurement the sediment was pushed up in the core liner so that the sediment-water interface was ca. 8 cm below the rim. The liner was left filled to the rim with *in situ* seawater and the water surface was covered by clear polyethylene film (food wrap) as an oxygen barrier. The oxygen distribution in the upper 120 mm was measured with needle-shaped optical microsensors (optodes) driven through the plastic film and into the sediment at 0.1–3 mm steps by a motorized stage (Micos, Germany). The optical signal was read on a MICROX TX3 (PreSens Precision Sensing GmbH) oxygen meter with automatic temperature compensation. A two-point calibration was performed in anoxic and in air-saturated seawater at 2°C giving a calibrated measurement of oxygen partial pressure. Conversion to molar concentrations was calculated at the appropriate temperature and salinity (García and Gordon, 1992).

Deep penetration of oxygen in the North Pacific Gyre was measured by inserting the microsensors sideways into the unopened sediment cores through holes drilled through the core liner. A second hole adjacent to the one for the oxygen sensor was drilled for the temperature probe for thermal compensation. Cores with deep O_2 penetration were allowed to equilibrate to room temperature for 24 hours before measurement to eliminate any thermal gradients between the oxygen sensor and the thermistor. The low rates of oxygen consumption ensure that the O_2 concentrations do not change measurably during 24 hours. The 5-cm distance from the core-liner to the centre of the core does not allow diffusion of oxygen from the outer surface to influence the measurements within this period (Fischer et al., 2009).

Porosity was calculated from the weight loss of known sediment volumes upon drying at 95°C until constant weight. Organic carbon content was measured on an 1112 series elemental analyzer (Thermo Fischer). Formation factor (F) was calculated from the ratio of sediment resistivity to seawater resistivity at the same temperature (measured on a Metrohm 712 with

dual platinum electrodes). F is used to relate tabulated seawater diffusivity (D_m) to sediment diffusivity (D_s). Furthermore, F is used to calculate high resolution porosity data (Boudreau, 1996).

Oxygen fluxes (J) were calculated from the slope of the oxygen concentration with depth (dC/dz) just below the sediment-water interface: $J = -D_m F(dC/dz)$ where F is the formation factor and D_m is the diffusion coefficient for oxygen in seawater at the appropriate pressure, temperature and salinity.

The volumetric oxygen consumption rate down-core in the deep oxygen profiles was calculated from the mass balance of dissolved oxygen, taking into account molecular diffusion and oxygen consumption. We modeled the oxygen consumption rates at each depth as the product of the organic carbon pool and an initially unknown reactivity (k) of that pool. For simplicity we assume a 1:1 ratio between organic carbon oxidation and O_2 consumption. We assume that k decreases monotonously with time (t), and that the decrease can be described by a power law function (12): $k = A \times (t + t_0)^B$ (Eq. 3.1). The mass balance of oxygen down core was solved with the software Comsol Multiphysics. Measured depth dependent values for porosity, D_m, C_{org} and sediment age were fed into the model as smoothed tabulated data and interpolated to fit the modeling grid. The fit parameters in Eq. 3.1 were varied to find the best fit to the measured deep oxygen profiles. The result is the volumetric oxygen consumption rate down-core and the relation between carbon age and reaction rate.

A model for predicting oxygen and organic carbon distributions in the top 100 meters of the sediment column as a function of sedimentation rate and carbon flux was set up very similar to the interpretative model above: Sedimentation was modeled as an advective term downwards and was varied in increments from 0.05 to 5 mm per 1000 years. The boundary condition for organic carbon was a constant influx across the sediment-water interface of 70 mmol organic carbon m^{-2} $year^{-1}$ taken from the calculated flux of organic matter to the seabed in the gyre (see below). The boundary condition at the bottom of the modeled domain (100 meter below seafloor (mbsf)) was a calculated advective flux (concentration times sedimentation rate). Organic carbon was not allowed to diffuse. The boundary condition for oxygen at the sediment-water interface was a constant concentration of 150 µmol L^{-1} as measured in the bottom water at Site 11. At the bottom of the modeled domain a calculated advective flux was used as for carbon. Porosity and diffusivity were set to the average values for the Site 11 core. Carbon consumption rates were calculated from sediment (and C_{org}) age following Eq. 3.1 and the fit parameters achieved from Site 11.

Table 3.1: *Position, water depth, and total sediment thickness of coring sites. Note that the oxygen fluxes at sites 8-11 are likely to be underestimated because the coarse spatial resolution conceals oxygen consumption in the top few cm. The volumetric oxygen consumption rates were calculated by dividing the surface oxygen flux by the oxygen penetration depth for the sites on the Equator and from modeling for Site 11. The O_2 penetration at sites 9 to11 was deeper than the core obtained. The O_2 profile at Site 9 was similar in shape to sites 10 and 11, but only 4 m was recovered. The volumetric oxygen consumption data for Site 11 represent the range calculated between 1m and 30 m below seafloor.*

Site	Latitude	Longitude	Water depth	Sediment thickness	Oxygen flux	Oxygen penetration	Volumetric oxygen consumption
	N	E	(m)	(m)	(mmol m^{-2} $year^{-1}$)	(m)	(µmol L^{-1} $year^{-1}$)
3	0°2’	105°25’	3624	120	60	0.06	1000
4	0°7’	112°36’	3993	350	90	0.05	1800
5	0°4’	123°01’	4394	340	45	0.08	562
6	0°2’	130°53’	4403	370	39	0.08	482
7	0°0’	139°19’	4314	400	45	0.09	474
8	0°0’	147°47’	4336	380	45	0.09	474
9	15°7	149°29’	5250	90	18	$>$ 4 m	-
10	20°41	143°21’	5412	100	3	$>$30 m	-
11	30°21	157°52’	6000	100	4	$>$30 m	14 - 0.0007

Primary production in the surface waters was estimated from Sea-WiFs remote sensing data converted into integrated primary productivity averaged over 10 years by the IMCS Ocean Primary Productivity Team (Rutgers, State University of New Jersey) using the algorithms from Behrenfeld and Falkowski (1997). The primary production data were converted to flux of particular organic carbon to the sediment based on ocean depth (Antia et al., 2001). See Fischer et al. (2009) for details.

Prokaryotic cells in the sediment were extracted from sediment samples and enumerated according to Kallmeyer et al. (2008).

4 Detection and quantification of microbial activity in the subsurface

The subsurface harbors a large fraction of Earth's living biomass, forming complex microbial ecosystems. Without a profound knowledge of the ongoing biologically mediated processes and their reaction to anthropogenic changes it is difficult to assess the long–term stability and feasibility of any type of geotechnical utilization, as these influence subsurface ecosystems.

Despite recent advances in many areas of subsurface microbiology, the direct quantification of turnover processes is still in its infancy, mainly due to the extremely low cell abundances. We provide an overview of the currently available techniques for the quantification of microbial turnover processes and discuss their specific strengths and limitations. Most techniques employed so far have focused on specific processes, e.g. sulfate reduction or methanogenesis. Recent studies show that processes that were previously thought to exclude each other can occur simultaneously, albeit at very low rates. Without the identification of the respective processes it is impossible to quantify total microbial activity. Even in cases where all simultaneously occurring processes can be identified, the typically very low rates prevent quantification. In many cases a simple measure of total microbial activity would be a better and more robust measure than assays for several specific processes. Enzyme or molecular assays provide a more general approach as they target key metabolic compounds. Depending on the compound targeted a broader spectrum of microbial processes can be quantified. The two most promising compounds are ATP and hydrogenase, as both are ubiquitous in microbes. Technical constraints limit the applicability of currently available ATP-assays for subsurface samples. A recently developed hydrogenase radiotracer assay has the potential to become a key tool for the quantification of subsurface microbial activity.

4.1 Introduction

For centuries, coal and hydrocarbons are extracted from the subsurface, which–until recently–was considered to be largely devoid of any life. Due to increasing energy demands and decreasing resources as well as greater awareness to environmental issues, unconventional energy resources have moved into focus over the last few years, leading to a new wave of exploration of the subsurface. Due to improved microbiological techniques we are now aware that there are many products of microbial activity in the subsurface, e.g. biodegraded hydrocarbon reservoirs or biogenic methane, which are now being exploited as an energy resource. Also, microbial activity influences the utilization of subsurface resources, e.g. biocorrosion, biological formation

of minerals, biofilm formation in geothermal plants. Underground storage of CO_2 is considered to be a key factor to make energy production from fossil fuels more climate-friendly. However, despite recent advances, our knowledge about microbially mediated processes in the subsurface is still in its infancy. Due to our lack of knowledge about these processes and our inability to measure them with sufficient accuracy (sometimes to detect them at all), it is difficult to develop appropriate techniques to control microbial activity in order to guarantee the long-term stability of geotechnical plants.

The deep subsurface biosphere harbors a large fraction of Earth's biomass and probably exceeds the number of microbes in any other environment on Earth. Whitman et al. (1998) have estimated that 75–94% of Earth's prokaryotes reside in the subsurface. Of these subsurface microbes, about 60% can be found in the marine realm. However, recent data from the South Pacific Gyre indicate that previous estimates of total subseafloor microbial biomass are inflated due to the fact that the selection of sampling sites was biased towards high-productivity areas (D'Hondt et al., 2009). The sediments underlying the ultraoligotrophic South Pacific Gyre reveal cell abundances that are 3 to 4 orders of magnitude lower than at the same depths in all previously explored subseafloor sediments. Almost half of the world ocean may approach conditions similar to the South Pacific Gyre, therefore such low-productivity sites need to be taken into greater account for global estimates of subsurface biomass.

Independent of the geological setting, microbes in the subsurface face common challenges, mainly the limitation of electron donors and/or acceptors as well as increasing pressure and temperature. Although much progress in the field of subsurface geomicrobiology has been made over the last decade, many fundamental questions remain unanswered, not only about the total biomass in the subsurface microbial community, but also about its genetic diversity and metabolic capabilities.

Most of the microorganisms found in the subsurface have no cultured or known relatives in the surface world and so far their only known characteristic is their genetic code. Recent geochemical and molecular biological studies have shed light on the ways in which subsurface microbes differ from their relatives in the surface world and on the energy sources that support life in this buried ecosystem (Amend and Teske, 2005; Biddle et al., 2006; D'Hondt et al., 2004).

Despite recent advances in molecular biology, the coupling between phylogenic information (e.g. 16S ribosomal ribonuclic acid (rRNA) genes) and functional genes in the same genome is still largely unknown, preventing the relation between identity and function. Organic

geochemical analyses have become an alternative means of identification and quantification of microbial populations (e.g., Elvert et al., 1999; Hinrichs et al., 1999; Lipp et al., 2008). So far, a comparison of the different methods has only been carried out once and the results were largely contradictory, even on the basic question whether archaea or bacteria are dominant (Biddle et al., 2006; Mauclaire et al., 2004; Schippers et al., 2005). In order to obtain a full picture of the biogeochemical processes in the subsurface, a quantitative study of microbial activity is as important as molecular taxonomic studies. Despite the difficulties mentioned above, molecular, microbiological and biogeochemical studies made great progress in the characterization of the microbial populations in recent years (Jones et al., 2008). However, the quantification of microbial activity is still difficult due to extremely low metabolic rates and insufficient sensitivity of the methods. Modeling approaches based on chemical concentration profiles and/or thermodynamical calculations have shown to be a powerful tool in detecting and quantifying microbial activity at depth (e.g., D'Hondt et al., 2002; Horsfield et al., 2006; Jørgensen et al., 2001; Schrum et al., 2009), but the results may not be unequivocal because the boundary conditions set for the modeling (e.g. temperature, porosity, tortuosity, nondiffusive transport processes, etc.) may not represent true *in-situ* conditions (Jørgensen et al., 2001).

Even with cell abundances in the subsurface being significantly lower than previously thought, these microbes still represent a large fraction of the total living biomass on Earth. The energy supply for this huge population remains a mystery. Based on published data, Jørgensen and D'Hondt (2006) calculated the mean doubling time of sulfate reducing bacteria (SRB) in the deep marine subsurface to be over 1000 years, which cannot be reconciled with our current understanding of the minimum maintenance energy requirements of life. The perhaps easiest explanation, subsurface cells are dormant and not metabolically active, has been ruled out through the work of Schippers et al. (2005) who targeted rRNA with catalyzed reporter deposition- fluorescence *in situ* hybridization (CARD-FISH). They showed that there are abundant and diverse communities of archaea and bacteria, which are alive and metabolically active. Similar results, also indicating a living subsurface biosphere were obtained through organic geochemical analysis of intact phospholipids, which are constituents of microbial cell walls. However, when compared with the CARD-FISH results of Schippers et al. (2005) the organic geochemical data point towards a significantly different ratio between archaea and bacteria (Biddle et al., 2006).

Due to lack of available samples, it is still unclear how deep microbial life reaches below the sedimentary layer into the oceanic basement. D'Hondt et al. (2004) showed an upward flux of

electron acceptors from the basement into the sediment, therefore life should in principle be possible in oceanic basalts. However, obtaining uncontaminated basalt samples and having techniques available to study life in the oceanic basement is still a major challenge.

Although marine sediments differ considerably in mineralogy, they are overlain by seawater with basically the same composition globally. Therefore, porewater profiles of dissolved compounds have the same starting point at the sediment–water interface. In contrast, chemical composition and concentration in terrestrial sedimentary porewater profiles show much greater variability, which makes it much more difficult to draw general conclusions from studies of one particular environment. Several studies, e.g. from deep goldmines (Baker et al., 2003) or aquifers (Onstott et al., 1998) have confirmed the viability and metabolic activity of subsurface microbial communities in terrestrial environments.

One of the most fundamental questions in subsurface research is how the microbial communities are supplied with energy. The largest pool of organic carbon is sedimentary organic matter, but due to preferential microbial degradation of easily degradable, energy–rich compounds it becomes increasingly recalcitrant during burial (Jørgensen, 1982a,b). It still remains a mystery how microbial activity can be sustained over geologic timescales on such recalcitrant organic matter as an energy source. Horsfield et al. (2006) showed that elevated temperature, acting over geological time leads to the massive thermal breakdown of the organic matter into volatiles, including petroleum. Because these processes occur at extremely low rates they cannot be measured directly but have to be inferred through kinetic modeling based on pyrolysis data. Because microbes can directly utilize these abiotically produced products, there is an overlap between the abiotic zone of catagenesis and the biological realm. A combination of direct biogeochemical and microbiological analysis (cell counts, radiotracer turnover experiments, porewater concentration profiles) together with organic geochemical techniques (Rock-Eval pyrolysis) and kinetic modeling was used to identify processes that occur at such low rates that they can be supported over geologic timescales.

Recent results show that other sources of energy also have to be taken into account. Research has mainly focused on molecular hydrogen (H_2), as it can be generated by alteration of young basaltic crust (Holm and Charlou, 2001) or radiolysis of water (Lin et al., 2005a). In extremely nutrient-poor environments like aquifers in deep goldmines or in sediments of the South Pacific Gyre, a hydrogen-fuelled metabolism may actually be the dominant metabolic pathway due to lack of other redox-couples. Although the total net respiration rate of South Pacific Gyre sediments is over 5 times lower than of any other sediment explored so far, cell abundances are

lower by up to three orders of magnitude. Therefore, D'Hondt et al. (2009) found the per-cell rates in the oxic South Pacific Gyre sediments to be up to two orders of magnitude higher than in anoxic sediments. Despite these apparently higher per-cell rates, a quantitative study of the metabolic activity in the deep biosphere remains a major challenge due to the fact that the turnover per volume of sediment is extremely low. It is therefore of utmost importance to develop new or refine existing techniques for turnover quantification in order to lower their minimum detection limit. Great care has to be taken to understand the physicochemical limits of any technique, below which no meaningful results can be achieved.

There are different methods to quantify microbial activity, the most common ones are metabolic and enzymatic assays. Metabolic assays measure either changes in concentration of substrates and/or products over time or the conversion of a labeled substrate. There are several options for labeling, the most common ones are stable or radioactive isotopes, fluorescent labeling is very popular in biochemistry but its use in sediments has so far been limited due to the interference of sediment particles on the quantification of the fluorescence signal. Currently the most sensitive and accurate techniques are radiotracer experiments. However, even these techniques may not be sensitive enough when metabolic turnover is extremely low.

Several studies showed the importance of hydrogen in microbial ecosystems (Chapelle et al., 2002; Conrad et al., 1985; Hinrichs et al., 2006; Hoehler et al., 2002; Jin, 2007; Jørgensen et al., 2001; Nealson et al., 2005). Despite the importance of molecular hydrogen in microbial ecosystems, its quantification did not become a standard measurement in many studies, mainly due to the technical challenges associated with detection of concentrations in the sub-nM range. In a study about H_2 cycling sedimentary ecosystem Hoehler et al. (2002) showed that the partial pressure of H_2 in phototrophic microbial fluctuates over orders of magnitude on a daily basis, depending on light levels. Still, except for the highest concentrations most measurements were at the lower limit of detection, even with highly sophisticated equipment. Another issue is the extremely short turnover time of seconds to minutes, which makes sample storage problematic. High flux rates combined with low concentrations leads to a very small hydrogen pool; even small physicochemical changes in the sample will affect metabolic processes, and thereby influencing the hydrogen pool, which in turn can have profound effects on other H_2 sensitive microbial processes in the ecosystem.

The key role of the enzyme H_2ase has long been identified (Stephenson and Stickland, 1931). Schink et al. (1983) were the first to use a radioassay to quantify H_2ase activity in environmental samples. This work was later adapted for use in subsurface sediments by Soffientino et al. (2006) and applied to subsurface sediments of the Gulf of Mexico (Nunoura et al., 2009). Further applications to other subsurface environments are still lacking.

4.2 Methods for quantification of microbial activity in the subsurface, an overview

4.2.1 Sulfate reduction

sulfate reduction (SR) can be broadly divided into two categories:

1. Organoclastic SR where either hydrogen or low molecular weight substrates (e.g. volatile fatty acids) derived from the fermentation of particulates dissolved organic matter, are used as electron donors (Jørgensen, 1982a,b; Martens and Berner, 1974). Examples are given in Eqs. 4.1 and 4.2.

2. Methanotrophic SR where CH_4 is oxidized (Martens and Berner, 1974). This process is also called anaerobic oxidation of methane (anaerobic oxidation of methane (AOM)). Eq. 4.3 describes the overall process.

$$2CH_2O + SO_4^{2-} \rightleftharpoons 2HCO_3^- + H_2S \quad (4.1)$$

$$4H_2 + SO_4^{2-} + H^+ \rightleftharpoons HS^- + 4H_2O \quad (4.2)$$

$$CH_4 + SO_4^{2-} \rightleftharpoons HCO_3^- + HS^- + H_2O \quad (4.3)$$

Over 30 years ago, Jørgensen wrote the first and still most complete review about the different techniques for the quantification of SR rates. The different techniques can be divided into three major categories:

1. radiotracer incubation followed by distillation (Jørgensen, 1978a);

2. mathematical modeling based on interpretation of chemical gradients (Jørgensen, 1978b);

3. estimation from chemical and bacteriological field data (colony counts of SRB, chemical gradients, degree of pyritization) (Jørgensen, 1978c).

The first two approaches have been used frequently in many different environments. However, since the work of Jørgensen few studies have been conducted where modeling and tracer measurements were directly compared (Fossing et al., 2000; Jørgensen et al., 2001). Both studies show that in deeper layers where the distribution of sulfate is only controlled by molecular diffusion, modeling can be a powerful tool for the estimation of sulfate reduction rates (SRR). However, in shallow sediments were advective transport and reoxidation are influencing the concentration and distribution of sulfate, models tend to underestimate the true SRR. This may also be of major concern in terrestrial environment, were there is lateral fluid flow in aquifers. Without good understanding of the hydrologic properties of the sampling area, mathematical models will not be able to provide meaningful results. Radiotracer incubation experiments should designed to be so short that there is no significant change in concentration of any compound involved (Fossing, 1995). Thereby, radiotracer experiments provide a measure of the gross rate of SR whereas modeling is based on net concentration changes.

Much of the current understanding of SR has been derived from experiments conducted with $^{35}SO_4{}^{2-}$ radiotracer. $^{35}SO_4{}^{2-}$ radiotracer is relatively inexpensive and can be obtained with high specific activity in carrier-free form. Ivanov (1956) first described the use of radiotracer $^{35}SO_4{}^{2-}$ incubation for quantification of SRR. His work was later adopted and modified by others to accommodate the different experimental needs (see King, 2001, for a review). The technique has recently been improved to quantify SRR in the nano- to picomolar cm^{-3} d^{-1} range (Kallmeyer et al., 2004). A recent study by Leloup et al. (2007) showed that novel phylogenetic lineages of putative sulfate reducing microbes (SRM) are present even below zone where sulfate is present. Although SR could not be detected below the sulfate zone, SRM were detected by targeting their metabolic key gene, the dissimilatory (bi)sulfite reductase (dsrA). This raises the question whether the analytical methods are still not sensitive enough to measure SRR in such environments or whether these organisms employ as yet undiscovered life strategies to thrive in low-sulfate habitats that are apparently inhospitable for SRM.

Geochemical data from ODP Leg 201 indicate that barite dissolution supplies sulfate in sediment horizons where no dissolved sulfate could be detected in the porewater (Riedinger et al., 2006). Dissolved barium concentrations vary antithetically with sulfate concentrations and aremost probably controlled by barite solubility. The microcrystalline barite is finely dispersed in the sediment; all sulfate that is liberated by dissolution is immediately consumed by AOM, leaving dissolved barium behind. Production/consumption models based on porewater

concentration profiles of sulfate, methane and barium suggest, that most of the barite dissolution actually fuels AOM (Fig. 4.1).

Recent work of Schrum et al. (2009) showed the thermodynamic feasibility of SR via ammonium oxidation based on porewater profiles from two organic rich sediments (coastal North Atlantic, Gulf of Bengal). The coastal sediment data suggest that the process may also occur in anoxic sediment where the ammonium concentration profile shows no net loss of ammonium. If sulfate-reducing ammonium oxidation occurs globally, it may be a significant sink for fixed nitrogen.

4.2.2 Methanogenesis

Methanogenesis plays an important role in the degradation of organic compounds because it is the terminal step in the carbon flow in anaerobic habitats. Methane can be produced via different pathways, the two best described pathways involve the use of carbon dioxide (Eq. 4.4) and acetate (Eq. 4.5) as substrates (for a review see Ferry, 1992).

$$CO_2 + 4H_2 \rightarrow CH_4 + 2H_2O \tag{4.4}$$

$$CH_3COOH \rightarrow CH_4 + CO_2 \tag{4.5}$$

However, it has been shown that methanogenesis utilizes carbon from other small organic compounds and, depending on the environment, certain substrates are predominant. In anoxic freshwater environments acetate is the dominant electron acceptor (Cappenberg, 1974), whereas in marine sediments methanogenic archaea use methanol and methylamines because these substrates cannot be consumed by SRB (Oremland et al., 1982). However, through radiotracer experiments it was shown that methanogenesis from bicarbonate, methanol, hexadecane, benzoate and acetate also occurs in marine subsurface sediments (Horsfield et al., 2006).

Biogenic methane in the granitic subsurface is mainly produced from H_2 and CO_2 but it has been shown that other substrates (acetate, methanol and methylamines) can be utilized as well (Kotelnikova and Pedersen, 1998), although they are quantitatively not significant. Especially in hard rock environments rates of methanogenesis are usually much too low for any direct detection through radiotracer experiments. Unless some new and much more sophisticated techniques become available, a direct quantification will remain impossible for most hard rock environments. For a variety of environments, e.g. rice paddies (Lu and Conrad, 2005), subseafloor sediments (Horsfield et al., 2006) and aquifers (see Kotelnikova and Pedersen,

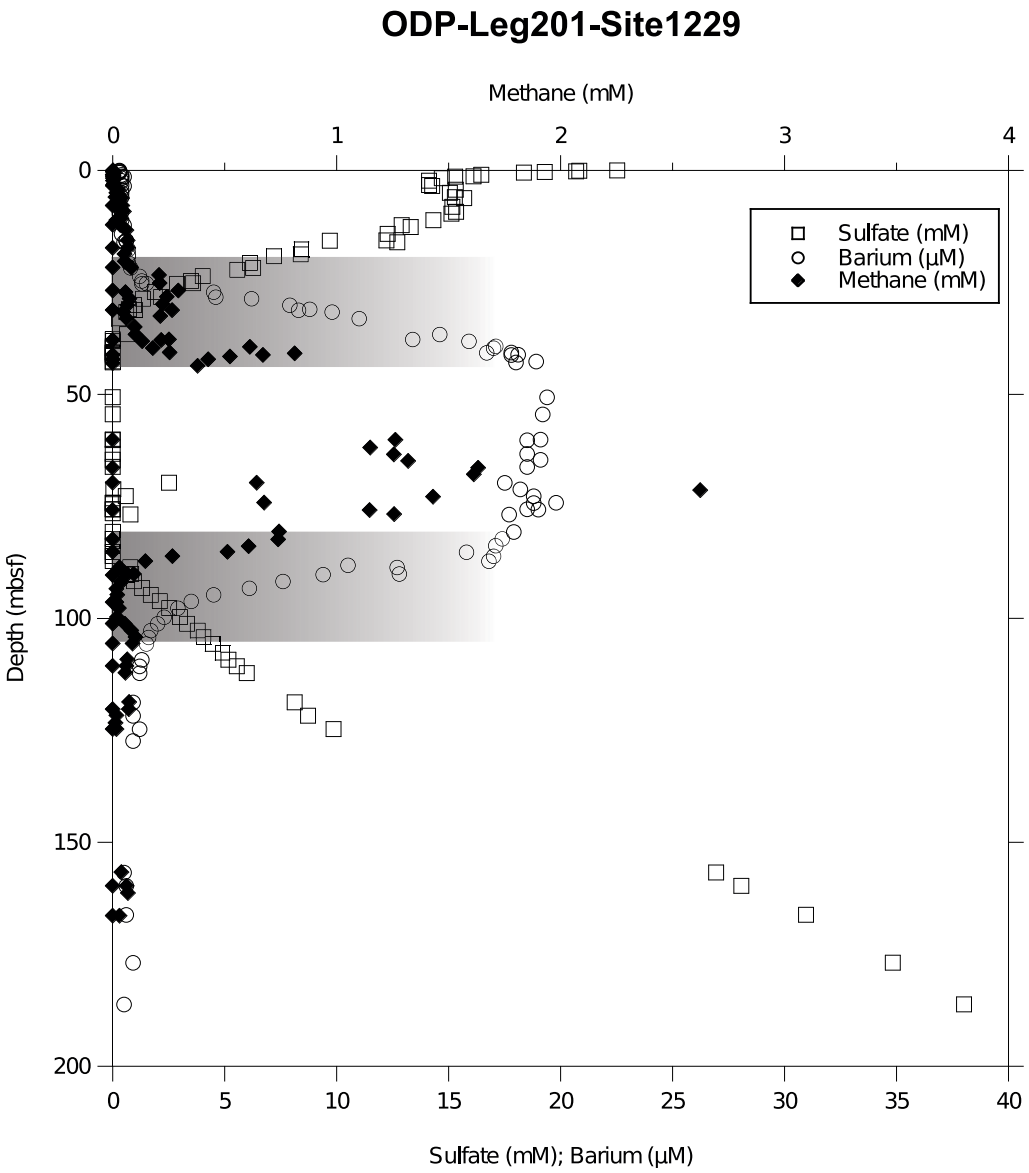

Figure 4.1: *Porewater concentration profiles from IODP Leg 201, Site 1229 (D'Hondt et al., 2003). Sulfate drops from the sediment–water interface down to zero around 40 mbsf. A unique feature of this site is the influx of saline brine from below. Sulfate reappears at depth and forms an almost mirror profile of the upper section. Methane is produced between ca. 40 and 80 mbsf, and diffuses upwards and downwards, forming two sulfate methane transition zones (gray shaded areas). Dissolved Ba^{2+} concentrations vary antithetically with sulfate concentrations and are most probably controlled by Barite solubility.*

1998, for a review) the direct quantification of methanogenesis via tracer experiment is being done routinely. However, most approaches only focus on a selection of substrates, usually acetate, formate and bicarbonate, and do not use all simply due to logistical reasons as every incubation requires additional sediment and processing capacities. Very soon practical limits are reached, especially when the number of samples becomes larger. Modeling of production and consumption of methane based on porewater methane concentration profiles has successfully

been used in marine sediments, but only in those horizons with methane concentrations below the maximum solubility of ca. 1.3 mmo $^{-L}$ at atmospheric pressure (Yamamoto et al., 1976). At elevated pressure methane solubility increases accordingly, but retrieval and processing of samples under *in-situ* pressure is rarely being done due to massive technical issues.

An identification from which substrate the methane was formed is usually not possible. Concentrations of the typical substrates are too low to be measured with sufficient precision, and gaseous substrates often get lost during porewater extraction or have too short turnover times, like hydrogen (Hoehler et al., 2002). In many cases the detection of biogenic methane as compared to abiotically produced thermogenic methane was done through stable carbon isotopic analysis.

4.2.3 Anaerobic oxidation of methane

Methane is the most abundant hydrocarbon in the atmosphere and a potent greenhouse gas (Knittel and Boetius, 2009). The largest fraction of the CH_4 flux from the subsurface to the atmosphere is efficiently controlled by anaerobic oxidation of methane (AOM) via sulfate as an electron acceptor (Martens and Berner, 1974; Nauhaus et al., 2002), converting methane to bicarbonate, which either remains in solution or precipitates as carbonate.

The almost quantitative conversion of methane to carbon dioxide through AOM is a significant contribution to the global carbon and sulfur cycle (Hinrichs and Boetius, 2002; Jørgensen, 1982a,b). Sulfate diffuses into the sediment from the overlying ocean. Where it is converted to hydrogen sulfide through organiclastic SR, using dissolved organic matter (volatile fatty acids, etc.) as an electron donor. Deeper in the sediment column methane produced from either abiotic or biological processes diffuses upwards and eventually the zones of sulfate and methane overlap. In this sulfate–methane-transition zone (sulfate–methane–transition zone (SMTZ)) anaerobic oxidation of methane (AOM) takes place.

The organisms responsible for this process have long been elusive. Boetius et al. (2000) provided the first identification of a microbial consortium consisting of SRB and anaerobic methanotrophic archaea (ANME). Since then different morphological and phylogenetic types have been found (Knittel et al., 2005). AOM also leads to carbon isotopic fractionation, where lighter ^{12}C of the methane is preferred, resulting in the produced carbon dioxide being isotopically lighter than the consumed methane. Depending on CH_4 supply, AOM can occur at depths ranging from a few millimeters to hundreds of meters below the sea floor. Rates also vary significantly, ranging from a few pmol cm^{-3} day^{-1} in deep SMTZ to mmol cm^{-3} day^{-1}

close to the sediment–water interface. AOM can be quantified by different techniques, the most common ones are radiotracer incubations and modeling based on porewater concentration profiles.

Radiotracer incubations are usually performed with $^{14}CH_4$, approaches with C^3H_4 were also carried out, but the separation of the produced tritiated water from the sediment is much more complicated than the separation of the radiolabeled $H^{14}CO_3^-$ (A. Boetius, pers. comm.). Many studies incubated samples with $^{14}CH_4$ and $^{35}SO_4^{2-}$ tracers in parallel to obtain two independent measurements for the process. Although rather labor-intensive, such experiments provided the strongest evidence that sulfate and methane react with a 1:1 stoichiometry (Iversen and Jørgensen, 1985; Nauhaus et al., 2002). Due to the fact that ^{14}C and ^{35}S are both beta-emitters with a very similar energy spectrum (ca. 160 keV), they cannot be detected separately in the same sample. The quantification of AOM through $^{14}CH_4$ radiotracer incubation was introduced by Iversen and Blackburn (1981) and refined by (Treude et al., 2003). Compared to radiotracer incubations for the quantification of SRR, AOM experiments suffer from a much lower sensitivity, which is due to the fact that solubility of methane in water is rather low. Even with carrierfree $^{14}CH_4$, 1ml of methane-saturated water contains only ca. 0.5 kBq. The amount of liquid that can be injected into a sample is limited, usually 10 to 30 ml are injected into a 5 cm^{-3} sample. For comparison, SRR experiments have been carried out with up to 1 MBq per sample. Although the long half-life of ^{14}C would allow for much longer incubation times as for ^{35}S (half-life 88 days), an increase in incubation times very soon reaches practical limits. The theoretical limit for radiotracer incubation times is solely controlled by the half-life of the isotope, any longer incubation times will not increase the amount of radiolabeled product independent of the activity of the tracer and the turnover rate (Kallmeyer et al., 2004). For ^{35}S the maximum incubation time is 127 days, whereas for ^{14}C it is 8266 years. In routine work, incubation times are usually in the range of hours to a few days. Longer incubation times are a major technical challenge because the samples have to be maintained at a constant temperature and, especially in the case of AOM rate measurements, degassing of the sample has to be avoided at any cost. For marine expeditions, the maximum incubation time is usually determined by the duration of the cruise. During transport back to the home lab temperatures may fluctuate, and such fluctuations during incubations make it difficult to interpret the final results.

Modeling has been used extensively to quantify AOM rates in SMTZs. As these zones are usually deep enough in the sediment to be controlled only by diffusion, modeling is relatively

straightforward and can provide reliable results (Jørgensen et al., 2001). Recently it has been shown that AOM can also proceed with nitrate as an electron acceptor (Raghoebarsing et al., 2006). Interestingly, Ettwig et al. (2008) showed that denitrifying bacteria anaerobically oxidize methane in the absence of archaea, providing a completely new concept of how AOM can proceed.

Froelich et al. (1979) were the first to show the typical zonation of electron acceptors according to the energy production per mole of organic carbon being oxidized. In simplified terms (excluding reoxidation reactions), the typical sequence of electron acceptors is oxygen, nitrate, manganese and iron oxides and sulfate, the latter providing the least energy gain. Nitrate and sulfate being identified as electron acceptors for AOM and having the highest and lowest energy yield, respectively, it would have been highly surprising if this reaction will not proceed with metal oxides or other electron acceptors as well. Only a short time after Raghoebarsing et al. (2006) showed that AOM proceeds with nitrate as an electron acceptor, Beal et al. (2009) could prove that the reaction can indeed utilize iron and manganese oxides.

4.2.4 ATP

adenosin 5'-triphosphate (ATP) quantification has long been used to measure microbial biomass in surface sediments (Tan and Rüger, 1989). Since ATP is used to store and distribute energy inside a cell, quantification of ATP would be the logical choice to quantify microbial activity. However, methodological problems are a great obstacle that needs to be overcome in order to obtain reliable results, especially in subsurface sediments. If there were a fairly constant ratio between ATP and the amount of living biomass, ATP could be a reliable tool for microbial biomass quantification. So far, such ratios have only been determined very rarely (Karl, 1980), therefore it is not clear how much this ratio varies between different sites and sediment types. In surface sediments ATP may also originate from protozoans and small infauna, making it difficult to assess microbial activity. As we focus mainly on deeper sediments below the depth of bioturbation (usually <1 mbsf, see Fossing et al., 2000, for a review) this is not much of an issue.

In sediment samples with low microbial activity and low biomass, the estimation of ATP is a major challenge. Since the abundance of cells is extremely low in the deep subsurface, a large sample volume is needed to extract enough ATP for the quantification. According to the data of Fagerbakke et al. (1996), the carbon content in environmental cells varies between 7 to 31 fg. For comparison, the carbon content of cultured cells is between 10 and 50 times higher.

Cell abundance in surface sediments is often in the range of 10^8 cells cm^{-3} (Parkes et al., 2000), resulting in a total amount of 0.7 to 3.1 mg cellular C cm^{-3}. Using a the conversion factor of 0.004 between ATP and cellular carbon (Tan and Rüger, 1989), there is a total of 2.8 to 12.4 ng ATP cm^{-3}, which translates to 11.2 to 24.5 pmol ATP cm^{-3}. Such a concentration would be in the range of commercially available ATP assay kits, which claim to measure ATP in the picomole range. However, cell abundances in subsurface sediments are usually several orders of magnitude lower than 10^8 cells cm^{-3} and can be as low as 10^3 cells cm^{-3} (D'Hondt et al., 2009). Such a drop in cell abundance cannot be countered by an increase in sampling size as there is usually only very little material available and sample handling would become increasingly difficult. For example, a drop in cell abundance by three orders of magnitude would increase the sample size from 1 cm^3 to 1 L of wet sediment. For the lowest cell abundances in the South Pacific Gyre, sample size would be in the order of 100 L. Therefore it is reasonable to conclude that standard fluorometrical ATP quantification is not suitable for subsurface environments at present.

The matrix of the sediment is another factor, which makes the extraction procedures difficult (Martens, 2001). The ATP-biomass quantification study by Tan and Rüger (1989) in the Northwest African upwelling region showed the highest ATP concentrations in the upper few centimeters of the sediment column, decreasing with sediment depth. This is not surprising, as cell abundance is usually highest close to the sediment–water interface. For the ATP quantification, they calculated a conversion factor of 0.004 for biological organic carbon to biological ATP (Karl, 1980; Tan and Rüger, 1989). The factor was taken as a constant over the entire sediment depth (0–6 cm), and no independent determination was carried out. Although ATP quantification has been used in numerous cases to determine microbial biomass in the water column and surface sediments (see review in Karl, 1980), this technique still has not been applied to deeper subsurface environments. The reason for this lack of application is most probably lack of sensitivity.

Other enzymes were also used to quantify biomass in sediments. Fabiano and Danovaro (1998) quantified enzymatic activities for aminopeptidase and beta-glucosidase from different sampling sites in the Antarctic Ross Sea. The sites differed in trophic conditions, and enzymatic activity was correlated with bacterial distribution and organic composition over different depths and between sites. Not too surprisingly, the result showed that enzyme activities decrease with increasing depth, following the microbial biomass distribution pattern.

4.2.5 Iron and Manganese reduction

Many metals play an important role in biogeochemical cycles as they allow easy exchange of electrons. The solubility of many metals depends on their oxidation state, e.g. reduced Fe^{2+} is much more soluble than oxidized Fe^{3+}, which usually forms oxides or oxyhydroxides, whereas it is the opposite for uranium, where U^{6+} is more soluble than U^{4+}, of course, quantitatively iron plays a much more significant role than uranium. Detection of the dissolved species in porewaters is usually rather simple, total metal concentration can be determined after complete digestion of the sample. The ratio between total metal and dissolved species and especially the changes of this ratio provide information about microbial activity after considering potential abiotic processes that may cause the same reaction.

An alternative approach is the use of radiotracers. For many metals that are commonly studied in natural environments there are radiotracers commercially available (Fe, Mn, V, U). However, the radiation emitted by some of them requires extensive safety precautions. The technical and formal requirements discourage many scientists from using these isotopes, but there are several studies that illustrate their great potential (Oremland et al., 2000; Schippers and Jørgensen, 2001). However, an application to deep subsurface environments is still lacking.

4.2.6 Hydrogenases

Hydrogenases (H_2ases) were first described by Stephenson and Stickland (1931) have been a prominent focus of research interests ever since. Hydrogenase is an exclusively intracellular enzyme expressed by almost all microorganisms, mostly prokaryotes, but also eukaryotes like algae, protozoa and fungi (Vignais et al., 2001). Hydrogenases are mostly periplasmic, where they cleave molecular hydrogen. The function of periplasmic enzyme is to reducemolecular hydrogen. For example, in the case of SR, the protons produced from the oxidation of hydrogen are used to drive ATP synthesis, and the electrons produced are transferred into the cytochrome network and delivered through the cytoplasmic membrane to the cytoplasm for the anaerobic reduction of sulfate or thiosulfate, thus harnessing the energy from hydrogen (Caffrey et al., 2007; Adams et al., 1981; Cammack et al., 2001). The cytoplasmic enzymes remove the excess reductants during microbial fermentation.

Stephenson and Stickland (1931) demonstrated hydrogen gas production during E. coli growth. Based on this observation, they named the enzyme involved for the reaction mechanism– H_2ase. During their study of anaerobic fermentation of fatty acids to methane by mixed cultures

from river mud, a culture was obtained which reduced sulfate to sulfide, and decomposed formate quantitatively to methane, CO_2 and water. The same culture synthesized methane from a mixture of carbon dioxide and hydrogen and simultaneously reduced sulfate to sulfide at the expense of hydrogen. This led to the conception that carbon dioxide and sulfate were acting as hydrogen acceptors in a system with molecular hydrogen as a proton donor, and it seemed likely that bacteria present in the mixed culture are capable of activating molecular hydrogen with the help of the enzyme.

The H_2ases play a central role in controlling the energy budget of many microbes (Cammack, 1999). Most H_2ases are highly sensitive to molecular oxygen, therefore, H_2ase-containing microorganisms predominantly live under anaerobic conditions. In some cases, oxygen can be an electron acceptor in microaerophillic environment, e.g. in Knallgas bacteria (Schink and Zeikus, 1984). In anoxic environments microbes release hydrogen as a result of fermentation of organic matter or as a side product in the course of nitrogen fixation. Molecular hydrogen is employed as an electron source by microorganisms to generate reducing equivalents, e.g. for CO_2 fixation. In other words, they utilize molecular H_2 either as a source of low potential electron or, upon evolution of hydrogen, as a means of reoxidizing the redox pool of the cell.

Numerous microorganisms can produce hydrogen by reactions linked to their energy metabolism. They use protons from water as electron acceptors to dispose the excess reducing power in the cell and to reoxidize their coenzymes. This process of utilization of hydrogen may be the only energy source in the deep subsurface (Hellevang, 2008; Vignais, 2008). In complex microbial communities such as those found in mammalian gut, it has recently been demonstrated that pathogenic bacteria such as Helicobacter pylori are able to utilize hydrogen as an energy source (Olson and Maier, 2002).

Figure 4.2 describes the three central functions of the enzyme. First, the organisms use hydrogen as an energy source by coupling molecular hydrogen oxidation to the reduction of electron acceptors such as CO_2, $SO_4{}^{2-}$, or elemental sulfur. The uptake H_2ases act as an electron donor for electron transfer proteins or the respiratory chain. By accumulating protons in one compartment, proton gradients are generated which are used later for the synthesis of ATP. Second, the production of H_2ases is usually found in obligate anaerobic bacteria. They catalyze the reduction of protons to hydrogen and facilitate the reoxidation of reduced cofactors (e.g. nicotinamide adenine dinucleotide (NADH)) or serve to dispose excess reducing equivalents. Most H_2ases are bidirectional and able to either cleave or produce molecular hydrogen as necessary. The third function is H_2-sensing on a genetic level, which regulates the

expression of further H_2ases in the cell. These H_2-sensing regulations are found in alpha and beta proteobacteria.

4.2.7 Hydrogenases, a potentially new tool for the sensitive detection and quantification of microbial activity

Hydrogenases catalyze the interconversion of molecular H_2 into protons and electrons or vice versa (Krasna and Rittenberg, 1954, 1956). The direction of the reaction depends on the redox potential of the available reactants to interact with the enzyme and the demands of the host organism. In the presence of molecular H_2 and an electron acceptor, the H_2ase functions as a H_2 uptake enzyme, and in the presence of an electron donor of low potential, it may use the protons from the H_2O molecule producing molecular hydrogen (Eq. 4.6).

$$H_2 + E \rightleftharpoons E : H + H^+ \quad (E = \text{H}_2\text{ase enzyme}) \tag{4.6}$$

Hoberman and Rittenberg (1943) demonstrated the catalytic properties of H_2ase by showing the function of H_2ase as an activator for the H_2 molecule and as a catalyst for the isotopic exchange reaction between water and the hydrogen molecule. The strong reducing power of H_2 is caused by the efficient catalysis of the reaction. The affinity of H_2ase for hydrogen has to be very high, since the solubility of hydrogen in water is very low (at $P(H_2)$ = 1 atm, T = 15°C, $[H_2]$ H_2O = 0.8 x 10^{-3} M (Collman, 1996; Crozier and Yamamoto, 1974).

Later, Anand and Krasna (1965) demonstrated the isotopic exchange through isotope experiment in which deuterium (Eq. 4.7) and tritium (Eq. 4.8) were exchanged with water in the presence of H_2ase.

$$HD + H_2O \rightleftharpoons H_2 + HDO \tag{4.7}$$

$$HT + H_2O \rightleftharpoons H_2 + HTO \tag{4.8}$$

The isotope exchange reaction is catalyzed by the reaction center of H_2ase without the need of any external electron acceptor. Because of the irrelevance of the external electron acceptor, a tritium exchange is a useful assay for the quantitative study of enzyme activity in

the laboratory (Schink et al., 1983; Vignais, 2008). A kinetic model for syntrophic butyrate fermentation was constructed by Jin (2007) considering the mechanism of reverse electron transfer. The model proposed that the net amount of energy, saved by microorganisms as ATP, depends on hydrogen partial pressure. Thus hydrogen partial pressure not only controls the energy available in the environment, but also the energy conserved by microorganisms. Most of the organisms able to produce hydrogen are also able to consume it, i.e. to oxidize hydrogen. A study by Hellevang (2008) has shown that hydrogen is the most important electron source in the deep biosphere.

Due to the very low concentrations of dissolved hydrogen, quantifying its production and consumption in sediments or porewater is not as straightforward as with other dissolved species, e.g. methane or sulfate. Due to the apparently important role of hydrogen as an energy source in subsurface ecosystems, the quantification of hydrogen turnover would have the potential to provide a measurement of total microbial activity in subsurface environments, independent of the specific processes that actually occur. Even if this measurement would not be as exact as the measurement of a specific process (e.g. SR, AOM), it would provide a rough estimate about total microbial activity. Especially in sediments with very low activity, there are significant deviations from the standard succession of electron acceptor processes (Froelich et al., 1979). Wang et al. (2008) provided quantitative evidence that multiple respiration pathways co-exist in the same depth intervals in deep subseafloor sediments. Until then it was assumed that these processes exclude each other based on thermodynamical calculations.

An analytical technique that could quantify total microbial activity in sediments with low biomass and/or metabolic activity would greatly improve our understanding of subsurface life. So far, only specific processes (e.g. SR, AOM) can be measured with sufficient sensitivity, there is no *catch all* measurement. Assays of ubiquitous enzymes appear to be the most promising approach. However, most available assays lack the necessary sensitivity for application in subsurface sediments. A new radiolabeled enzymatic assay, targeting H_2ase has the potential to be best subsurface microbial biomass activity quantification technique as it is highly sensitive and has already been proven to work in subsurface sediments (Nunoura et al., 2009; Schink et al., 1983; Soffientino et al., 2006).

In short, samples are incubated with a tritium gas headspace and due to the activity of the H_2ase enzyme tritiated water will be produced, its activity can be quantified by liquid scintillation counting. Although it is still not possible to convert H_2ase activity directly into total microbial metabolic activity, it allows the detection of very low levels of activity without

having to identify the specific metabolic processes. However, the current technique is rather labor-intensive and requires time-course experiments for each sample. Future efforts should focus on making this method more user friendly and allowing for higher sample throughput in order to make it become a standard technique for monitoring microbial activity in subsurface sediments.

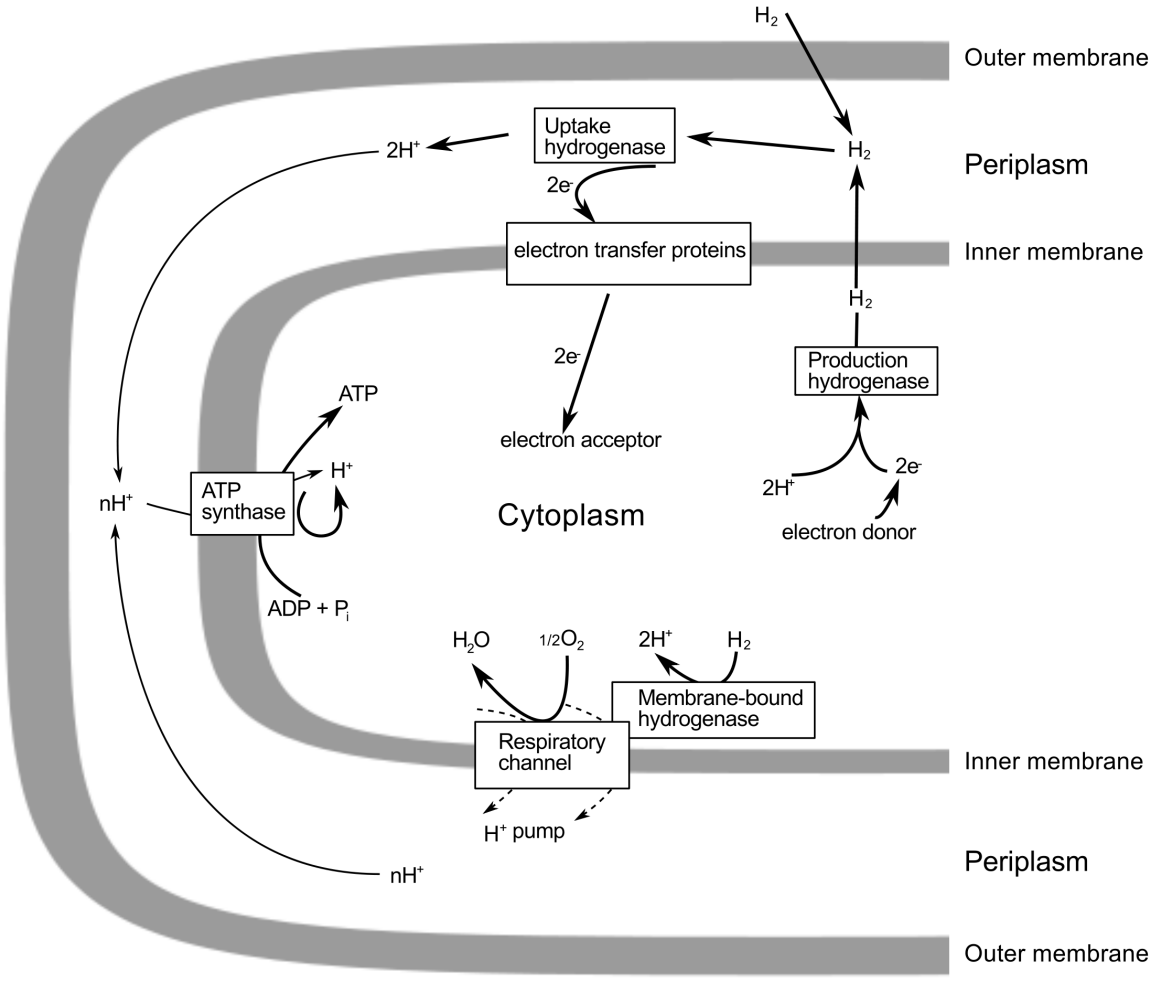

Figure 4.2: *Energy conservation pathways in microbial cells involving H_2ase (redrawn from Cammack et al., 2001). Oxidation of H_2 by a periplasmic uptake enzyme. Release of H^+ into the periplasm generates a proton gradient across the embrane. The proton gradient powers ATP production by the ATPase.*

4.3 Conclusions and Outlook

Quantification of microbial turnover in deep sediments is still in its infancy. The techniques used for quantifying sulfate reduction (SR) and anaerobic oxidation of methane (AOM) have already been refined and reached their absolute limits, which are set by logistical constraints (amount of sample that can be processed, duration of incubation) as well as physical and

technical limits (decay of radiotracer, minimum sensitivity of scintillation counter). Still, they are not sensitive enough to detect the extremely low rates with which these processes occur in the subsurface. In these cases modeling may be the only tool available. Other radiotracer techniques may still have some great potential for refinement and may become powerful tools in the future. Additional to the quantification of single specific processes, an estimate of total microbial activity will provide very valuable information about the location of hotspots of activity. Such quantification needs to focus on ubiquitous compounds or processes, and enzymes appear to be the best option. Due to low cell abundances in deep sediments, enzyme concentrations are also low, causing the minimum detection limit to become a major issue again. Especially for fluorometric assays the minimum detection limit is constrained by the amount of photons produced per reacting molecule and the minimum number of photons that can be detected. As cell abundances vary by many orders of magnitude in different environments, variations in sample size will not be able to counter this problem. A radiotracer assay targeting the ubiquitous and exclusively intracellular enzyme H_2ase has the greatest potential to become a standard tool for the quantification of total microbial activity in the future.

Meeting future energy needs and protecting our climate at the same time will require heavy utilization and exploitation of the subsurface. However, like any ecosystem on the Earth's surface we need to understand the complex interactions and processes in the subsurface. Due to the problematic access and the very low rates this is even more challenging. Although some progress has been made and certain processes can now be measured with sufficient accuracy, many others cannot. This is where microbiology has to come up with new ideas in order to secure our future energy resources.

4.4 Acknowledgements

The manuscript benefitted from the comments of the two reviewers, T. Treude and C. Hubert. Financial support was provided through the BMBF Forschungsverbundvorhaben GeoEn (Grant 03G0671A/B/C).

5 Distribution and activity of hydrogenase enzymes in subsurface sediments

Activity and distribution of hydrogenase enzyme activity were quantified in sediment samples from four different aquatic subsurface environments using a tritium-based assay. Enzyme activity was found at all sites and depths. Volumetric hydrogenase activity did not show much variability, whereas cell-specific activity ranged from 10^{-5} to 1 nmol H_2 $cell^{-1}$ d^{-1}. Activity was lowest in sediment layers where nitrate was detected. Higher activity was associated with samples in which sulfate was the dominant electron acceptor. Highest activity was found in samples from environments with >10 ppm methane in the pore water. The results show cell-specific hydrogenase enzyme activity increases with decreasing energy yield of the electron acceptor used. It is not possible to convert volumetric or cell-specific hydrogenase activity into a turnover rate of a specific process like sulfate reduction. However, the cell-specific hydrogenase activity can be used to estimate the size of the metabolically active microbial population. The conversion factors vary according to the respective electron acceptor process.

5.1 Introduction

Microorganisms in subsurface environments compete for electron donors and acceptors like in most surface environments (D'Hondt et al., 2002). Availability of these electron donors/acceptors usually decreases with depth. Utilization of different electron acceptors is controlled by the amount of energy per mole of organic matter that is being oxidized, leading to a distinct depth zonation in the sediment. In the uppermost sediment layer oxygen is used as an electron acceptor as it yields the most energy, followed by NO_3^-, Fe^{3+}/Mn^{4+}, SO_4^{2-} and ultimately methanogenesis. The sequence of electron acceptor utilization is controlled by thermodynamic constraints (Froelich et al., 1979) .The actual thickness of each electron acceptor zone varies dramatically, depending on the availability of the respective compound, which is controlled by concentration, diffusivity and rate of consumption. For example, in organic-rich sediments (e.g. coastal and upwelling areas) oxygen is depleted within a few millimeters to centimeters because the aerobic remineralization of organic matter consumes so much oxygen that diffusion can only meet the demand over very short distances (Glud et al., 1994). In more oligotrophic areas with lower organic matter content microbial activity and oxygen consumption decrease accordingly, leading to much deeper oxygen penetration depths. A recent study in the North Pacific Gyre showed that aerobic respiration persists down to

tens of meters (Røy et al., 2012), and in the ultra-oligotrophic South Pacific Gyre the entire sedimentary column is fully oxygenated down to the basaltic basement (D'Hondt et al., 2009).

The variable thickness of the different electron acceptor zones poses a challenge to precisely identify and quantify each specific metabolic process in the sediment column (Wang et al., 2008; Teske, 2012) in order to quantify overall microbial activity. There are two approaches to determine total microbial activity: 1) separately determining every quantitatively important individual metabolic processes and summing them up or, 2) determining total metabolic activity in a single measurement, by measuring a parameter that is ubiquitous in all microbes but independent of any specific metabolic process.

Conventionally, individual specific turnover rates are quantified in order to understand the occurrence and distribution of a specific process. For several processes, e.g. sulfate reduction (SR) and anaerobic oxidation of methane (AOM) this can be done with high sensitivity through radiotracer experiments (Treude et al., 2005). However, due to the very low turnover rates in subsurface environments, even these techniques reach their minimum detection limit in subsurface sediments. There are other processes like denitrification for which there are no radiotracers available, in such cases turnover rates can be modeled based on pore water profiles (Review in Boudreau, 1997).

Since only a specific metabolic process is targeted, all these approaches only provide a measure of a single process. Still, such measurements or modeling results provide valuable data, because in many cases one or two processes are quantitatively dominating carbon turnover so that measurements of these processes might provide a relatively robust estimate of total microbial activity (Jørgensen, 1982b).

However, new results challenge the notion that electron acceptor processes occur in distinct geochemical horizons. For example, Wang et al. (2008) showed that multiple respiration pathways co-exist in the same depth intervals of deep subseafloor sediments. Sulfate reduction was assumed to cease at the bottom of the sulfate–methane–transition zone (SMTZ), but Holmkvist et al. (2011) identified a cryptic sulfur cycle in the methane zone. Such deviations from the generally assumed order of electron acceptor utilization represent significant challenges when trying to estimate total microbial activity in subsurface sediments.

It would be a major step forward to have a universal proxy that covers all types of microbial activity. Several approaches have been made in recent years, the two most promising ones being adenosin 5'-triphosphate (ATP) and hydrogenase (H_2ase) enzyme activity. Recently

Vuillemin et al. (2013) quantified total microbial activity by ATP measurements in subsaline maar lake sediment from Laguna Potrok Aike, Southeastern Patagonia, Argentina. They took small subsamples immediately after retrieval of the core, mixed them with a luciferase solution and measured *in situ* ATP activity in the sediment with a handheld luminometer. These data were compared with total microbial abundance using diamidinophenylindole (DAPI) cell counts and found reasonable agreement between the two parameters. Due to the lack of other turnover rate measurements it is not possible to relate ATP activity to microbial activity, only to microbial cell abundance. However, as ATP should only be present in live cells, the ATP measurement should be a better proxy for live cells than DAPI cell counts, which also stain dead cell that still contain double-stranded deoxyribonuclic acid (DNA).

Adhikari and Kallmeyer (2010) compared various techniques for microbial activity quantification and explained their strengths and weaknesses in subsurface sediments. Among the various techniques discussed, a H_2ase assay was considered to be the most promising tool in comparison to other methods in subsurface environments especially with low microbial activity because metabolic reactions with molecular hydrogen, which occur in all microbes, is catalyzed by H_2ase enzymes.

Molecular hydrogen is an important substrate for fermenters (Laanbroek et al., 1982), methanogens (Zeikus, 1977), and sulfate reducers (Jørgensen, 1978b). Due to the low energy of activation and ability of dissociation into protons/electrons, hydrogen plays an important role in many biogeochemical reactions (Hoehler et al., 1998; Nealson et al., 2005; Jørgensen et al., 2001). Despite the importance of molecular hydrogen in microbial ecosystems, its quantification did not become a standard measurement in many studies, mainly due to technical challenges associated with detection in very low concentration. Although hydrogen is present in very low concentrations, turnover rates in subsurface sediments are high (Hoehler et al., 2001). In subsurface environments H_2 can be generated by alteration of young basaltic crust (Stevens and McKinley, 1995; Bach and Edwards, 2003) or radiolysis of water (Lin et al., 2005a; Blair et al., 2007; Holm and Charlou, 2001). Several studies have shown that hydrogen is a controlling factor for microbial activity in subsurface environments (Stevens and McKinley, 1995; Hinrichs et al., 2006; Anderson et al., 2001). For every terminal electron accepting reactions i.e. for nitrate reduction, Fe^{3+}/Mn^{4+} reduction, sulfate reduction, or methane production, hydrogen is necessary (Lovley and Goodwin, 1988), so quantification of hydrogen utilization would be a useful parameter to understand terminal electron accepting processes in anaerobic sedimentary environments (Hoehler et al., 2001).

Since hydrogen is a key component in anaerobic metabolism and H_2ases catalyze hydrogen utilization, quantification of H_2ase activity could be a catch all parameter for anaerobic metabolism. Soffientino et al. (2006) developed a method for the quantification of H_2ase activity by using a tritium-based assay. This technique was successfully employed in several studies of microbial activity in subsurface sediments (Soffientino et al., 2006, 2009; Nunoura et al., 2009).

Hydrogenases are typically intracellular and are present in all microbes (Schink et al., 1983; Vignais and Billoud, 2007). One of the main functions of H_2ases is to catalyze the reversible interconversion of molecular hydrogen gas into protons and electrons (Eq. 5.1). During the catalytic conversion of hydrogen, protons and electrons are produced or consumed according to what is needed to facilitate cellular metabolism, for example proton gradient formation in the cell membrane to synthesize ATP (Odom and Peck, 1984). Microbes utilize the available electrons for their metabolic activity by reduction of electron acceptors or methanogenesis. Moreover, H_2ases catalyze hydrogen isotope exchange between water and hydrogen as shown in the Eq. 5.2 below (Schink et al., 1983; Stephenson and Stickland, 1931).

$$H_2 \rightleftharpoons 2H^+ + 2e^- \tag{5.1}$$

$$HT + H_2O \rightleftharpoons HTO + H_2 \tag{5.2}$$

where T = Tritium (^{3}H)

Biological transformation of molecular hydrogen into electrons and protons occurs via the H_2ase enzyme by catalyzing the reversible reaction (Stephenson and Stickland, 1931). The reaction results in either H_2 consumption or production. Instead of hydrogen ($^1H_2$), tritium ($^3H_2$) gas can also be cleaved by H_2ase producing $^3H^+$. Through isotope exchange with water tritiated water is generated. Although the concentration of $^3H_2$, H_2 and water greatly influence microbial activity, the isotopic exchange reaction is strongly favored because of the higher concentration of water (55.56 mol L^{-1}) compared to all other reactants (Schink et al., 1983). During the incubation of sediments with tritium gas the isotopic exchange reaction takes place over time. The increase in tritiated water over time yields a rate of tritium incorporation that is proportional to the total activity of H_2ase in the sediment sample.

It was shown previously that most microbes in subsurface sediments are alive and metabolically active (Schippers et al., 2005). A great number of different metabolic processes occur in

sediments, many of them can proceed simultaneously (Wang et al., 2008). It was hypothesized that H_2ase activity provides a measure of total microbial activity in subsurface environments irrespective of the specific metabolic processes (Adhikari and Kallmeyer, 2010). However, the different electron acceptor processes utilize different amounts of hydrogen (per mole carbon oxidized) and involve different numbers of H_2ase enzymes, which makes it rather unlikely to translate H_2ase activity directly into a specific turnover rate. We hypothesize that if such a conversion of H_2ase activity into another turnover process is possible, it would require different conversion factors for each process.

In order to evaluate whether H_2ase activity can be translated into a rate measurement of a specific microbial process or whether it provides an independent quantification of the metabolically active microbial population, we measured H_2ase activity in sediment cores from very different environments in which different electron acceptors were quantitatively most important.

5.2 Materials and methods

5.2.1 Site description

Lake Van, Turkey

Lake Van, one of the largest soda lakes on Earth (Kadioglu et al., 1997), is located in eastern Anatolia, Turkey. It covers an area of 3570 km^2 and has a maximum depth of 460 m (Litt et al., 2009). High alkalinity of 155 mEq L^{-1} and a pH of ca. 10 are mainly due to evaporation processes and weathering of nearby volcanic rocks (Kempe et al., 1991).

Sediment samples were taken during International Continental Scientific Drilling Program (ICDP) PALEOVAN drilling operation in summer 2010. For our study, short gravity cores of ca. 0.8 m length were taken from the Northern Basin (NB) and Ahlat Ridge (AR) in a water depth of 375 m and 260 m, respectively. The cores were sectioned immediately after retrieval and the anoxic sediment samples were packed in gas tight aluminum bags, flushed with nitrogen gas and frozen immediately at -20°C until analysis.

Barents Sea

The Barents Sea is located between the Norwegian Sea in the southwest and the Arctic Ocean in the north. Our sampling area is located between the southwestern part of the Loppa High and Ringvassoy-Loppa fault complex (Fig. 5.2; Nickel et al., 2012). The morphology of the

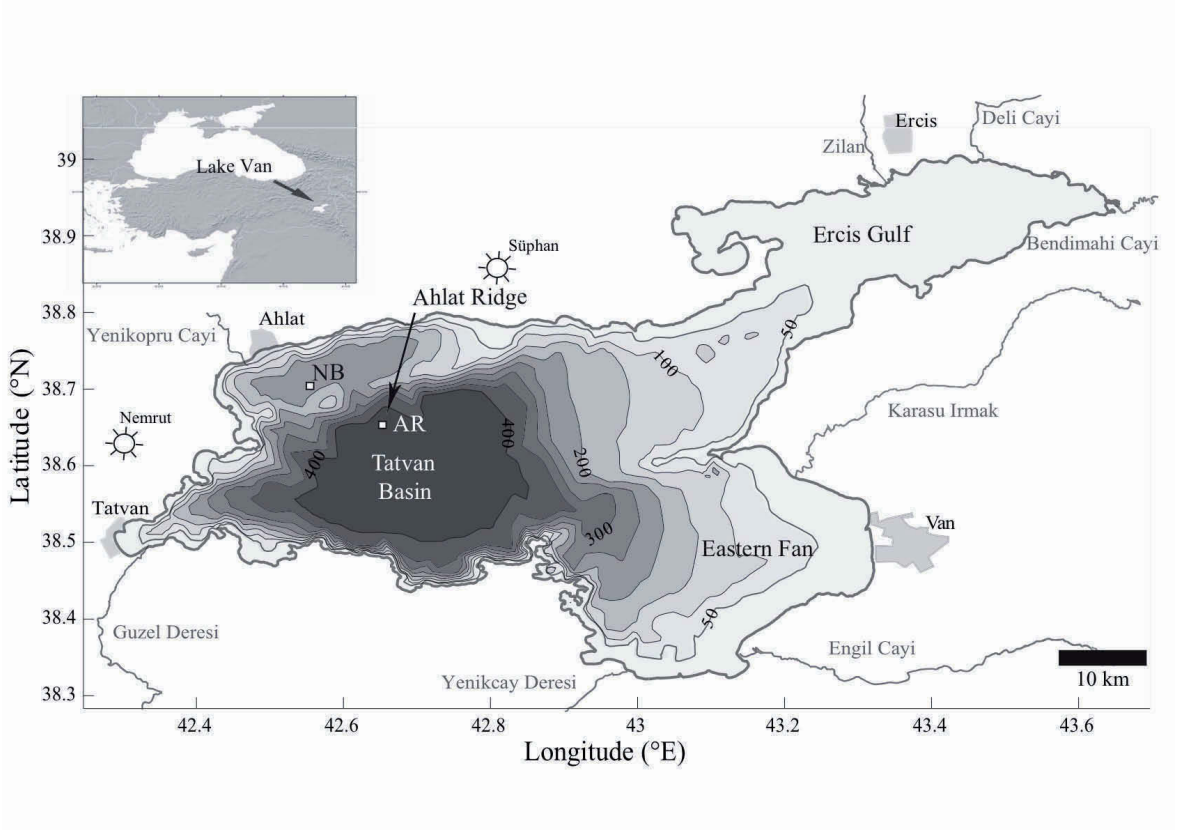

Figure 5.1: *Map of Lake Van showing lake bathymetry contours (in meters) and the sampling locations Ahlat Ridge (AR) and Northern Basin (NB) (Glombitza et al., 2013)*

seabed in our sampling area B is rather peculiar as it contains an average of ca. 100 pockmarks per square kilometer. The randomly distributed pockmarks are thought to be formed by sudden expulsion of fluids or gas from the sediments (Solheim, 1991). The pockmarks are between 10 and 50 m in diameter with an average depth of ca. 1-3 m and currently inactive. Average water depth and temperature in the investigated area were around 350 m and 6°C, respectively. Short gravity cores of ca. 1.5-1.8 m length were taken in the pockmarks at two locations (B1 and B9). Immediately after core retrieval, whole round cores of 10 cm length were packed into gas tight aluminum bags, flushed with N_2, heat sealed and frozen at -20°C until processing onshore. The sediment is a very sticky silt clay, brown to dark brown in color with a total organic carbon (TOC) of 0.4-1.6% (Nickel et al., 2012).

Equatorial Pacific

Samples were retrieved during the R/V Knorr Cruise 195-III in early 2009. The sites EQP-05 and EQP-07 are located in the eastern equatorial Pacific upwelling area with relatively high primary productivity of ca. 15 mmol C m^{-2} $year^{-1}$ (Røy et al., 2012). Water depths at EQP-05 and EQP-07 are 4394 m and 4314 m, respectively. Using the large piston corer of Woods

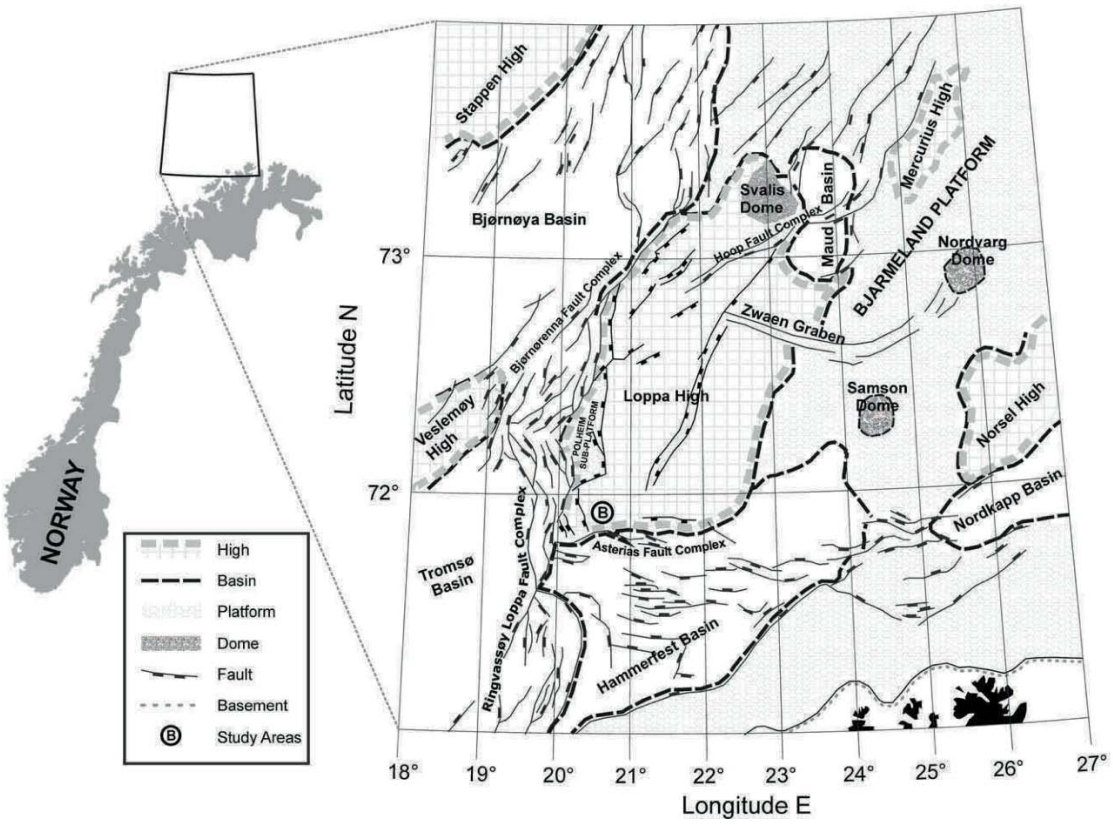

Figure 5.2: *Barents Sea tectonic framework and sampling area (Gabrielsen et al., 1990; Nickel et al., 2012)*

Hole Oceanographic Institution (WHOI), sediment cores with a maximum length of 35 meter were recovered. Soon after the core was retrieved, samples for H_2ase activity measurements were taken with 20 cm^3 cut-off plastic syringes. The syringes were immediately packed into gas-tight aluminum foil bags, flushed with N_2 gas and frozen at -80°C for further analysis onshore.

Gulf of Mexico (IODP Expedition 308)

Sediment cores were retrieved during Integrated Ocean Drilling Program (IODP) Exp. 308 using advanced piston corer (APC) and extended core barrel (XCB). Samples were collected from two holes (U1319 and U1320) at the Brazos-Trinity (BT) Basin and two holes (U1322 and U1324) at the Mars-Ursa Basin (Flemings et al., 2006). Volumetric H_2ase activity and cell count data were digitalized from a publication (Nunoura et al., 2009) using freeware (`http://nick-r.pisem.net/digiter_e.htm`), all other data were obtained from the IODP database (`http://iodp.tamu.edu/janusweb/general/dbtable.cgi`).

5.2.2 Methods

Hydrogenase enzyme assay

We used a tritium-based assay to measure H_2ase activity (Soffientino et al., 2006). Previous studies on tritiated H_2ase assay (Schink et al., 1983; Doherty and Mayhew, 1992; Nunoura et al., 2009; Soffientino et al., 2009) have shown the potential of the method for the quantification of microbial activity in subsurface sediments.

Sample preparation

For the measurement of H_2ase activity, ca. 2 g of frozen sediment was placed into a 50 cm^3 glass syringe barrel fitted with a 3-way stopcock, and mounted vertically on a manifold (Fig. 5.3). Under a continuous stream of N_2 the sediment was slurried with 10 ml of sterile NaCl solution of the corresponding salinity for 5 minutes to remove traces of oxygen contamination. Each sample was processed in triplicate plus a negative control that was treated with 0.5 ml saturated $HgCl_2$. All four slurries were then incubated with 30 cm^3 gas headspace (tritium mixed with 20/80% H_2/N_2) gas on a shaker at 250 rpm. Five subsamples of ca. 0.5 ml were taken at 0.5 h, 1 h, 2 h, 3 h and 4 h from each of the slurries. Unreacted $^3H_2$ was removed by bubbling the subsample with N_2 for 10 minutes and the sediment particles were removed by centrifugation. 100 µl of supernatant were mixed with 4 ml Perkin Elmer® Ultima Gold LLT scintillation cocktail for radioactivity quantification by liquid scintillation counting on a Perkin Elmer® TriCarb TR2800.

Headspace preparation

For the incubation of the sediment slurry, a tritium headspace gas was prepared by mixing tritium gas (American Radiolabeled Chemicals) with a non-radioactive (20/80% H_2/N_2) gas. To store, dilute and dispense the gas, a manifold was constructed according to Soffientino et al. (2009) with some minor modifications (Fig. 5.3). In brief, the manifold consists of a 1-liter stainless steel cylinder (Fig. 5.3A) for the storage of 37 GBq of tritium gas in a mixture of 20% H_2 and 80% N_2. The cylinder is connected to the headspace reservoir (Fig. 5.3C) via a stainless steel loop with a volume of 11.4 ml (Fig. 5.3B). To prepare the desired specific activity of tritiated gas, one or several volumes of the loop are diluted with known volumes of non-radioactive gas. Different to Soffientino et al. (2009) we have added an oxygen scrubber (Fig. 5.3F) to remove traces of O_2 from the system between the headspace cylinder (Fig. 5.3A) and dilution gas cylinder (Fig. 5.3E). The oxygen scrubber consists of two graduated cylinders

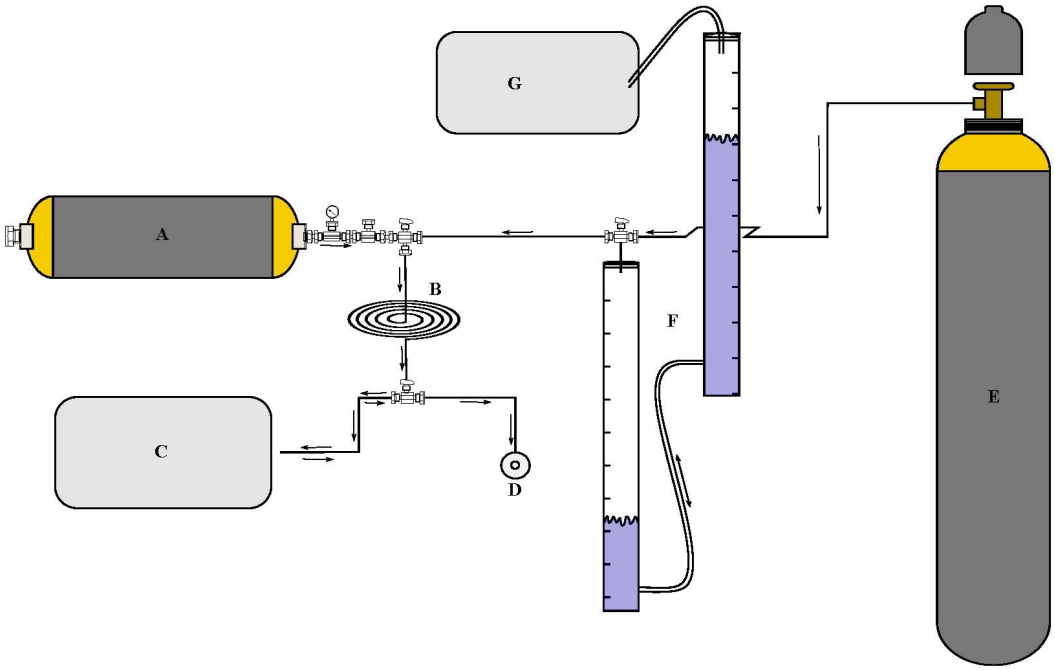

Figure 5.3: *Headspace (tritiated H_2/N_2) manifold for storing, diluting and dispensing tritiated hydrogen gas to the incubation syringes. A, 1-L stainless steel cylinder filled with 37 GBq tritiated stock gas; B, tubing loop; C, secondary headspace reservoir; D, headspace port*

filled with chromous chloride ($CrCl_2$) solution produced by reacting 1 mol L^{-1} $CrCl_3.6H_2O$ in 0.5 N HCl with zinc granules under a stream of nitrogen. One of the cylinders is connected to a non-radiolabelled 20%/80% H_2/N_2 gas cylinder and the headspace loop (Fig. 5.3B) via a 3-way valve. The other is connected to a gas-tight aluminum bag (Fig. 5.3G) filled with N_2 gas to maintain oxygen-free conditions (Fig. 5.3). Additional to being an oxygen scrubber, the graduated cylinders were also used to measure the volume of dilution gas. Finally the diluted tritium gas is filled into the glass syringes via a sample port (Fig. 5.3D).

Specific activity of the headspace gas was measured as described by Soffientino et al. (2009). In brief 500-µl tritiated H_2/N_2 gas was reacted with air in a Knallgas-reactor in the presence of a heated platinum catalyst to form tritiated water. The tritiated water was trapped with 5 ml distilled water and radioactivity of the tritiated water was quantified by liquid scintillation counting.

Cell extraction and enumeration

Lake Van, Barents Sea and EQP samples for cell enumeration were taken immediately after the core was retrieved. Using cut-off plastic syringes (2 cm^3) subsamples were taken and placed in a 15 ml centrifuge tube containing 8 ml NaCl solution of the respective salinity with 2% formalin as a fixative. The tubes were shaken vigorously to create a homogenous slurry and stored at

4°C until analysis. Cell counts were done using the cell extraction protocol of Kallmeyer et al. (2008). The separated cells were filtered onto 0.2 µm polycarbonate filters, stained with SYBR Green I according to Morono et al. (2009) and counted using epifluorescence microscopy. Cell counts of samples from IODP Exp. 308 were performed according to Nunoura et al. (2009). In brief, 1 ml sediment samples were fixed in 9 ml of 3.7% formaldehyde with phosphate buffered saline (PBS) and stored in 1:1 (v/v) ethanol:PBS solution. Subsamples were filtered on a polycarbonate membrane and stained with both acridine orange (AO) and DAPI. The stained cells were enumerated with an epifluorescence microscope onboard.

Sulfate, nitrate and methane analysis

Pore water extraction and sulfate, nitrate and methane analyses of IODP Exp. 308 samples were carried out on board according to IODP standard protocols (Flemings et al., 2006).

Pore water from Barents Sea, Lake Van and Equatorial Pacific samples was extracted with an IODP-style titanium/PTFE pore water extraction system (Manheim, 1966) in a hydraulic press (2-column bench top laboratory press, 22 ton max load, Carver Inc., USA). The pore water was filtered through a 0.45 mm syringe filter and stored frozen until analysis. On previous subseafloor microbiological research cruises, it was learned that squeezing generated a high nitrate blank corresponding to between 1 and 5 µmol L^{-1} NO_3^- in the sample. Because of this problem, nitrate concentrations in the pore water samples of the Equatorial Pacific expedition were measured using samples from Rhizon™ samplers. This practice allowed us to effectively quantify even the lowest concentrations of nitrate (< 1 µmol L^{-1}).

Lake Van and Barents Sea samples were analyzed using an IC system equipped with an LCA A14 column, a suppressor (SAMS™, SeQuant, Sweden) and a SYKAM S3115 conductivity detector. The mobile phase was a 6.25 mmol L^{-1} Na_2CO_3 with 0.1 vol% modifier (1 g 4-hydroxy-benzonitrile in 50 ml methanol). Elution was performed at isocratic conditions. The eluent flow was set to 1 ml min^{-1}. A blank sample and a standard solution were measured every 15 samples. Standard deviation of both standard and sample analysis was below 1% (determined from replicate analysis).

On the Equatorial Pacific expedition sulfate and chloride were quantified with a Metrohm 861 Advanced Compact IC. The IC was comprised of an 853 CO_2 suppressor, a thermal conductivity detector, a 150×4.0 mm Metrosep A SUPP 5 150 column, and a 20 µl sample loop. A Metrohm 837 IC Eluent/Sample Degasser was coupled to the system. The column oven was set at 32°C. The eluent solution was 3.2 mmol L^{-1} Na_2CO_3, and 1.0 mmol L^{-1}

$NaHCO_3$. A 1:50 dilution of interstitial water with 18 MOhm cm^{-1} deionized water was analyzed. If samples were anaerobic, 5 µL of 10% Zn-acetate, per ml of analyte was added to precipitate ZnS.

Nitrate concentrations were analyzed with a Metrohm 844 UV/VISCompact IC. A 150×4.0 mm Metrosep A SUPP 8 150 column was used. The column oven was set at 30°C. The eluent was a 10% NaCl solution filtered through a 0.45-micron filter. Approximately 0.8 ml of interstitial water was injected manually into a 250 µL sample loop. Absorption at the 215 nm channel was used for quantification.

5.3 Results

Using the tritium-hydrogenase assay, we measured H_2ase activity in sediment samples collected from two locations each in Lake Van (AR and NB), Barents Sea (B1 and B9) and Equatorial Pacific Ocean (EQP-05 and EQP-07) (Fig. 5.4 and 5.5). Enzyme activity could be quantified in all samples at all depths but differed significantly between sites and depths. Additionally, we compiled data from four different sites from the Gulf of Mexico (U1319, U1320, U1322, U1324) drilled during IODP Exp. 308 (Flemings et al., 2006; Nunoura et al., 2009). Hydrogenase activity and cell count data were extracted from the published data (Nunoura et al., 2009), whereas porewater geochemical data and methane gas concentration were taken from IODP database (Fig. 5.6).

Lake Van

In AR samples, a minimum activity of 1.67 µmol H_2 cm^{-3} d^{-1} was quantified in the uppermost layer at 0.08 meter below lakefloor (mblf). An increase in H_2ase activity over depth was observed, reaching a maximum activity of 17.85 µmol H_2 cm^{-3} d^{-1} at a depth of 0.43 mblf before decreasing down to 11.6 µmol H_2 cm^{-3} d^{-1} at the bottom of the core (0.72 mblf). Unlike at the AR site, H_2ase activity in samples from the NB site decreased with depth. A maximum activity of 3.44 µmol H_2 cm^{-3} d^{-1} was measured in the uppermost sediment layer at 0.06 m, which is ca. 3 times higher than in the AR sample of the same depth interval. Activity decreased by an order of magnitude within a few centimeters and remained in the range of 0.2 to 1.2 µmol H_2 cm^{-3} d^{-1} between 0.14 and 0.74 mblf (Fig. 5.4A).

At AR microbial cell numbers remained constant around 10^6 cells cm^{-3} and show only little variation with depth. The cell numbers at NB are slightly higher (10^6 to 10^7 cells cm^{-3}) but also show higher scatter (Fig. 5.4B).

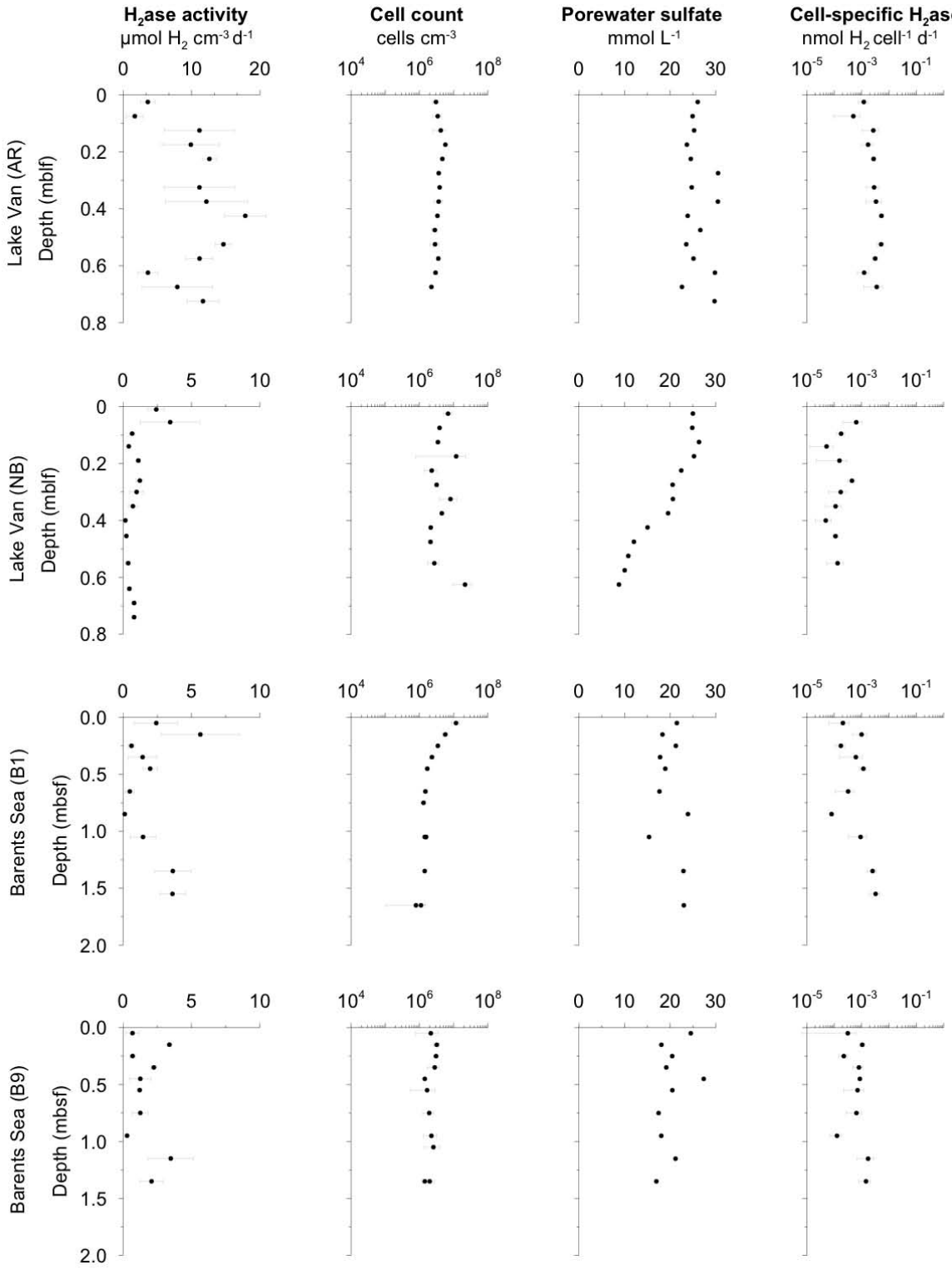

Figure 5.4: *Microbial activity distribution in sediments of Lake Van and Barents Sea (A) hydrogenase activity; (B) total cell counts; (C) porewater sulfate concentration (D) cell specific hydrogenase activity*

Almost identical pore water sulfate concentrations of ca. 26 mmol L^{-1} were observed in the uppermost sediment layer of both sites. At the NB site sulfate concentration decreases to 8 mmol L^{-1} at 0.65 mblf whereas at the AR site, sulfate concentration remains fairly constant throughout the core despite some scatter. In both cores microbial sulfate reduction was detected by radiotracer incubations, with maximum rates around 20 and 2 nmol cm^{-3} d^{-1} at NB and AR, respectively (Glombitza et al., 2013).

Throughout the water column nitrate concentrations are below 1 µmol L^{-1} (Reimer et al., 2009) and the bottom water is anoxic at both sites (Kaden et al., 2010). Our porewater analysis could not detect any nitrate. Methane gas could also not be detected in any samples.

Barents Sea

Hydrogenase activity in both Barents Sea sites (B1, B9) scattered between 1 and 3 µmol H_2 cm^{-3} d^{-1} in the upper 1 meter below seafloor (mbsf). Below this depth an increase in activity to values up to ca. 5 µmol H_2 cm^{-3} d^{-1} was observed (Fig. 5.4).

Cell counts varied between depths and sites by an order of magnitude. At B1 ca. 10^7 cells cm^{-3} sediment were counted at the uppermost 0.05 m, decreased down to 10^6 at 0.75 mbsf and remained constant until the end of the core. At site B9 cell numbers remained fairly constant between 10^6 and 10^7 cells cm^{-3} sediment at all depths.

An average sulfate concentration of 20 mmol L^{-1} with some scatter is observed at both sites B1 and B9 throughout the entire core. The sulfate profiles indicate that microbial sulfate reduction is very low. This was confirmed in another study (Nickel et al., 2012) that found sulfate reduction rates to be very low (max. $<$100 pmol cm^{-3} d^{-1}), 20 to 200-fold lower than at Lake Van. Nitrate and methane could not be detected in any Barents Sea sample.

Equatorial Pacific Ocean

At both EQP sites H_2ase activity is relatively low with values between 0.09 nmol and 1.23 nmol H_2 cm^{-3} d^{-1}. Below 23.3 mbsf a slight increase in activity in the two lowermost samples of both sites could be observed (Fig. 5.5).

Up to 10^9 cells cm^{-3} were found at both sites in the uppermost sediment layer, much more than in any other sediment analyzed in this study. Cell numbers decreased exponentially and remained between10^5 to 10^6 cells cm^{-3} below 5 mbsf (Fig. 5.5).

Sulfate profiles remained around seawater values over the entire length of the cores at both sites. As a unique feature of the EQP sites, nitrate was detectable with maximum

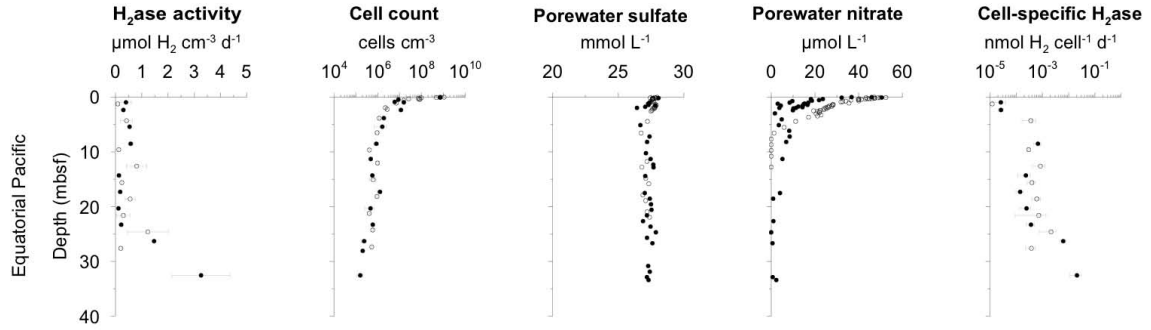

Figure 5.5: *Microbial activity distribution in sediments from Equatorial Pacific Ocean. EQP-05 (filled circles) and EQP-07 (open circles) (A) hydrogenase activity; (B) total cell counts; (C) porewater sulfate concentration; (D) porewater nitrate concentration; (E) cell specific hydrogenase activity*

concentrations of ca. 50 µmol L^{-1} close to the sediment-water interface. Concentrations decreased steadily and fell below the minimum detection limit (MDL) of ca. 1 µmol L^{-1} around 2 and 7 mbsf at site EQP-05 and EQP-07, respectively (Fig. 5.5). In some scattered samples of EQP-05, nitrate was detectable in very low concentrations over the entire length of the core (Fig. 5.5).

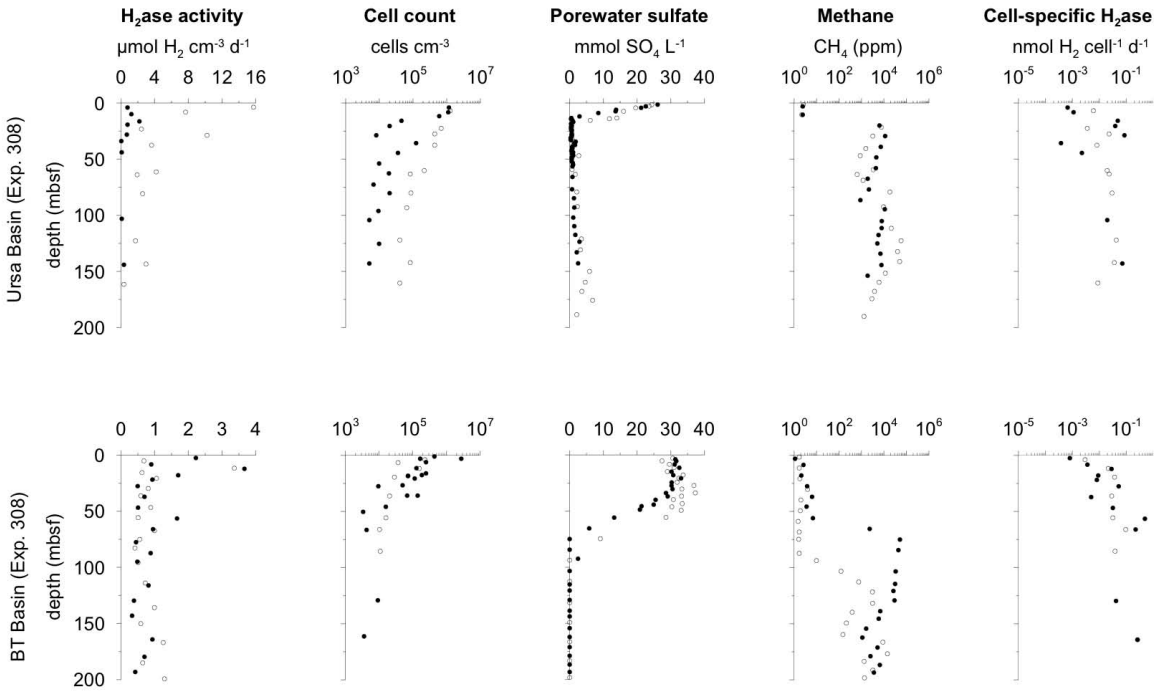

Figure 5.6: *Microbial activity distribution in sediments taken during IODP expedition 308. Sites U1319 and U1322 (filled circles) and sites U1320 and 1324 (open circles). (A) hydrogenase activity; (B) total cell counts; (C) porewater sulfate concentration; (D) headspace methane gas measurement; (E) cell specific hydrogenase activity (the data were taken from IODP data bank and from Nunoura et al. (2009)*

Gulf of Mexico (IODP Expedition 308)

At all investigated sites of IODP Exp. 308 (U1319, U1320, U1322 and U1324), H_2ase activity remained below 5 µmol H_2 cm^{-3} d^{-1} at all depths except for three samples from the upper 30 mbsf at site U320, which revealed activities of up to 16 µmol H_2 cm^{-3} d^{-1}.

Close to the sediment-water interface cell counts were in the range of 10^6–10^7 cells cm^{-3} and decreased down to 10^3–10^4 cells cm^{-3} at depth. Contrary to sites U1319, U1322 and U1324 that showed a logarithmic decline with depth, cell counts at site U1320 exhibit an almost linear decrease but with relatively high scatter.

At sites U1319 and U1320 porewater sulfate was completely consumed within the upper 10 mbsf, whereas at sites U1322 and U1324 sulfate did not show any decrease over the upper 30 m and 50 m, respectively, and remained at or slightly above normal seawater level. Deeper, porewater sulfate concentrations drop almost linearly and reach zero between 80 and 100 mbsf. The sulfate profile is mirrored by methane, with values between 10^4 and 10^5 ppm in the sulfate-free zone and low but detectable concentrations (1-10 ppm) where sulfate is present. There are SMTZs at all four sites, but they differ in their depth position in the sediment and thickness.

5.4 Discussion

Four sets of samples from widely different environments (alkaline Lake Van, shallow Barents Sea and deep Equatorial Pacific and the Gulf of Mexico) were analyzed and the results show that the enzyme assay was able to detect microbial activity at all sites and depths, indicating the presence of an active microbial population. Hydrogenase activity was not restricted to a specific sediment layer or chemical porewater zone. Unlike most other radioassay techniques the H_2ase assay detects different metabolic processes that utilize a variety of electron acceptors.

Despite being from very different environments with different biogeochemical conditions, volumetric H_2ase activity (hydrogen turnover per volume sediment) varies only very little between sites and depth, whereas organic matter reactivity – which ultimately controls microbial activity (Røy et al., 2012) – decreases with depth over several orders of magnitude (Rothman and Forney, 2007; Middelburg, 1989). Considering this apparent discrepancy it appears unlikely that these volumetric H_2ase data can be translated directly into a turnover rate of a specific process, e.g. denitrification, sulfate reduction or methanogenesis. Also, given the recent findings of several processes occurring simultaneously (Wang et al., 2008; Teske,

2012) or cryptic element cycles (Holmkvist et al., 2011), any direct conversion of H_2ase activity into a specific turnover rate would be associated with a considerable error margin.

In order to find a possible relationship between H_2ase activity and specific metabolic processes, we calculated cell-specific H_2ase activity based on our measurements of volumetric H_2ase rates and cell numbers (Figs. 5.4, 5.5 and 5.6). Between all sites and depths, cell-specific H_2ase activity ranged from 10^{-5} to 1 nmol H_2 cell^{-1} d^{-1}.

The different sites that were analyzed in our study differ considerably with regard to their porewater composition and therefore also in the predominant electron acceptor process. All samples from Lake Van, Barents Sea and the Equatorial Pacific had high sulfate concentrations and no detectable methane. Nitrate was detected in the upper few mbsf of both Equatorial Pacific cores, but was absent at all other sites. At the IODP Exp. 308 sites methane was detectable above the SMTZ, almost up to the sediment-water interface. This is rather unusual, as methane is usually completely consumed in the SMTZ (e.g., Treude et al., 2005). We grouped the samples based on their porewater composition. The first group contains all samples with detectable nitrate (nitrate group). The second group is defined by the presence of sulfate and the absence of methane (sulfate group). Samples with detectable methane were labeled methane group, irrespective of their sulfate content. This group was differentiated into a low (<10 ppm) and a high (>10 ppm) methane group. The samples from the high methane group do not contain any sulfate.

The lowest per-cell H_2ase activity rates of ca. 10^{-5} nmol H_2 cell^{-1} d^{-1} were found in the nitrate zone of EQP-05 and EQP-07. It is known that some H_2ases are inhibited by the presence of molecular oxygen (Fisher et al., 1954; Stripp et al., 2009). At the EQP sites this can be ruled out because oxygen was fully depleted in the upper 0.1 mbsf (Røy et al., 2012). However, in the suboxic zone of nitrate reduction (Chapelle, 2001), redox conditions might still be unfavorable for H_2ase enzymes. So far the influence of suboxic conditions on H_2ase activity has not been studied. However, considering the fact that per-cell H_2ase activities increase with decreasing redox levels, the question arises whether nitrate inhibits H_2ase activity or whether microbes involved in denitrification utilize fewer H_2ases than those employing different electron acceptor processes. Per-cell H_2ase activity in the sulfate group samples from Lake Van, Barents Sea and the Equatorial Pacific mostly ranged between 10^{-4} to 5×10^{-2} nmol H_2 cell^{-1} d^{-1}, which is higher than in nitrate group samples.

In the low methane zone (<10 ppm), cell specific H_2ase activity falls in the range of 10^{-3} to 5×10^{-1} nmol H_2 cell^{-1} d^{-1}. There is quite some overlap with the sulfate zone on the

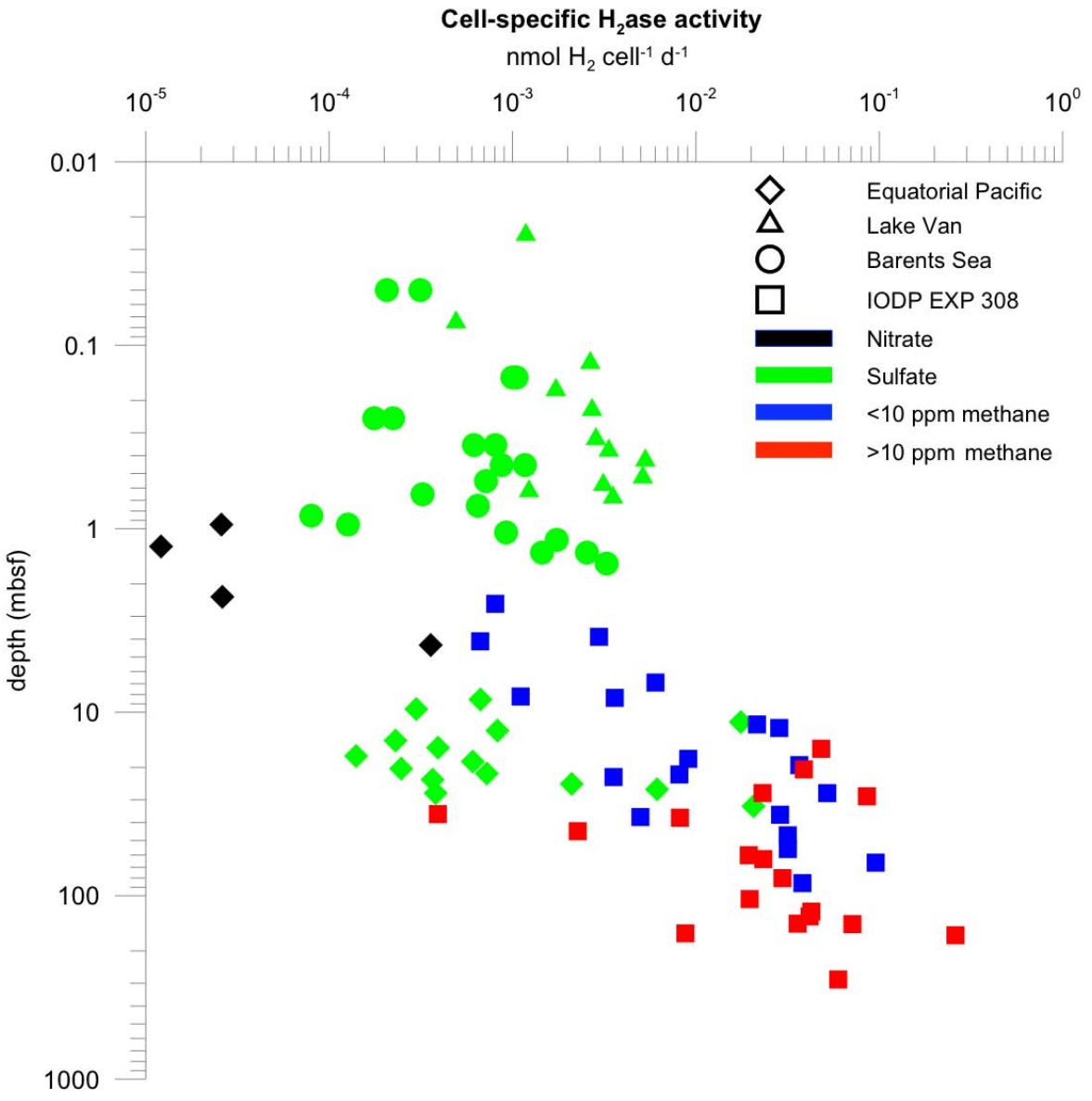

Figure 5.7: *Cell-specific hydrogenase activity distribution along depth. Different colors represent different geochemical zones. Different shapes represent different locations*

low end and the high methane zone on the high end. In the high methane zone (>10 ppm) cell specific H_2ase activity is highest with values between 10^{-2} and 1 nmol H_2 cell^{-1} d^{-1}. This indicates that per-cell H_2ase activity increases when moving down the chain of electron acceptors. Highest values in the high methane zone might be explained by the fact that hydrogen is directly involved in hydrogenotrophic methanogenesis ($CO_2 + 4H_2 \rightarrow CH_4 + 2H_2O$) and indirectly through acetogenesis also in acetoclastic methanogenesis. In comparison to other metabolic activities, higher number of protons and molecular hydrogen are necessary for these processes, requiring a greater number of H_2ases per cell or a higher H_2ase activity to facilitate this process (Vignais, 2008).

When plotting all cell-specific H_2ase activity data against depth and color-coding them according their respective biogeochemical zone (Fig. 5.7) the relationship between per cell H_2ase activity and the predominant metabolic process becomes obvious. Despite considerable scatter the plot shows cell-specific H_2ase activity increasing in the following order: nitrate zone < sulfate zone < low methane zone < high methane zone (Fig. 5.7).

The results were obtained from experiments that were run at room temperature and atmospheric pressure. It is not known what roles temperature and hydrogen availability play in enzyme activity in natural environments, but especially hydrogen has a strong effect on energy yields and may promote or hamper specific reactions (Hinrichs et al., 2006).

Experiments under *in situ* temperature and hydrogen partial pressure might provide more accurate results. However, the processing these samples under high pressure would create significant technical challenges (Sauer et al., 2012) that were beyond the scope of this study. Hydrogenases are a large and structurally diverse family of enzymes (Vignais et al., 2001), so far it is not known what types of H_2ases are involved in particular electron acceptor processes in natural sediment samples. Furthermore, we are unaware of any isotopic discrimination of cellular H_2ase and its impact in our results.

The results show the H_2ase assay is a powerful tool to detect microbial activity in different biogeochemical environments, regardless of porewater chemistry. However, a direct translation into a specific turnover rate is not possible.

Although there is now general consensus that the majority of the microbial population in subsurface sediments is alive and metabolically active (Teske, 2005; Schippers et al., 2005; Parkes et al., 1994), recent findings stress the importance of a more detailed study not just of living and active cells but also spores and necromass (Lomstein et al., 2012). Vuillemin et al. (2013) showed a good correlation between ATP activity and total cell counts in lacustrine sediment drill cores. There were however two horizons that did not correlate. In these horizons there was a considerable amount of bacterial necromass.

Depending on the biogeochemical zone per cell H_2ase activity values vary by several orders of magnitude. Each zone is characterized by its own specific per-cell H_2ase activity value. Despite some scatter this activity can be used as a conversion factor to have an independent quantification of the metabolically active microbial population.

Acknowledgements

This research was funded by the Federal Ministry of Education and Research (BMBF), Germany through the Forschungsverbundvorhaben GeoEn (Grant 03G0671A/B/C), the German Science Foundation (DFG) through the ICDP Priority Program (SPP 1006). We thank the crews and scientific parties of the ICDP PaleoVan drilling campaign, R/V HU Sverdrup, R/V Knorr, and R/V JOIDES Resolution (IODP Expedition 308).

6 Impact of seismogenic fault activities on deep subseafloor life

One sentence summary: Gigantic earthquake and tsunami-genic fault activities have strongly impacted deep subseafloor microbial communities in the accretionary wedge of the Nankai Trough.

Subducting oceanic plates at convergent plate boundaries generate devastating earthquakes and tsunamis through slips propagated in accretionary wedges. The transient faulting decomposes sedimentary structures and produces frictional heat and chemically transforms matter. Here we demonstrate that both the habitat and activity of subseafloor sedimentary microbial communities have been impacted by episodic fault activities in the Nankai Trough seismogenic zone. Cell abundances were up to two orders of magnitude higher above and below the megasplay fault zone. Combined evidence from microbial DNA and lipids as well as hydrogenase activities showed that community compositions, structures, and metabolic activities near the fault zone differed from those in the overlying stratified sediment. Distributions and isotopic compositions of archaeal lipids putatively record a microbial habitat at elevated temperature and with isotopically distinct substrates. We conclude that deep sedimentary microbial habitats on tectonically active continental margins are affected by large fault activities, with the communities being adapted to the associated drastic habitat perturbations.

Marine subsurface sediments on global continental margins harbor remarkably abundant microbial life (Lipp et al., 2008; Parkes et al., 2000; Whitman et al., 1998). Its abundance decreases logarithmically with increasing subseafloor depth (Morono et al., 2009; Parkes et al., 2000), except for sharp increases at geochemical interfaces such as sulfate-methane transition zones (Parkes et al., 2005). Analysis of 16S ribosomal ribonuclic acid (rRNA) gene clone libraries revealed the presence of diverse Bacteria and Archaea in the sedimentary habitats, most of which are uncultured and hence physiologically unknown (Inagaki et al., 2006). The metabolic activity of these organisms is generally extremely low, in correspondence to the slow supply of nutrients to the subseafloor environment (D'Hondt et al., 2004; Jørgensen, 2011). As a result, most subseafloor microbial cells are believed to live under conditions of extreme energy limitation, with mean generation times of up to thousands of years (Jørgensen, 2011; Morono et al., 2011).

At the Nankai Trough, the Philippine Sea plate is subducting below southwest of Japan, making it one of the world's most geologically active accretionary wedges. This site has been the source of multiple gigantic earthquakes and tsunamis (Fukao, 1979). Geological

and geophysical studies suggest that the megasplay fault, which is the primary co-seismic plate boundary-associated thrust structure, slipped during the 1944 Tonankai earthquake and thereby generated devastating tsunamis (Ando, 1975; Moore et al., 2007).

The upper sedimentary strata at Site C0004 at the Nankai Trough seismogenic zone off the Kii Peninsula of Japan, was drilled and investigated down to 398 meter below seafloor (mbsf) during Expedition 316 of the Integrated Ocean Drilling Program (IODP) using the drilling vessel *Chikyu* (Fig. 6.3) (Supplementary Materials Kinoshita et al., 2009). The sedimentary structure has been classified into four lithostratigraphic units: Pleistocene upper slope apron (Unit I, 0–78 mbsf), Pliocene accretionary complex (Unit II, 78–258 mbsf), Pliocene megasplay fault-bounded unit (Unit III, 258–307.5 mbsf), and Pleistocene under-thrust slope basin (Unit IV, 307.5–398.8 mbsf) (Fig. 6.1A) (Supplementary Materials Strasser et al., 2009). Mass-wasting deposits were observed in the upper accretionary prism (i.e., Unit II); zones of intensely brecciated or fractured sediments were observed in sediments under the lower accretionary prism (i.e., Unit IV).

Microbial cell concentrations, determined by computer-based fluorescent image analysis with SYBR Green I stain (Supplementary Materials Morono et al., 2009), decrease logarithmically with increasing depth in the well-stratified upper slope apron sediment from 3.4×10^7 cells cm^{-3} at 0.6 mbsf to 1.2×10^5 cells cm^{-3} at 36.5 mbsf (Fig. 6.1B and Table 6.1). These results are consistent with observations in other continental margin sediments (Whitman et al., 1998; Morono et al., 2009; D'Hondt et al., 2004). However, drastic elevations of cell concentrations by two orders of magnitude were observed in sediments above (225.6 mbsf) and below (320.4 mbsf) the megasplay fault zone (3.7×10^7 and 1.5×10^7 cells cm^{-3}, respectively).

Bulk intracellular deoxyribonuclic acid (DNA) was aseptically extracted from the innermost sub-core samples, purified and concentrated using size-filtration membranes, and then fluorometrically quantified (see Supplementary Materials). The extracted DNA concentrations logarithmically decreased with depth, except for some anomalies from the upper accretionary prism and the underlying megasplay fault zone, where notably high concentrations of DNA ($\sim$38 ng g^{-1} wet sediment) were observed (Fig. 6.1C and Table 6.1). Also, high concentrations of archaeal intact polar lipids (IPLs) were extracted from the megasplay fault boundary ($\sim$44 ng g^{-1} wet sediment) (see Supplementary Materials), while in most other horizons, IPLs were below detection (Fig. 6.1C and Table 6.1). Using the extracted DNA, we quantified relative abundance of bacterial and archaeal 16S rRNA genes using quantitative PCR (Morono et al., 2009, also see Supplementary Materials). Increasing ratios of archaeal 16S rRNA genes were

observed in mass-wasting deposits below the unconformity (∼48% in total prokaryotic 16S rRNA genes) and fault-associated sediments (∼91% in total prokaryotic 16S rRNA genes) (Fig. 6.1F and Table 6.1).

It is worth noting that mismatching primer sequences, which prevents amplification of some archaeal genes, and/or generally low DNA extraction efficiency of archaea and some specific cell forms might cause biases in molecular-based assay. Nevertheless, the cumulative cellular and molecular data strongly suggest microbial responses to geologic processes in sediments associated with the megasplay fault; these processes have repeatedly occurred over the timescales integrated by these various microbial tracers. The proliferation of microbial populations in sediment near the unconformity and megasplay fault zones suggests that the

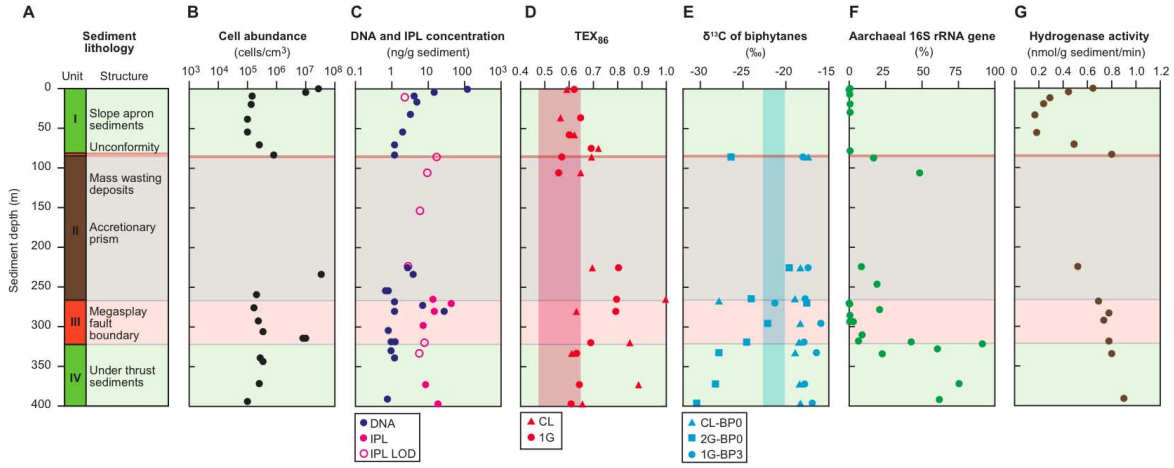

Figure 6.1: *Depth profiles of lithological and microbiological characteristics in sediment at the IODP Site C0004 in the Nankai Trough seismogenic zone: (A) lithologic units; (B) cell abundance evaluated by a fluorescent image-based cell count (Morono et al., 2009); (C) concentration of DNA and intact polar lipid (IPL); glycosidic and diglycosidic GDGT from Archaea), open symbols indicate level of detection of IPL analysis (see Supplementary Materials); (D) Molecular distribution, expressed as the temperature-sensitive TEX_{86} proxy (Schouten et al., 2002), of archaeal GDGT lipids, which were detected as either monoglycoside (1G) or core lipid (CL); shaded area reflects predicted TEX_{86} values based on reconstructed minima and maxima of sea surface temperatures during the late Quaternary (Yamamoto et al., 2004) and during the mid Pliocene (Dowsett et al., 1996) in the NW Pacific around Japan, resulting in a range of 13° C to 24° C, in combination with the temperature calibration (Schouten et al., 2002); (E) stable carbon isotopic compositions, ^{13}C, of biphytanes derived from CL-GDGT, 1G-GDGT, and diglycosidic (2G) GDGT; bp0 designates the acyclic biphytane, bp3 the tricyclic, crenarchaeol-related derivative with two cyclopentane and one cyclohexane moieties; for reference, the shaded area designates the typical range of carbon isotope values of found in bps from planktonic archaea (Hoefs et al., 1997); availability of bp isotope values in some samples for which IPL concentration in panel C indicates "below level of detection" is due to different analytical protocol involving purification of selected compounds (see Supplementary Materials); (F) relative ratio of archaeal 16S rRNA genes in total prokaryotic (archaeal and bacterial) 16S rRNA genes estimated by quantitative PCR (see Supplementary Materials); (G) hydrogenase activity measured by radiotracer incubation experiments using trititated hydrogen (see Supplementary Materials Soffientino et al., 2009). The data reported in this figure are tabulated in the Supplementary Materials.*

physical and energetic conditions that affect habitability in the sedimentary complex differ from the stratified sedimentary sequences that have previously been explored by scientific ocean drilling. We infer that disturbance of sedimentary structures caused by the episodic fault activities in the Nankai Trough generates niches for microbial life (Sleep and Zoback, 2007; Sherwood Lollar et al., 2007).

Recently, Hirose et al. (2012) have demonstrated that notable concentrations of hydrogen can be produced via mechano-radicals formed by friction of marine sediment in the course of fault activities. To examine the potential effect of hydrogen on the extant subseafloor microbial communities, we examined hydrogenase enzyme activities (see Supplementary Materials Soffientino et al., 2009); activity was observed in all sediment samples examined. In the slope

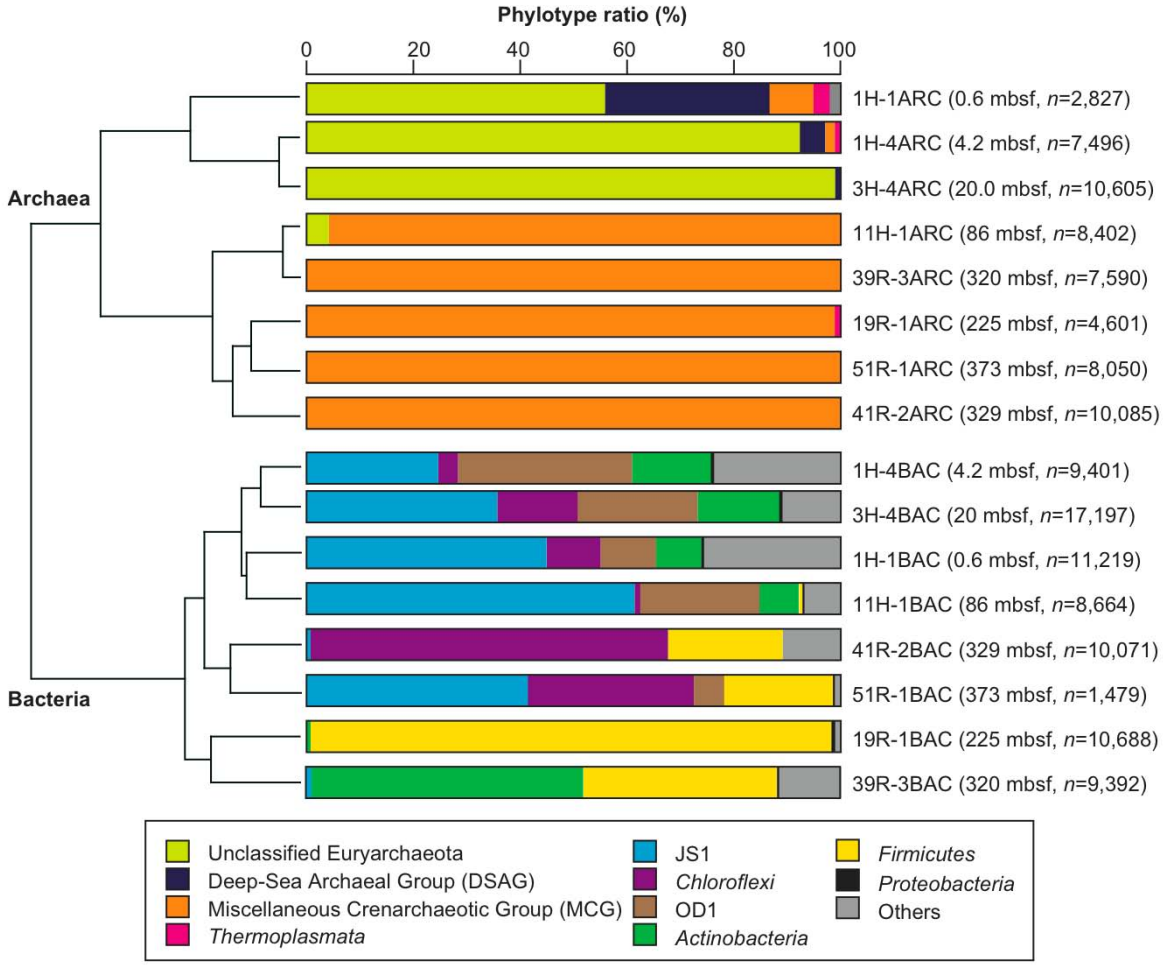

Figure 6.2: *Comparison of bacterial and archaeal communities at Site C0004 using phylogenetic information of 16S rRNA gene tag-sequence data. The UniFrac tree indicates the similarities and phylogenetic relationships among the communities from multiple depth layers (see Supplementary Materials). Bar graphs show the ratio of 16S rRNA gene fragments based on cluster analysis at the phylum level (see Supplementary Materials). Following each sample code, depth (meters below the seafloor: mbsf) and number of sequence reads (n) are provided in parentheses (see Table 6.1).*

apron sediment (i.e., Unit I), hydrogenase activity decreased with increasing depth before sharply increasing to a maximum mean value of 0.8 nmol min^{-1} g^{-1} wet sediment above the fault unconformity (Fig. 6.1G). In deeper horizons, a constant increase in hydrogenase activity to generally higher values than those in shallow sediment was observed (Fig. 6.1G). These data suggest that microbial activity and population size are stimulated by hydrogen, which may have been generated by the fault activity.

The response of deep-subseafloor biosphere to geological processes associated with seismogenic fault activity was also observed by the analysis of 16S rRNA gene-tagged PCR fragments using a 454 sequencer (see Supplementary Materials Sogin et al., 2006; Hoshino et al., 2011). Bacterial communities were generally more diverse than archaeal communities (Table 6.1). Phylogenetic clustering analysis of bacterial and archaeal 16S rRNA gene tagged-sequences revealed that microbial compositions clearly differed between the stratified slope apron (Unit I) and the fault-associated sedimentary habitats (Unit II, III and IV) (Fig. 6.2). In upper slope apron sediments, 45% of the bacterial tag-sequences were affiliated with the JS1 candidate division, and archaeal tag-sequences were predominantly composed of previously unclassified members within the Euryarchaeota and the Deep-Sea Archaeal Group (DSAG). By contrast, 53% of bacterial tag-sequences from megasplay fault-associated layers were affiliated with the Firmicutes, and almost 99.9% of the archaeal sequences were affiliated with the Miscellaneous Crenarchaeaotic Group 1 (MCG-1). Statistic analysis of tag-sequence assemblages using the UniFrac software Lozupone et al. (2007) clearly demonstrated the compositional change of microbial communities in these sedimentary habitats (Fig. 6.2). Interestingly, most bacterial tag-sequences obtained from the fault-associated core samples were related to the phyla that include spore-forming bacteria (i.e., Firmicutes, Actinobacteria), suggesting that seismogenic fault activities have stimulated the germination of spores buried in the sedimentary habitat.

Important complementary information on microbial responses to geologic processes associated with the megasplay fault was obtained via analysis of archaeal CLs and IPLs (see Supplementary Materials). While the first lipid group is generally considered to be largely reflective of planktonic archaeal communities (Liu et al., 2011), the latter is viewed as diagnostic of sedimentary archaea (e.g., Lipp and Hinrichs, 2009). In analogy to DNA-based assays applied to sediments (Dell'Anno and Donavaro, 2005), IPLs in low-activity subseafloor environments may comprise a fossil component (cf. Lipp and Hinrichs, 2009; Schouten et al., 2010) but given the long residence time of sediment and the hosted microbial communities in the megasplay fault, both lipid pools probably record microbial responses to geological processes in this

unique habitat. Indeed, both lipid pools exhibit anomalous signals in depth horizons in or close to the megasplay fault that are consistent with lipid biosynthesis under elevated temperatures by sedimentary archaeal communities such as the dominant MCG-1.

Specifically, TEX_{86} ratios, i.e., molecular paleo-sea surface temperature proxies based on the relative distribution of the minor cyclopentane and cyclohexane-bearing archaeal glycerol dialkyl glycerol tetraethers (GDGT) (Schouten et al., 2002), show anomalously high values of close to 1 in strata around the megasplay fault (Fig. 6.1D) and coincide with the peaks in archaeal IPLs (Fig. 6.1C); these high TEX_{86} values are inconsistent with the paleoceanographic regime during the geologic period recorded at Site C0004 (see Supplementary Materials Dowsett et al., 1996; Yamamoto et al., 2004) and strongly suggest an overprint of the planktonic lipid population by benthic lipid biosynthesis at elevated temperature. This overprint is further corroborated by the isotopic composition of acyclic biphytane (bp0; Fig. 6.1E), which is predominantly derived from acyclic GDGT, a putative major lipid of benthic archaeal communities (Liu et al., 2011; Lipp and Hinrichs, 2009). The most variable as well as lowest carbon isotopic compositions of bp0 coincide with horizons, in which both IPL concentrations and TEX_{86} values indicate new production of archaeal lipids. The cumulative lipid signals provide strong evidence that recent geophysical and/or geochemical processes have repeatedly affected microbial communities located near the megasplay fault zone. The temperature signal recorded in the lipid distribution as well as the inferred stimulation of microbial growth by heat-generated substrates is consistent with friction due to fault activity causing locally confined transient temperature increases as recorded by vitrinite reflectance of organic matter in the megasplay fault zone (suggesting temperatures of up 390±50°C, ref. Sakaguchi et al., 2011) and mineralogical alterations (e.g., smectite-illite reaction, ref. Yamaguchi et al., 2011).

Alternatively, it can be explained by other geochemical and/or geophysical factors that potentially impact on nutrient and energetic conditions of indigenous subseafloor life: e.g., geochemical analyses of pore waters showed anomalies such as lower pH (∼6.5), and peaks in concentrations of iron (∼100 µmol L^{-1} and manganese (∼12 µmol L^{-1}) near the upper unconformity and megasplay fault boundaries (Kinoshita et al., 2009). These anomalies are also consistent with enhanced microbial activity linked to metal reduction and diagenesis of organic matter in these zones.

Multiple converging lines of evidence strongly suggest that tectonically mediated physical and chemical alterations, triggered by frictional heat released within the fault, result in unique type of geosphere-biosphere interaction. New generations of microbial assemblages,

which could have survived drastic environmental changes as spores or other dormant cell forms, were potentially activated at such geological interfaces. Consequently, we infer that dynamic movement of oceanic plates may play significant geobiological and ecological roles in physiological adaptation and evolution of subseafloor life and the deep biosphere.

Acknowledgments

This research used samples and data provided by the Integrated Ocean Drilling Program (IODP). We thank the crews, technical staffs and shipboard scientists of the drilling vessel Chikyu for their support of sampling during the IODP Expedition 316. We thank S. Tanaka, S. Fukunaga and N. Masui for technical support and N. Ohkouchi, M. Strasser and A. Kopf for useful discussion. This study was supported in part by the Strategic Fund for Strengthening Leading-Edge Research and Development (to JAMSTEC) and the Funding Program for Next Generation World-Leading Researchers (NEXT Program, to F.I.) by the Japan Society for the Promotion of Science (JSPS) and the Ministry of Education, Culture, Sports, Science and Technology, Japan (MEXT). Support for K.-U.H. and J.S.L. was provided by the Deutsche Forschungsgemeinschaft through grant HI 616-9 (C-Nankai). The work of Y.T. was supported in part by a research grant from the J-DESC internship program between Japan and Germany (FY2009). The work was also supported by the Academy of Finland (no. 122394), the Finnish Funding Agency for Technology and Innovation (no. 40149/07), the Osk Huttunen's Foundation, and the Finnish Cultural Foundation (to A.H.K.).

Supplimentary Materials

Materials and Methods

Sample preparation

All sediment samples were subsampled onboard the deep-earth drilling vessel *Chikyu* during the IODP Expedition 316 in 2008 (Fig. 6.3). Ten centimeter of whole round cores were taken at the QA/QC laboratory on *Chikyu* after core recovery, and immediately stored at -80°C. After the frozen cores were delivered to the shore-based laboratory, they were cut with diamond powder-etched band saw (RYOWA, Chiba, Japan), into pieces of approximately 0.5 cm×1 cm×10 cm geometry bars without melt (Masui et al., 2009). The innermost part of core samples was used for molecular analyses to avoid potential contamination from the seawater-based drilling fluid.

For cell count, 1 cm^3 of the innermost sediment was taken from 10 cm whole round cores by 3 ml tip-cut sterilized syringe in a lamina-flow clean bench, and then fixed with 2% (wt/v) paraformaldehyde in phosphate buffered saline (PBS) buffer (pH 7.6) for 6 hours at 4°C. The fixed slurry samples were washed twice with PBS buffer, filled up to 10 ml with PBS-ethanol (1:1) solution, and then stored at -20°C. All sample preparation was performed in the microbiology laboratory on *Chikyu*.

Cell count

Fifty microliter of fixed slurry was mixed with 3% NaCl, sonicated at 20 W for 1 min, treated with 1% hydrofluoric acid for 20 min, and then filtered through a polycarbonate membrane (0.22 µm in pore size, Millipore, Japan). The membrane retained on the filtration device (Millipore, Japan) was immersed in 1 ml of 0.1 mol L^{-1} HCl for 5 min, washed with 5 ml of TE buffer (10 mM Tris-HCl, 1.0 mM EDTA, pH 8.0) containing approximately 1×10^8 os beads that fluoresce only under UV excitation, and air-dried. Approximately a quarter of the membrane was cut, placed on a cellulose acetate membrane (ADVANTEC, Japan) and placed in SYBR Green I staining solution (1:40 [v/v] SYBR-I in TE buffer) for 10 min. The staining solution was removed by vacuum filtration and the membranes were placed on glass microscope slides and mounted with 3 µL of mounting solution (2:1 mixture of VECTASHIELD mounting medium H-1000 and TE buffer). Cell number on the membrane was counted using an automated epifluorescent microscope (Olympus BX-51) and slide-loader system with a

band-pass filter of 490/20 nm (center wavelength/bandwidth) for excitation and a long-pass filter at 510 nm-cutoff (Morono et al., 2009; Morono and Inagaki, 2010).

DNA extraction, purification and quantification

Bulk environmental DNA was extracted from 10 g of the frozen sediment using a Power Max Soil DNA Isolation Kit (MoBIO Lab. Inc., CA) with 3 additional autoclaved metal beads (5 mm in diameter) per tube according to the manufacturer's instructions, followed by the concentration of DNA with Montage PCR centrifugal filter devices (Millipore, MA). The final

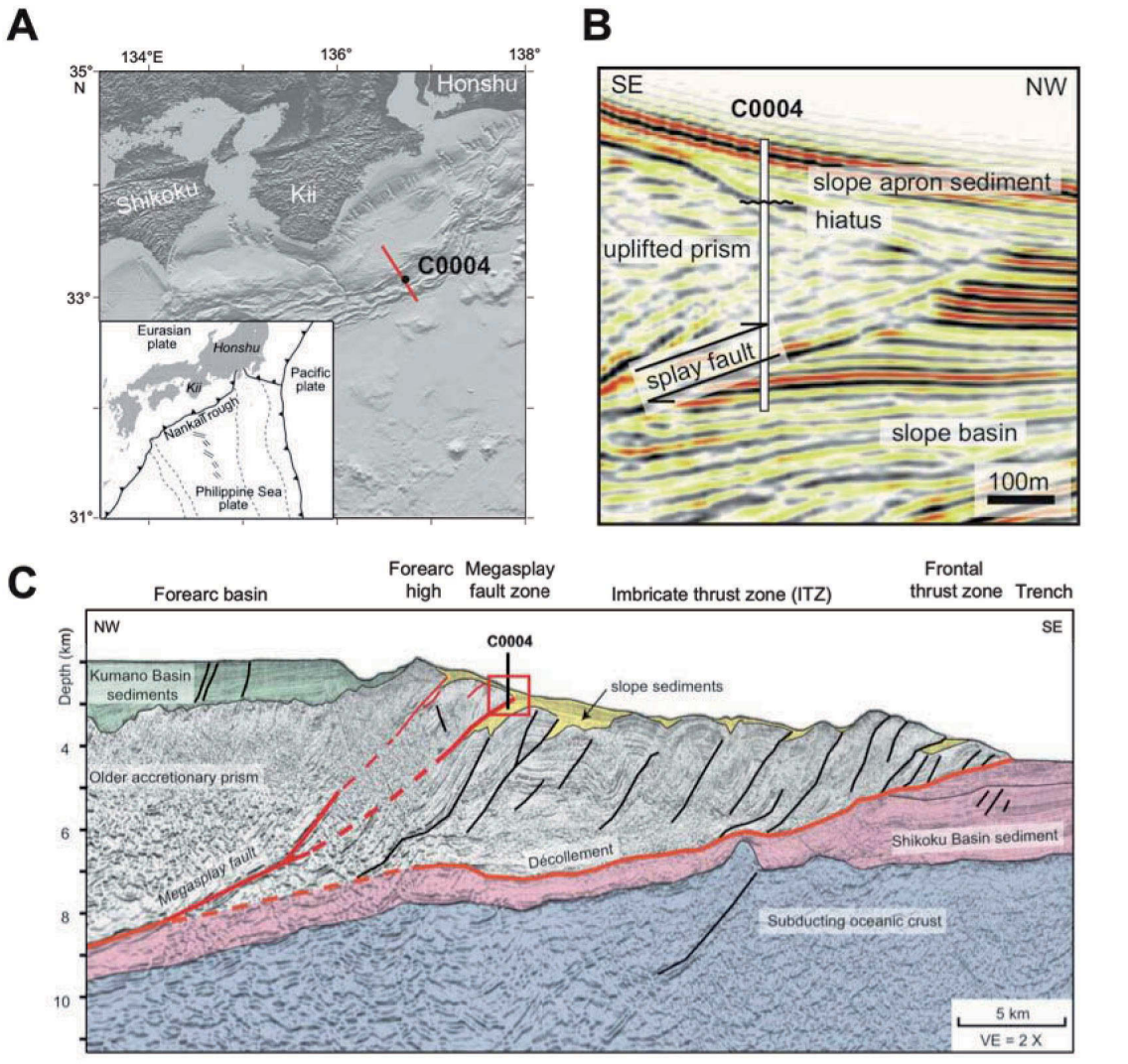

Figure 6.3: *Geological setting of Site C0004 in the Nankai Trough seismogenic zone. (A) Location map of Site C0004 in the Nankai Trough off Kii Peninsula of Japan. The red line shows the seismic transect as in (C). (B) Structural interpretation of the shallow megasplay fault zone based on the seismic line (IL2675) crossing Site C0004. (C) Interpreted composite seismic line of the Nankai subduction zone (Strasser et al., 2009).*

concentration of DNA was measured using a Quanti-iT DNA assay kit (Life technologies, CA), and the DNA samples were stored at -20°C until further use. Since several trials for PCR amplification of bacterial and archaeal 16S rRNA genes yielded negative results, DNA samples were amplified with multiple displacement amplification using GenomiPhi V2 Kit (GE Healthcare) for the subsequent PCR amplification. Genome amplifications were monitored by real-time PCR with SYBR Green I (Lipp et al., 2008). No amplifications from negative control samples (i.e., without sediment samples) were observed. To estimate relative abundance of archaeal and bacterial 16S rRNA genes was performed with a Power SYBR Green PCR Master Mix by ABI 7300 real-time PCR system (Applied Biosystems, Foster City, CA) according to the published method by Lipp et al. (2008).

DNA sequence analysis

PCR amplification of 16S rRNA gene fragments was conducted with the primers EUB27F (Amann et al., 1990) and EUB338Rmix (I: 5'-ACTCCTACGGGAGGCAGC-3', II: 5'-ACACCTA CGGGTGGCTGC-3', III: 5'-ACACCTACGGGTGGCAGC-3') (Frank et al., 2008) for bacteria, and ARC21F (5'-TTCCGGTTGATCCYGCCGGA-5') (DeLong, 1992) and ARC912R (I: 5'- CCCCCGCCAATTCCTTTAA -3', II: 5'-CCCCCGTCAATTCCTTCAA -3', III: 5'-CCCCCGCCAATTTCTTTAA -3') (Miyashita et al., 2009) for archaea, with some modifications from the sequences in the original publication as shown above. For sequencing using a GS FLX pyrosequencer (454 Life Sciences, Branford, CT), another amplification (6 cycles) was performed using primers (EUB27F and EUB338Rmix for bacteria, and UNIV530F [I: 5'-GTGCCAGCMGCCGCGG-3', II: 5'-GTGTCAGCCGCCGCGG-3'] and ARC912R for archaea) with 454 FLX Titanium adapters A, B, and a 6-base sample identifier tag. Purification of the amplified product, quality checks, and sequencing with the GS FLX pyrosequencer were conducted by TaKaRa Bio Inc. (Shiga, Japan).

All of the reads, including sample identifier tags and primer sequences, were first processed with Pipeline Initial Process (`http://pyro.cme.msu.edu/init/form.spr`), which is part of the Ribosomal Database Project (Cole et al., 2009). Parameters for Pipeline Initial Process are; forward primer max edit distance: 2, max number of N's: 0, minimum average exp. quality score: 20, reverse primer max edit distance: 0, min sequence length: 150. Reads that did not match the tags and primer sequences were also eliminated through this process. Chao-1 estimator (Chao, 1987) and Shannon diversity index (Krebs, 1989) were calculated with OTU cut-off of 97% sequence similarity (Table 6.1). Taxonomic classification of each processed read

was assigned by BLAST analysis with a customized computer script using the ARB SILVA sequence package (Pruesse et al., 2007) as the database.

Hydrogenase assay

Hydrogenases are a family of ubiquitous enzymes that catalyze the heterolytic cleavage of molecular hydrogen into electrons and protons to be used for adenosin 5'-triphosphate (ATP) synthesis, thereby coupling energy-generating metabolic processes to electron acceptors such as carbon dioxide or sulfate (Stephenson and Stickland, 1931; Vignais, 2008). Because of the important role of hydrogen in basically all metabolic strategies and the fact that hydrogenases occur only intracellularly, hydrogenase enzyme activity can be used as a robust measure of total metabolic activity without the need to identify any specific metabolic process (Adhikari and Kallmeyer, 2010; Soffientino et al., 2009). Hydrogenases also facilitate isotopic exchange reactions between hydrogen gas and water molecules (Schink et al., 1983). In our study we measured the rate of production of tritiated water facilitated by the enzyme.

The gas handling system and sample processing are similar to Soffientino et al. (2009). Trititated hydrogen (37 GBq) is stored in a 1-L stainless steel cylinder that is connected to a headspace reservoir, in which the tritiated gas is diluted to the desired specific radioactivity with an ultrapure H_2/N_2 (20/80 [v/v]) gas mixture. Hydrogenases are very sensitive to oxygen; therefore last traces of oxygen present in the diluent gas are removed by bubbling through $CrCl_2$ solution.

About 2-3 g of frozen sediments were placed in 50 ml ground glass syringes with the plunger removed and mixed with 10 ml anoxic autoclaved synthetic seawater under a continuous stream of N_2 gas. After insertion of the plunger, and complete removal of the N_2 headspace, 30 cm^3 tritiated gas headspace as described above were loaded into the syringe. For a negative control 500 µL of saturated $HgCl_2$ solution was added to the slurry and processed like a regular sample. Incubation is performed at room temperature on a rotary shaker to facilitate sufficient gas exchange between the headspace and the slurry. Subsamples were taken after 30, 60, 120, 180, and 240 minutes by withdrawing few drops of slurry. The subsample was degassed to remove unreacted dissolved gas and then centrifuged to remove sediment particles. 100 µL of the supernatant was taken off and radioactivity of the tritiated water quantified by liquid scintillation counting.

The rate of hydrogen exchange, which is proportional to enzyme activity, was calculated using the specific activity of the headspace, sample weight, and the volume of synthetic

seawater added. For quantification of the specific activity of the headspace, tritiated water was produced by reacting 500 µL of headspace gas with oxygen inside a reaction chamber containing a platinum catalyst. The tritiated water was then trapped in 5 ml of distilled water and the activity was measured by liquid scintillation counting.

Extraction of membrane lipids

About 50 g to 100 g of wet sediment was extracted using a modified Bligh and Dyer protocol (Sturt et al., 2004) after addition of 10 µg of internal standard (PAF, 1-O-hexadecyl-2-acetyl-sn-glycero-3-phosphocholine). In brief, 4 extraction steps with each 120 ml of a mixture consisting of methanol, dichloromethane (DCM), and aqueous buffer in a ratio of 2:1:0.8 (v:v:v) were added. The first two steps used phosphate buffer (8.7 g L^{-1} KH_2PO_4, pH 7.4) and the last two steps used trichloroacetic acid buffer (50 g L^{-1}, pH 2). The mixture was ultrasonicated for 15 min in an ultrasonic bath and after centrifugation at 800 ×g for 10 min. the supernatant was transferred to a separatory funnel. After the last extraction step, phase separation was achieved by the addition of 120 ml DCM and 120 ml Milli-Q water. The aqueous phase was washed three times with 30 ml DCM and the combined organic phases were then washed three times with 30 ml Milli-Q water. The organic phase was then evaporated to dryness under a nitrogen stream and stored as total lipid extract (TLE) at -20°C until further analysis.

Analysis of intact polar lipids by high-performance liquid chromatography

An aliquot of the TLE was analyzed by injection on a ThermoFinnigan Surveyor HPLC system coupled to a ThermoFinnigan LCQ Deca XP Plus ion trap mass spectrometer according to the methods published by Sturt et al. (2004) and Lipp et al. (2008). The intact polar lipids were separated according to head group polarity on an Alltech LiChrospher Diol-100 column (150×2.1 mm, 5 µm particle size) with a gradient from 100% A to 65% B over 45 min and the following eluent composition: eluent A is a mixture of 79 : 20 : 0.12 : 0.04 (hexane, isopropanol, formic acid, ammonia) and eluent B is mixed from 89 : 10 :0.12 : 0.04 (isopropanol, Milli-Q water, formic acid, ammonia). Quantification was done with peak areas from mass chromatograms of compounds of interest relative to the peak area of the internal standard PAF assuming an identical response factor. The level of quantification was calculated from the peak area of a typical noise peak assuming a signal-to-noise ratio of three (Lipp et al., 2008).

Preparation of fractions containing core, monoglycosidic, and diglycosidic tetraether lipids by preparative chromatography

A subset of 13 samples was selected for preparation of pure fractions containing only core, monoglycosidic, and diglycosidic GDGTs. Fractions were prepared using a preparative high-performance liquid chromatography (HPLC) system with a fraction collector following established parameters (Biddle et al., 2006; Lipp and Hinrichs, 2009). The TLE was injected in three aliquots on a Alltech LiChrospher Si60 column (250×10 mm, 5 µm particle size, Alltech, Germany) and separated with the following gradient: 100% A to 100% B in 120 min, followed by 30 min reequilibration with 100% A; eluent A consisted of a mixture of 79 : 20 : 0.12 : 0.04 of hexane : isopropanol : formic acid : ammonia, and eluent B was comprised of a mixture of 89 : 10 : 0.12 : 0.04 of isopropanol : Milli-Q water : formic acid : ammonia. Three fractions were collected: F1 containing core GDGTs (10–15 min), F2 containing monoglycosidic GDGTs (20–45 min), and F3 containing diglycosidic GDGT (45–50 min). All fractions were evaporated and checked for purity by analytical HPLC-mass spectrometry (HPLC-MS) before further treatment.

Analysis of ring distribution of apolar and polar tetraether lipids and calculation of TEX_{86} and ring indices

After preparative separation of the three lipid classes containing zero, one, and two sugars as head groups, the ring distribution was determined from apolar derivatives by HPLC-MS. The mono- and diglycosidic GDGT were first hydrolyzed by addition of 1 ml of a mixture of DCM : methanol : 6 N HCl (1 : 10 : 1) and heated to 80°C for 1 h according to the procedure outlined in Lipp and Hinrichs (2009). The untreated apolar fraction and the freshly prepared hydrolyzed derivatives were analyzed according to a procedure modified from Hopmans et al. (2000). In brief, an aliquot was injected to an Alltech Prevail Cyano column (150×2.1 mm, 3 µm particle size) used in a ThermoFinnigan Surveyor HPLC system coupled to a ThermoFinnigan LCQ Deca XP Plus ion trap mass spectrometer or an Agilent 1100 MSD. The gradient was as follows: 99% A/1% B to 98.2% A/1.8% B in 45 min, followed by flushing of the column with 10% B for 10 min before re-equilibration for 15 min; eluent A was hexane and eluent B was isopropanol. The relative distribution of GDGT with different numbers of rings were quantified from mass chromatograms of m/z 1302, 1300, 1298, 1296, and 1292 for GDGT-0, GDGT-1, GDGT-2, GDGT-3, and GDGT-5 (crenarchaeol, including crenarchaeol regioisomer GDGT-5'), respectively.

TEX_{86} was calculated according to the equation by Schouten et al. (2002):

$$TEX_{86} = \frac{[GDGT-2]+[GDGT-3]+[GDGT-5']}{[GDGT-1]+[GDGT-2]+[GDGT-3]+[GDGT5']}$$

Preparation of biphytane derivatives

An aliquot of 90% of the fractions containing purified GDGT was ether-cleaved to yield biphytanes following the procedure outlined in Jahn et al. (2004). In brief, 200 µL of a 1M solution of BBr_3 in DCM was added to a dry aliquot of the organic phase. After reaction at 80°C for 2 h, the mixture was evaporated to dryness and 300 µL of superhydride (1M lithium triethylborohydride in tetrahydrofuran) was added. The reaction was done at 80°C for 2 h before 500 µL deionized water was added for quenching. The water phase was washed six times with 500 µL hexane and the organic phase was evaporated before purification by elution with 8 ml of hexane from a column packed with 500 mg silica gel. As internal standard, 200 ng of cholestane was added before injection.

Table 6.1: *Microbial community structure analyzed by 16S rRNA gene-tagged sequences obtained from sediment core samples at Site C0004 in the Nankai Trough seismogenic zone.*

Sample ID	Depth (mbsf)	Target domain	Number of sequence read	Shannon index (H')	Chao-1 estimate	Evenness (E)
1H-1	0.6	Archaea	2827	4.63	440.2	0.80
1H-1	0.6	Bacteria	11219	5.15	1264.4	0.75
1H-4	4.2	Archaea	7496	3.20	250.5	0.59
1H-4	4.2	Bacteria	9401	3.87	149.2	0.84
3H-4	20	Archaea	10605	2.64	162.4	0.52
3H-4	20	Bacteria	17197	4.20	691.8	0.66
11H-1	86	Archaea	8402	2.53	154.2	0.51
11H-1	86	Bacteria	8664	2.52	54.5	0.66
19R-1	225	Archaea	4601	2.78	121.0	0.59
19R-1	225	Bacteria	10688	3.30	265.3	0.60
39R-3	320	Archaea	7590	2.80	167.7	0.55
39R-3	320	Bacteria	9392	3.69	432.0	0.64
41R-2	329	Archaea	10085	2.58	162.0	0.51
41R-2	329	Bacteria	10071	3.01	329.9	0.54
51R-1	373	Archaea	8050	3.41	185.7	0.66
51R-1	373	Bacteria	1479	3.05	152.8	0.66

Analysis of concentrations and carbon isotopic composition of biphytanes

Concentrations of biphytanes were determined by gas chromatography–flame ionization detector (GC-FID) on a ThermoFinnigan Trace gas chromatography (GC) equipped with a Rxi-5ms capillary column (Restek GmbH, Bad Homburg, Germany), or an Ultra-2 capillary column

(Agilent Technology, USA). The GC used helium as carrier gas at a constant flow rate of 1 ml min^{-1} and 1 µL of sample was injected in splitless mode. The temperature program used was: hold at 60°C for 1 min, then ramp up at 10°C min^{-1} to 150°C, then heat at 4°C min^{-1} to 320°C before holding for 27 min at 320°C. Stable carbon isotopic compositions were analyzed on a Trace GC Ultra GC (Thermo Scientific GmbH, Bremen, Germany) or a Agilent 6890N GC (Agilent Technologies, USA) coupled to a GC Combustion III interface and a Delta Plus XP Plus isotope mass spectrometer (Thermo Scientific GmbH, Bremen, Germany). The GC temperature program was identical to the one used for GC-FID analysis. The resulting stable carbon isotope values are expressed as $\delta^{13}C$ values in ‰ relative to the Vienna PeeDee Belemnite standard.

7 Conclusions and outlook

Conclusions

The aim of this thesis was to estimate total living biomass and to understand its role in biogeochemical cycles in various subsurface environments using different methods including cell enumeration and microbial turnover rate measurements. Microbial cell enumeration and cell size determination provide information about total biomass but can neither differentiate between living and dead cells and between metabolically active and dormant microbes. A tritium-based hydrogenase enzyme assay provides information about the activity of metabolically active microbial biomass.

In order to understand microbial abundance and its variation in subsurface sediments cell abundance was measured at several sites. Additionally published subseafloor cell count data were compiled. Microbial cell numbers in these environments range from 10^9 to 10^3 cells cm^{-3} sediment. The highest number of microbes was found close to the sediment-water interface, where relatively high amounts of nutrients are available for microbial metabolism. Cell numbers decreased logarithmically with depth, eventually reaching the current limit of detection of $\sim 10^3$ cells cm^{-3}. The variation in subseafloor microbial abundance is strongly correlated to the mean sedimentation rate and distance from land. Based on these correlations the global subseafloor sedimentary microbial population was estimated to be 2.9×10^{29} cells, which is ca. 0.6% of Earth's total living biomass. This new estimate is significantly lower than all previous estimates, because a much larger database was used, covering all major oceanic provinces.

In order to better understand the impact of subseafloor microbes on biogeochemical cycles, microbial metabolic activity and abundance in equatorial Pacific and north Pacific Gyre sediments were measured. In the north Pacific Gyre sedimentation rate is extremely low (1 mm ky^{-1}), concomitantly the supply of fresh organic matter is also extremely low. Due to the low input of organic matter the sediments remain oxygenated down to tens of meters below the seafloor. At the equatorial Pacific sites, where primary productivity in the surface waters is higher, the input of fresh organic matter also increases. At these sites oxygen is consumed within a few centimeters due to higher rates of microbial activity.

To deal with the questions how microbes can survive in subsurface environments, we reviewed currently available techniques for quantification of microbial activity in subsurface sediments. Most of these techniques are designed to identify and quantify a single specific metabolic

process rather than an overall microbial activity. ATP analysis and hydrogenase enzyme assay were the most promising techniques to quantify activity of total living microbes. Since ATP analysis has some major technical issues, especially in subsurface sediments with extremely low microbial metabolism, a tritium hydrogenase enzyme assay turned out to be the most promising technique.

For the quantification of microbial activity in subsurface sediments, a tritium-based hydrogenase enzyme assay was applied to samples from various sites, covering a wide range of environmental conditions and ranging from a few centimeters below the sediment surface to hundreds of meters below the sea floor. Since the assay measures the catalytic activity of hydrogenase enzymes which are ubiquitous in all microbes and only occurs intracellularly, it should represent the total activity of the microbial population. We measured hydrogenase activity in various subsurface environments and found that hydrogen turnover is ubiquitous in subsurface environment, which we interpret as the presence of hydrogenase enzymes. Although we consider the assay to be an important tool for the quantitative study of enzymatic metabolism in subsurface sedimentary environments, it does not allow for the direct conversion of hydrogenase activity into a turnover rate of a specific process. Instead, it rather provides an independent quantification of the metabolically active microbial population.

Hydrogenase activity in the sediment taken at the Nankai Trough seismogenic zone off the Kii Peninsula of Japan (IODP Expedition 316) was measured to examine the potential effect of hydrogen on the extant subseafloor microbial communities. In deeper horizons, a constant increase in hydrogenase activity to generally higher values than those in shallow sediments was observed. The measurements suggest that microbial activity and population size are stimulated by hydrogen, which may have been generated by the fault activity.

In our study about global subsurface biomass, we revised size and distribution of global subseafloor microbial biomass and reduced it significantly. Despite the major reduction, the subseafloor microbial biosphere remains an important but still enigmatic player in global biogeochemical cycles. A tritium-based hydrogenase enzyme assay was used to quantify the total microbial activity in subsurface sediments. Cell-specific hydrogenase activity data show that per-cell enzyme activity varies by several orders of magnitude and increases with decreasing energy yield, which is controlled by the different electron acceptors. The assay does not provide a direct measure of total microbial activity but rather for the quantification of the metabolically active microbial population.

Outlook

There are many challenges in understanding subsurface life; from access to samples over recreating *in situ* conditions in the laboratory to extrapolating results over geological time scales. So, in order to advance our current understanding of the subsurface biosphere, we need to develop new techniques and improve the current methods based on field, laboratory and theoretical studies.

In subsurface sediments several metabolic processes may occur simultaneously at the same time. In order to understand these processes, measuring only a single specific turnover rate would not provide a complete picture. So, an understanding of the limitations of these individual techniques and comparing them with other methods that measure overall activity is necessary for an accurate image of microbial activity. A tritium-based hydrogenase enzyme assay, which is one of the main topics of this thesis, provides information about the activity of metabolically active microbes in subsurface sediments.

Some general improvements and measurements are essential to improve our ability to explore the subsurface biosphere:

- Differentiation between live, dead, active and dormant cells
- Measurement and comparison of specific turnover rates for example SRR, AOM with hydrogenase and ATP activity
- Measurement of hydrogen concentration to better understand hydrogen metabolism and its utilization as energy source in deep subsurface
- PCR amplification or sequencing of hydrogenase genes to identify different types of hydrogenase enzymes

References

Adams, M. et al. (1990). The structure and mechanism of iron-hydrogenases. *Biochimica et biophysica acta*, 1020(2):115.

Adams, M. W. W., Mortenson, L. E., and Chen, J.-S. (1981). Hydrogenase. *Biochimica et Biophysica Acta*, 1118:167–204.

Adhikari, R. R. and Kallmeyer, J. (2010). Detection and quantification of microbial activity in the subsurface. *Chemie Der Erde-Geochemistry*, 70:135–143.

Albracht, S. P. (1994). Nickel hydrogenases: In search for the active site. *Biochimica et Biophysica Acta G General Subjects*, 1188:167–204.

Amann, R., Binder, B., Olson, R., Chisholm, S., Devereux, R., and Stahl, D. (1990). Combination of 16S rRNA-targeted oligonucleotide probes with flow cytometry for analyzing mixed microbial populations. *Applied and environmental microbiology*, 56(6):1919–1925.

Amend, J. P. and Teske, A. (2005). Expanding frontiers in deep subsurface microbiology. *Palaeogeography, Palaeoclimatology, Palaeoecology*, 219:131–155.

Anand, S. R. and Krasna, A. I. (1965). Catalysis of the H_2-HTO exchange by hydrogenase. A new assay for hydrogenase. *Biochemistry*, 4(12):2747–2753.

Anderson, R., Chapelle, F. H., and Lovley, D. R. (2001). Comment on "Abiotic controls on H_2 production from basalt-water reactions and implications for aquifer biogeochemistry". *Environmental Science & Technology*, 35(7):1556–1557.

Ando, M. (1975). Source mechanisms and tectonic significance of historical earthquakes along the Nankai Trough, Japan. *Tectonophysics*, 27(2):119–140.

Antia, A. N., Koeve, W., Fischer, G., Blanz, T., Schulz Bull, D., Scholten, J., Neuer, S., Kremling, K., Kuss, J., Peinert, R., Hebbeln, D., Bathmann, U., Conte, M., Fehner, U., and Zeitzschel, B. (2001). Basin-wide particulate carbon flux in the Atlantic Ocean: Regional export patterns and potential for atmospheric CO_2 sequestration. *Global Biogeochemical Cycles*, 15(4):845–862.

Bach, W. and Edwards, K. J. (2003). Iron and sulfide oxidation within the basaltic ocean crust: Implications for chemolithoautotrophic microbial biomass production. *Geochimica et Cosmochimica Acta*, 67(20):3871–3887.

Baker, B. J., Moser, D. P., MacGregor, B. J., Fishbain, S., Wagner, M., Fry, N. K., Jackson, B., Speolstra, N., Loos, S., Takai, K., Sherwood Lollar, B., Fredrickson, J., Balkwill, D., Onstott, T. C., Wimpee, C. F., and Stahl, D. A. (2003). Related assemblages of sulphate-reducing bacteria associated with ultradeep gold mines of South Africa and deep basalt aquifers of Washington State. *Environmental Microbiology*, 5(4):267–277.

Barz, M., Beimgraben, C., Staller, T., Germer, F., Opitz, F., Marquardt, C., Schwarz, C., Gutekunst, K., Vanselow, K. H., Schmitz, R., et al. (2010). Distribution analysis of hydrogenases in surface waters of marine and freshwater environments. *PLoS ONE*, 5(11):e13846.

Beal, E. J., House, C. H., and Orphan, V. J. (2009). Manganese- and iron- dependent marine methane oxidation. *Science*, 325(5937):184–187.

Behrenfeld, M. J. and Falkowski, P. G. (1997). A consumer's guide to phytoplankton primary productivity models. *Limnology and Oceanography*, 42(7):1479–1491.

Berg, P., Risgaard-Petersen, N., and Rysgaard, S. (1998). Interpretation of measured concentration profiles in sediment pore water. *Limnology and Oceanography*, 43(7):1500–1510.

Berger, W. H. and Wefer, G. (1990). Export production - seasonality and intermittency, and paleoceanographic implications. *Global and Planetary Change*, 89(3):245–254.

Berner, A. (1980). A rate model for organic matter decomposition during bacterial sulfate reduction in marine sediments: Biogeochimie de la matiere organique a l'interface eau-sediment marin. *Colloq. Int. CNRS*, 293(35).

Biddle, J. F., Lipp, J. S., Lever, M. A., Lloyd, K. G., Sorensen, K. B., Anderson, R., Fredricks, H. F., Elvert, M., Kelly, T. J., Schrag, D. P., Sogin, M. L., Brenchley, J. E., Teske, A., House, C. H., and Hinrichs, K. U. (2006). Heterotrophic archaea dominate sedimentary subsurface ecosystems off Peru. *Proceedings of the National Academy of Sciences of the United States of America*, 103(10):3846–3851.

Bird, D., Juniper, S., Ricciardi-Rigault, M., Martineu, P., Prairie, Y., and Calvert, S. (2001). Subsurface viruses and bacteria in Holocene/Late Pleistocene sediments of Saanich Inlet, BC: ODP Holes 1033B and 1034B, Leg 169. *Marine Geology*, 174(1):227–239.

Blair, C. C., D'Hondt, S., Spivack, A. J., and Kingsley, R. H. (2007). Radiolytic hydrogen and microbial respiration in subsurface sediments. *Astrobiology*, 7(6):951–970.

Boetius, A., Ravenschlag, K., Schubert, C. J., Rickert, D., Widdel, F., Giesecke, A., Amann, R., Jørgensen, B. B., Witte, U., and Pfannkuche, O. (2000). A marine microbial consortium apparently mediating anaerobic oxidation of methane. *Nature*, 407:623–626.

Bölter, M., Bloem, J., Meiners, K., and Möller, R. (2002). Enumeration and biovolume determination of microbial cells- A methodological review and recommendations for applications in ecological research. *Biology and Fertility of Soils*, 36(4):249–259.

Boudreau, B. P. (1996). The diffusive tortuosity of fine-grained unlithified sediments. *Geochimica et Cosmochimica Acta*, 60(3139).

Boudreau, B. P. (1997). Diagenetic models and their implementation: Modelling transport and reactions in aquatic sediments.

Boudreau, B. P. and Ruddick, B. R. (1991). On a reactive continuum representation of organic matter diagenesis. *American Journal of Science*, 291(5):507–538.

Breuker, A., Koeweker, G., Blazejak, A., and Schippers, A. (2011). The deep biosphere in terrestrial sediments in the Chesapeake Bay area, Virginia, USA. *Frontiers in Microbiology*, 2(156).

Caffrey, S. M., Park, H. S., Voordouw, J. K., He, Z., Zhou, J., and Voordouw, G. (2007). Function of periplasmic hydrogenases in the sulfate-reducing bacterium Desulfovibrio vulgaris Hildenborough. *J Bacteriol*, 189(17):6159–6167.

Cai, W. J. and Sayles, F. L. (1996). Oxygen penetration depths and fluxes in marine sediments. *Marine Chemistry*, 52(2):123–131.

Cammack, R. (1999). Hydrogenase sophistication. *Nature*, 397(6716):214–215.

Cammack, R., Frey, M., and Robson, R. (2001). Hydrogen as a fuel: Learning from nature.

Cappenberg, T. E. (1974). Interrelations between sulfate-reducing and methane-producing bacteria in bottom deposits of a fresh-water lake. I. Field observations. *Antonie Van Leeuwenhoek*, 40(2):285–95.

Chao, A. (1987). Estimating the population size for capture-recapture data with unequal catchability. *Biometrics*, 43:783–791.

Chapelle, F. (2001). *Ground-water microbiology and geochemistry*. John Wiley & Sons.

Chapelle, F. H. and Lovley, D. R. (1990). Rates of bacterial metabolism in deep coastal-plain aquifers. *Applied and Environmental Microbiology*, 56:1856–1874.

Chapelle, F. H., O'Neill, K., Bradley, P. M., Methé, B. A., Ciufo, S. A., Knobel, L. L., and Lovley, D. R. (2002). A hydrogen-based subsurface microbial community dominated by methanogens. *Nature*, 415(6869):312–315.

Chapelle, F. H., Zelibor, J., Grimes, D., and Knobel, L. (1987). Bacteria in deep coastal plain sediments of Maryland: A possible source of CO_2 to groundwater. *Water Resour. Res.*, 23:1625—1632.

Cole, J., Wang, Q., Cardenas, E., Fish, J., Chai, B., Farris, R., Kulam-Syed-Mohideen, A., McGarrell, D., Marsh, T., Garrity, G., et al. (2009). The Ribosomal Database Project: Improved alignments and new tools for rRNA analysis. *Nucleic acids research*, 37(suppl 1):D141–D145.

Collman, J. P. (1996). Coupling H_2 to electron transfer. *Nature Structural Biology*, 3(3):213–217.

Colwell, F., Onstott, T., Delwiche, M., Chandler, D., Fredrickson, J., Yao, Q.-J., McKinley, J., Boone, D., Griffiths, R., Phelps, T., Ringelberg, D., White, D., LaFreniere, L., Balkwill, D., Lehman, R., Konisky, J., and Long, P. (1997). Microorganisms from deep, high temperature sandstones: Constraints on microbial colonization. *FEMS Microbiology Reviews*, 20(3-4):425–435.

Conrad, R., Phelps, T. J., and Zeikus, J. G. (1985). Gas metabolism evidence in support of the juxtaposition of hydrogen-producing and methanogenic bacteria in sewage sludge and lake sediments. *Appl Environ Microbiol*, 50(3):595–601.

Cragg, B. (1995). The impact of fluid and gas venting on bacterial populations and processes in sediments from the Cascadia Margin Accretionary System (Sites 888-892) and the geochemical consequences. *Proceedings of the Ocean Drilling Program–Scientific Results*, 146:399–413.

Cragg, B., Law, K., Cramp, A., and Parkes, R. (1998). The response of bacterial populations to sapropels in deep sediments of the Eastern Mediterranean. *Proceedings of the Ocean Drilling Program–Scientific Results*, 160:303–308.

Cragg, B., Law, K., O'Sullivan, G., and Parkes, R. (1999). Bacterial profiles in deep sediments of the Alboran Sea, western Mediterranean, Sites 976-978. *Proceedings of the Ocean Drilling Program—Scientific Results*, 161:433–438.

Cragg, B. A., Parkes, R. J., Fry, J. C., Herbert, R. A., Wimpenny, J. W. T., and Getliff, J. M. (1990). Bacterial biomass and activity profiles within deep sediment layers. In Suess, E. and von Huene, R., editors, *Proceedings of the Ocean Drilling Program, Scientific Results*, volume 112, pages 607–619. Ocean Drilling Program.

Crozier, T. E. and Yamamoto, S. (1974). Solubility of hydrogen in water, seawater, and sodium chloride solutions. *Journal of Chemical and Engineering Data*, 19(3):242–244.

Davis, E., Fisher, A., and Firth, J. (1997). Initial Reports. *Proceedings of the Ocean Drilling Program*, 168.

Davis, E., Mottl, M., and Fisher, A. (1992). Initial Reports. *Proceedings of the Ocean Drilling Program*, 139.

DeLeon-Rodriguez, N., Lathem, T. L., Rodriguez-R, L. M., Barazesh, J. M., Anderson, B. E., Beyersdorf, A. J., Ziemba, L. D., Bergin, M., Nenes, A., and Konstantinidis, K. T. (2013). Microbiome of the upper troposphere: Species composition and prevalence, effects of tropical storms, and atmospheric implications. *Proceedings of the National Academy of Sciences*, 110(7):2575–2580.

Dell'Anno, A. and Donavaro, R. (2005). Extracellular DNA plays a key role in deep-sea ecosystem functioning. *Science*, 309(5744):2179–2179.

DeLong, E. (1992). Archaea in coastal marine environments. *Proceedings of the National Academy of Sciences*, 89(12):5685–5689.

Després, V. R., Huffman, J. A., Burrows, S. M., Hoose, C., Safatov, A. S., Buryak, G., Fröhlich-Nowoisky, J., Elbert, W., Andreae, M. O., Pöschl, U., et al. (2012). Primary biological aerosol particles in the atmosphere: A review. *Tellus B*, 64.

D'Hondt, S. L., Jørgensen, B., and Miller, D. J. (2003). Controls on microbial communities in deeply buried sediments, Eastern Equatorial Pacific and Peru Margin Sites 1225-1231. *Proceedings of the Ocean Drilling Program–Initial Reports*, 201.

D'Hondt, S. L., Jørgensen, B. B., Miller, D. J., and Party, O. L. S. S. (2004). Distributions of microbial activities in deep subseafloor sediments. *Science*, 306:2216–2221.

D'Hondt, S. L., Rutherford, S., and Spivack, A. J. (2002). Metabolic activity of subsurface life in deep-sea sediments. *Science*, 295(5562):2067–2069.

D'Hondt, S. L., Spivack, A. J., Pockalny, R., Ferdelman, T. G., Fischer, J. P., Kallmeyer, J., Abrams, L. J., Smith, D. C., Graham, D., Hasiuk, F., Schrum, H., and Stancin, A. M. (2009). Subseafloor sedimentary life in the South Pacific Gyre. *Proceedings of the National Academy of Sciences of the United States of America*, 106(28):11651–11656.

Divins, D. (2008). NGDC total sediment thickness for the world's oceans and marginal seas.

Divins, D. (2009). NGDC total sediment thickness for the world's oceans and marginal seas.

Doherty, G. M. and Mayhew, S. G. (1992). The hydrogen-tritium exchange activity of Megasphera elsdenii hydrogenase. *Eur. J. Biochem.*, 205:117–126.

Dowsett, H., Barron, J., and Poore, R. (1996). Middle Pliocene sea surface temperatures: A global reconstruction. *Marine Micropaleontology*, 27(1-4):13–25.

Ehrlich, H. L. (1998). Geomicrobiology: Its significance for geology. *Earth-Science Reviews*, 45(1):45–60.

Elvert, M., Suess, M., and Whiticar, M. J. (1999). Anaerobic methane oxidation associated with marine gas hydrates: Superlight C-isotopes from saturated and unsaturated C_{20} and C_{25} irregular isoprenoids. *Naturwissenschaften*, 86:295–300.

Ettwig, K. F., Shima, S., van de Pas-Schoonen, K. T., Kahnt, J., Medema, M. H., op den Camp, H. J., Jetten, M. S. M., and Strous, M. (2008). Denitrifying bacteria anaerobically oxidize methane in the absence of Archaea. *Environ Microbiol*, 10(11):3164–3173.

Fabiano, M. and Danovaro, R. (1998). Enzymatic activity, bacterial distribution, and organic matter composition in sediments of the Ross Sea (Antarctica). *Applied nad Environmental Microbiology*, 64(10):3838–3845.

Fagerbakke, K. M., Heldal, M., and Norland, S. (1996). Content of carbon, nitrogen, oxygen, sulfur and phosphorus in native aquatic and cultured bacteria. *Aquatic Microbial Ecology*, 10:15–27.

Fenchel, T. (2008). Motility of bacteria in sediments. *Aquatic Microbial Ecology*, 51(1):23–30.

Ferdelman, T. G., Lee, C., Pantoja, S., Harder, J., Bebout, B. M., and Fossing, H. (1997). Sulfate reduction and methanogenesis in Thioploca-dominated sediment off the coast of Chile. *Geochimica et Cosmochimica Acta*, 61(15):3065–3079.

Ferry, J. G. (1992). Biochemistry of methanogenesis. *Crit Rev Biochem Mol Biol*, 27(6):473–503.

Finkel, S. E. (2006). Long-term survival during stationary phase: Evolution and the GASP phenotype. *Nature Reviews Microbiology*, 4(2):113–120.

Fischer, J. P., Ferdelman, T. G., D'Hondt, S., Røy, H., and Wenzhoefer, F. (2009). Oxygen penetration deep into the sediment of the South Pacific Gyre. *Biogeosciences*, 6(8):1467–1478.

Fisher, H. F., Krasna, A. I., and Rittenbergs, D. (1954). The interaction of hydrogenase with oxygen. *Journal of Biological Chemistry*, 209:569–578.

Flemings, P., Behrmann, J., John, C., and Scientists, E. . (2006). Expedition Reports Gulf of Mexico Hydrogeology. *Proc. IODP*, 308.

Flood, R. D., Piper, D. J. W., and Klaus, A. (1995). Initial Reports. *Proceedings of the Ocean Drilling Program*, 155.

Fossing, H. (1995). ^{35}S-Radiolabeling to probe biogeochemical cycling of sulfur. In Vairavamurthy, M. A. and Schoonen, M. A. A., editors, *Geochemical Transformations of Sedimentary Sulfur*, volume 612. American Chemical Society. Washington, DC.

Fossing, H., Ferdelman, T. G., and Berg, P. (2000). Sulfate reduction and methane oxidation in continental margin sediments influenced by irrigation (South-East Atlantic off Namibia). *Geochimica et Cosmochimica Acta*, 64(5):897–910.

Frank, J., Reich, C., Sharma, S., Weisbaum, J., Wilson, B., and Olsen, G. (2008). Critical evaluation of two primers commonly used for amplification of bacterial 16S rRNA genes. *Applied and Environmental Microbiology*, 74(8):2461–2470.

Froelich, P. N., Klinkhammer, G. P., Bender, M. L., Luedtke, N. A., Heath, G. R., Cullen, D., Dauphin, P., Hammond, D., Hartman, B., and Maynard, V. (1979). Early oxidation of organic matter in pelagic sediments of the Eastern Equatorial Atlantic: Suboxic diagenesis. *Geochimica et Cosmochimica Acta*, 43:1075–1090.

Fry, J. C. (1998). Determination of biomass. *Methods in Aquatic Bacteriology*, pages 27–72.

Fry, J. C., Horsfield, B., Sykes, R., Cragg, B. A., Heywood, C., Kim, G. T., Mangelsdorf, K., Mildenhall, D. C., Rinna, J., Vieth, A., et al. (2009). Prokaryotic populations and activities in an interbedded coal deposit, including a previously deeply buried section (1.6–2.3 km) above 150 ma basement rock. *Geomicrobiology Journal*, 26(3):163–178.

Fukao, Y. (1979). Tsunami earthquakes and subduction processes near deep-sea trenches. *Journal of Geophysical Research*, 84(B5):2303–2314.

Gabrielsen, R., Faerseth, R., Jensen, L., Kalheim, J., and Riis, F. (1990). Structural elements of the Norwegian continental shelf. Part I: The Barents Sea Region. *Norwegian Petroleum Directorate - Bulletin*, 6:1–33.

García, H. E. and Gordon, L. I. (1992). Oxygen solubility in seawater: Better fitting equations. *Limnology and Oceanography*, 37(1307).

Gersonde, R., Hodell, D., and Blum, P. (1999). Initial Reports. *Proceedings of the Ocean Drilling Program*, 177.

Glombitza, C., Stockhecke, M., Schubert, C. J., Vetter, A., and Kallmeyer, J. (2013). Sulfate reduction controlled by organic matter availability in deep sediment cores from the saline, alkaline Lake Van (Eastern Anatolia, Turkey). *Frontiers in Microbiology*, 4(209).

Glud, R., Wenzhöfer, F., Middelboe, M., Oguri, K., Turnewitsch, R., Canfield, D. E., and Kitazato, H. (2013). High rates of benthic microbial activity at ca. 10.900 meters depth: Results from the Mariana Trench. *Nature Geoscience*, 6:284–288.

Glud, R. N., Gundersen, J. K., Revsbech, N. P., and Jørgensen, B. B. (1994). Effects on the benthic diffusive boundary-layer imposed by microelectrodes. *Limnology and Oceanography*, 39(2):462–467.

Hellevang, H. (2008). On the forcing mechanism for the H_2-driven deep biosphere. *International Journal of Astrobiology*, 7(2):157–167.

Himmelreich, R., Hilbert, H., Plagens, H., Pirkl, E., Li, B. C., and Herrmann, R. (1996). Complete sequence analysis of the genome of the bacterium Mycoplasma pneumoniae. *Nucleic Acids Research*, 24(22):4420–4449.

Hinrichs, K.-U. and Boetius, A. (2002). The anaerobic oxidation of methane: New insights in microbial ecology and biogeochemistry. *Ocean Margin System*, pages 457–477.

Hinrichs, K.-U., Hayes, J. M., Bach, W., Spivack, A. J., Hmelo, L. R., Holm, N. G., Johnson, C. G., and Sylva, S. P. (2006). Biological formation of ethane and propane in the deep marine subsurface. *Proceedings of the National Academy of Sciences of the United States of America*, 103(40):14684–14689.

Hinrichs, K.-U., Hayes, J. M., Sylva, S. P., Brewer, P. G., and DeLong, E. F. (1999). Methane consuming archaebacteria in marine sediments. *Nature*, 398:802–805.

Hinrichs, K.-U. and Inagaki, F. (2012). Downsizing the deep biosphere. *Science*, 338(6104):204–205.

Hirose, T., Kawagucci, S., and Suzuki, K. (2012). Correction to mechanoradical H_2 generation during simulated faulting: Implications for an earthquake-driven subsurface biosphere. *Geophysical Research Letters*, 39(23).

Hoberman, H. D. and Rittenberg, D. (1943). Biological catalysis of the exchange reaction between water and hydrogen. *Journal of Biological Chemistry*, 147:211–227.

Hoefs, M. J. L., Schouten, S., King, L. L., Wakeham, S. G., de Leeuw, J. W., and Damsté, J. S. S. (1997). Ether lipids of planktonic archaea in the marine water column. *Applied and Environmental Microbiology*, 63(8):3090–3095.

Hoehler, T. M., Albert, D. B., Alperin, M. J., Bebout, B. M., Martens, C. S., and Des Marais, D. J. (2002). Comparative ecology of H_2 cycling in sedimentary and phototrophic ecosystems. *Antonie Van Leeuwenhoek International Journal of General and Molecular Microbiology*, 81:575–585.

Hoehler, T. M., Alperin, M. J., Albert, D. B., and Martens, C. S. (1994). Field and laboratory studies of methane oxidation in an anoxic marine sediment: Evidence for a methanogen-sulfate reducer consortium. *Global Biogeochemical Cycles*, 8(4):451–463.

Hoehler, T. M., Alperin, M. J., Albert, D. B., and Martens, C. S. (1998). Thermodynamic control on hydrogen concentrations in anoxic sediments. *Geochimica et Cosmochimica Acta*, 62(10):1745–1756.

Hoehler, T. M., Bebout, B. M., and Des Marais, D. J. (2001). The role of microbial mats in the production of reduced gases on the early Earth. *Nature*, 412(6844):324–327.

Hoehler, T. M. and Jørgensen, B. B. (2013). Microbial life under extreme energy limitation. *Nature Reviews Microbiology*, 11:83–94.

Holm, N. G. and Charlou, J. L. (2001). Initial indications of abiotic formation of hydrocarbons in the Rainbow ultramafic hydrothermal system, Mid-Atlantic Ridge. *Earth and Planetary Science Letters*, 191:1–8.

Holmkvist, L., Ferdelman, T. G., and Jørgensen, B. B. (2011). A cryptic sulfur cycle driven by iron in the methane zone of marine sediment (Aarhus Bay, Denmark). *Geochimica et Cosmochimica Acta*, 75(12):3581–3599.

Hoos, E. and Schweisfurth, R. (1982). Untersuchungen über die Verteilung von Bakterien von 10 bis 90 Meter unter Bodenoberkante. *Vom Wasser*, 58:103—112.

Hopmans, E., Schouten, S., Pancost, R., van der Meer, M., and Sinninghe Damsté, J. (2000). Analysis of intact tetraether lipids in archaeal cell material and sediments by high performance liquid chromatography/atmospheric pressure chemical ionization mass spectrometry. *Rapid Communications in Mass Spectrometry*, 14(7):585–589.

Horsfield, B. and Kieft, T. L. (2007). The geobiosphere. In *Continental Scientific Drilling*, pages 163–211. Springer.

Horsfield, B., Schenk, H.-J., Zink, K., Ondrak, R., Dieckmann, V., Kallmeyer, J., Mangelsdorf, K., Di Primio, R., Wilkes, H., Parkes, R. J., and Fry, J. C. (2006). Living microbial ecosystems within the active zone of catagenesis: Implications for feeding the deep biosphere. *Earth and Planetary Science Letters*, 246:55–69.

Hoshino, T., Morono, Y., Terada, T., Imachi, H., Ferdelman, T., and Inagaki, F. (2011). Comparative study of subseafloor microbial community structures in deeply buried coral fossils and sediment matrices from the Challenger Mound in the Porcupine Seabight. *Frontiers in Microbiology*, 2.

Imshenetsky, A., Lysenko, S., and Kazakov, G. (1978). Upper boundary of the biosphere. *Applied and environmental microbiology*, 35(1):1–5.

Inagaki, F., Nunoura, T., Nakagawa, S., Teske, A., Lever, M., Lauer, A., Suzuki, M., Takai, K., Delwiche, M., Colwell, F. S., Nealson, K. H., Horikoshi, K., D'Hondt, S., and Jorgensen, B. B. (2006). Biogeographical distribution and diversity of microbes in methane hydrate-bearing deep marine sediments, on the Pacific Ocean Margin. *Proceedings of the National Academy of Sciences of the United States of America*, 103(8):2815–2820.

Ivanov, M. V. (1956). Isotopes in the determination of the sulfate-reduction rate in lake Belovod. *Microbiologiya*, 25:305–309.

Iversen, N. and Blackburn, T. H. (1981). Seasonal rates of methane oxidation in anoxic marine sediments. *Applied and Environmental Microbiology*, 41(6):1295–1300.

Iversen, N. and Jørgensen, B. B. (1985). Anaerobic methane oxidation rates at the sulfate-methane transition in marine sediments from Kattegat and Skagerrak (Denmark). *Limnology and Oceanography*, 30(5):944–955.

Jahn, U., Summons, R., Sturt, H., Grosjean, E., and Huber, H. (2004). Composition of the lipids of Nanoarchaeum equitans and their origin from its host Ignicoccus sp. strain KIN4/I. *Archives of microbiology*, 182(5):404–413.

Jahnke, R. A. (1996). The global ocean flux of particulate organic carbon: Areal distribution and magnitude. *Global Biogeochemical Cycles*, 10(1):71–88.

Jahnke, R. A. and Jackson, G. A. (1987). Role of sea-floor organisms in oxygen-consumption in the deep North Pacific Ocean. *Nature*, 329(6140):621–623.

Jin, Q. (2007). Control of hydrogen partial pressures on the rates of syntrophic microbial metabolisms: A kinetic model for butyrate fermentation. *Geobiology*, 5:35–48.

Jones, D. M., Head, I. M., Gray, N. D., Adams, J. J., Rowan, A. K., Aitken, C. M., Bennett, B., Huang, H., Brown, A., Bowler, B. F. J., Oldenburg, T., Erdmann, M., and Larter, S. R. (2008). Crude-oil biodegradation via methanogenesis in subsurface petroleum reservoirs. *Nature*, 451(7175):176–U176.

Jørgensen, B. (2011). Deep subseafloor microbial cells on physiological standby. *Proceedings of the National Academy of Sciences*, 108(45):18193–18194.

Jørgensen, B. B. (1978a). A comparison of methods for the quantification of bacterial sulfate reduction in coastal marine sediments. 1. Measurement with radiotracer techniques. *Geomicrobiology Journal*, 1(1):11–27.

Jørgensen, B. B. (1978b). A comparison of methods for the quantification of bacterial sulfate reduction in coastal marine sediments. 2. Calculation from mathematical models. *Geomicrobiology Journal*, 1(1):29–47.

Jørgensen, B. B. (1978c). A comparison of methods for the quantification of bacterial sulfate reduction in coastal marine sediments. 3. Estimation from chemical and bacteriological field data. *Geomicrobiology Journal*, 1(1):49–64.

Jørgensen, B. B. (1982a). Ecology of the sulfur cycle with special referene to anoxic-oxic interfaces. *Philosophical Tranactions of the Royal Society of London*, B298:543–561.

Jørgensen, B. B. (1982b). Mineralization of organic matter in the sea bed- the role of sulphate reduction. *Nature*, 296:643–644.

Jørgensen, B. B. (2012). Shrinking majority of the deep biosphere. *Proceedings of the National Academy of Sciences*, 109(40):15976–15977.

Jørgensen, B. B. and D'Hondt, S. (2006). A starving majority deep beneath the seafloor. *Science*, 314(5801):932–934.

Jørgensen, B. B., Schulz, H. D., and Zabel, M. (2000). Bacterial and marine biogeochemistry. *Marine Geochemistry*, pages 173–207.

Jørgensen, B. B., Weber, A., and Zopfi, J. (2001). Sulfate reduction and anaerobic methane oxidation in Black Sea sediments. *Deep Sea Research 1*, 48:2097–2120.

Kaden, H., Peeters, F., Lorke, A., Kipfer, R., Tomonaga, Y., and Karabiyikoglu, M. (2010). Impact of lake level change on deep-water renewal and oxic conditions in deep saline Lake Van, Turkey. *Water Resources Research*, 46(11).

Kadioglu, M., Sen, Z., and Batur, E. (1997). The greatest soda-water lake in the wolrd and how it is influenced by climatic change. *Annales Geophydicae-Atmospheres Hydrospheres and Space Sciences*, 15(11):1489–1497.

Kallmeyer, J. (2011). Detection and quantification of microbial cells in subsurface sediments. *Advances in applied microbiology*, 76(1113).

Kallmeyer, J., Ferdelman, T. G., Weber, A., Fossing, H., and Jørgensen, B. B. (2004). A cold chromium distillation procedure for radiolabeled sulfide applied to sulfate reduction measurements. *Limnology and Oceanography: Methods*, 2:171–180.

Kallmeyer, J., Pockalny, R., Adhikari, R. R., Smith, D. C., and D'Hondt, S. (2012). Global distribution of microbial abundance and biomass in subseafloor sediment. *Proceedings of the National Academy of Sciences*, 109(40):16213–16216.

Kallmeyer, J., Pockalny, R., D'Hondt, S., and Adhikari, R. R. (2009). A new estimate of total microbial subseafloor biomass. *Eos, Transactions, American Geophysical Union*, 90(52):B23C–0381.

Kallmeyer, J., Smith, D. C., Spivack, A. J., and D'Hondt, S. (2008). New cell extraction procedure applied to deep subsurface sediments. *Limnology and Oceanography: Methods*, 6:236–245.

Karl, D. M. (1980). Cellular nucleotide measurements and applications in microbial ecology. *Microbiological Reviews*, 44(4):739–796.

Kempe, S., Kazmierczak, J., Landmann, G., Konuk, T., Reimer, A., and Lipp, A. (1991). Largest known microbialites discovered in Lake Van, Turkey. *Nature*, 349(6310):605–608.

King, G. M. (2001). Radiotracer assays (^{35}S) of sulfate reduction rates in marine and freshwater sediments. *Academic Press: Methods in Microbiology*, 30.

Kinoshita, M., Tobin, H., Ashi, J., Kimura, G., Lallemant, S., Screaton, E., Curewitz, D., Masago, H., Moe, K., and the Expedition 314/315/316 Scientists (2009). Expedition 316 Site C0004. In *Proceedings of the Ocean Drilling Program*, volume 314/315/316, Washington, DC.

Knittel, K. and Boetius, A. (2009). Anaerobic oxidation of methane: Progress with an unknown process. *Annu. Rev. Microbiol*, 63:311–334.

Knittel, K., Losekann, T., Boetius, A., Kort, R., and Amann, R. (2005). Diversity and distribution of methanotrophic archaea at cold seeps. *Applied and Environmental Microbiology*, 71(1):467–479.

Knoblauch, C., Jørgensen, B. B., and Harder, J. (1999). Community size and metabolic rates of psychrophilic sulfate-reducing bacteria in Arctic marine sediments. *Applied and Environmental Microbiology*, 65(9):4230–4233.

Kotelnikova, S. and Pedersen, K. (1998). Distribution and activity of methanogens and homoacetogens in deep granitic aquifers at Äspö Hard Rock Laboratory, Sweden. *FEMS Microbiology Ecology*, 26:121–134.

Krasna, A. I. and Rittenberg, D. (1954). The mechanism of action of the enzyme hydrogenase. *Biochemistry*, 76:3015–3020.

Krasna, A. I. and Rittenberg, D. (1956). A comparison of the hydrogenase activities of different microorganisms. *Biochemistry*, 42.

Krebs, C. (1989). Ecological Methodology, 2nd Edition.

Kyte, F. T., Leinen, M., Heath, G. R., and Zhou, L. (1993). Cenozoic sedimentation history of the central North Pacific - inferences from the elemental geochemistry of core 1144-GPC3. *Geochimica et Cosmochimica Acta*, 57(8):1719–1740.

Kyte, F. T. and Wasson, J. T. (1986). Accretion rate of extraterrestrial matter: Iridium deposited 33 to 67 million years ago. *Science*, 232(4755):1225–1229.

Laanbroek, H., Veldkamp, H., Postgate, J., Lynch, J., and Le Roux, N. (1982). Microbial interactions in sediment communities [and discussion]. *Philosophical Transactions of the Royal Society of London. B, Biological Sciences*, 297(1088):533–550.

Laske, G. and Masters, G. (1997). A global digital map of sediment thickness. *Eos, Transactions, American Geophysical Union*, 78(46):S41E–1 (Suppl).

Leloup, J., Loy, A., Knab, N. J., Borowski, C., Wagner, M., and Jørgensen, B. B. (2007). Diversity and abundance of sulfate-reducing microorganisms in the sulfate and methane zones of a marine sediments, Black Sea. *Environmental Microbiology*, 9(1):131–142.

Lin, L.-H., Hall, J., Lippmann-Pipke, J., Ward, J. A., Sherwood Lollar, B., DeFlaun, M., Rothmel, R., Moser, D., Gihring, T. M., Mislowack, B., et al. (2005a). Radiolytic H_2 in continental crust: Nuclear power for deep subsurface microbial communities. *Geochemistry, Geophysics, Geosystems*, 6(7).

Lin, L.-H., Slater, G. F., Sherwood Lollar, B., Lacrampe-Couloume, G., and Onstott, T. C. (2005b). The yield and isotopic composition of radiolytic H_2, a potential energy source for the deep subsurface biosphere. *Geochimica et Cosmochimica Acta*, 69(4):893–903.

Lipman, C. B. (1928). The discovery of living micro-organisms in ancient rocks. *Science*, 68:272–273.

Lipman, C. B. (1931). Living micro-organisms in ancient rocks. *Journal of Bacteriology*, 22(3):183.

Lipp, J. and Hinrichs, K. (2009). Structural diversity and fate of intact polar lipids in marine sediments. *Geochimica et Cosmochimica Acta*, 73(22):6816–6833.

Lipp, J. S., Morono, Y., Inagaki, F., and Hinrichs, K.-U. (2008). Significant contribution of Archaea to extant biomass in marine subsurface sediments. *Nature*, 454:991–994.

Litt, T., Krastel, S., Sturm, M., Kipfer, R., Örcen, S., Heumann, G., Franz, S. O., Ülgen, U. B., and Niessen, F. (2009). 'PALEOVAN', International Continental Scientific Drilling Program (ICDP): site survey results and perspectives. *Quaternary Science Reviews*, 28(15):1555–1567.

Liu, X., Lipp, J., and Hinrichs, K. (2011). Distribution of intact and core GDGTs in marine sediments. *Organic Geochemistry*, 42(4):368–375.

Lomstein, B. A., Langerhuus, A. T., D'Hondt, S., Jørgensen, B. B., and Spivack, A. J. (2012). Endospore abundance, microbial growth and necromass turnover in deep sub-seafloor sediment. *Nature*, 484(7392):101–104.

Lovley, D. R. and Goodwin, S. (1988). Hydrogen concentrations as an indicator of the predominant terminal electron accepting reactions in aquatic sediments. *Geochimica et Cosmochimica Acta*, 52:2993–3003.

Lozupone, C., Hamady, M., Kelley, S., and Knight, R. (2007). Quantitative and qualitative β diversity measures lead to different insights into factors that structure microbial communities. *Applied and environmental microbiology*, 73(5):1576–1585.

Lu, Y. H. and Conrad, R. (2005). In situ stable isotope probing of methanogenic archaea in the rice rhizosphere. *Science*, 309(5737):1088–1090.

Lyon, E. J., Shima, S., Boecher, R., Thauer, R. K., Grevels, F.-W., Bill, E., Roseboom, W., and Albracht, S. P. (2004). Carbon monoxide as an intrinsic ligand to iron in the active site of the iron-sulfur-cluster-free hydrogenase H_2-forming methylenetetrahydromethanopterin dehydrogenase as revealed by infrared spectroscopy. *Journal of the American Chemical Society*, 126(43):14239–14248.

Manheim, F. T. (1966). A hydraulic squeezer for obtaining interstitial water from consolidated and unconsolidated sediments. *USGS Reference paper (C)*, pages 171–174.

Martens, C. S. and Berner, R. A. (1974). Methane production in the interstitial waters of sulfate-depleted marine sediments. *Science*, 185:1167–1169.

Martens, R. (2001). Estimation of ATP in soil: Extraction methods and calculation of extraction efficiency. *Soil Biology & Biochemistry*, 33:973–982.

Masui, N., Morono, Y., and Inagaki, F. (2009). Bio-archive core storage and subsampling procedure for subseafloor molecular biological research. *Scientific Drilling IODP/ICDP*, 8:35.

Mauclaire, L., Zepp, E., Meister, P., and McKenzie, J. A. (2004). Direct in-situ detection of cells in deep-sea sediment cores from the Peru Margin (ODP Leg 201, Site 1229). *Geobiology*, 2:217–223.

McKay, D. S., Gibson, E. K., ThomasKeprta, K. L., Vali, H., Romanek, C. S., Clemett, S. J., Chillier, X. D. F., Maechling, C. R., and Zare, R. N. (1996). Search for past life on Mars: Possible relic biogenic activity in Martian meteorite ALH84001. *Science*, 273(5277):924–930.

Middelburg, J. J. (1989). A simple rate model for organic-matter decomposition in marine-sediments. *Geochimica et Cosmochimica Acta*, 53(7):1577–1581.

Miquel, P. (1883). Les organismes vivants de l'atmosphère.

Miyashita, A., Mochimaru, H., Kazama, H., Ohashi, A., Yamaguchi, T., Nunoura, T., Horikoshi, K., Takai, K., and Imachi, H. (2009). Development of 16s rRNA gene-targeted primers for detection of archaeal anaerobic methanotrophs (anmes). *FEMS microbiology letters*, 297(1):31–37.

Moore, G., Bangs, N., Taira, A., Kuramoto, S., Pangborn, E., and Tobin, H. (2007). Three-dimensional splay fault geometry and implications for tsunami generation. *Science*, 318(5853):1128–1131.

Moore, G., Taira, A., and Klaus, A. (2001). Scientific Results. *Proceedings of the Ocean Drilling Program*, 190.

Morita, R. (1999). Is H_2 the universal energy source for long-term survival? *Microbial ecology*, 38(4):307–320.

Morita, R. Y. and ZoBell, C. E. (1955). Occurrence of bacteria in pelagic sediments collected during the Mid-Pacific Expedition. *Deep Sea Research (1953)*, 3(1):66–73.

Morono, Y. and Inagaki, F. (2010). Automatic slide-loader fluorescence microscope for discriminative enumeration of subseafloor life. *Scientific Drilling*, 9:32–36.

Morono, Y., Terada, T., Masui, N., and Inagaki, F. (2009). Discriminative detection and enumeration of microbial life in marine subsurface sediments. *ISME Journal*, 3:503–511.

Morono, Y., Terada, T., Nishizawa, M., Ito, M., Hillion, F., Takahata, N., Sano, Y., and Inagaki, F. (2011). Carbon and nitrogen assimilation in deep subseafloor microbial cells. *Proceedings of the National Academy of Sciences*, 108(45):18295–18300.

Müller, R. D., Sdrolias, M., Gaina, C., and Roest, W. R. (2008). Age, spreading rates, and spreading asymmetry of the world's ocean crust. *Geochemistry Geophysics Geosystems, Q04006*, 9.

Nauhaus, K., Boetius, A., Krüger, M., and Widdel, F. (2002). In vitro demonstration of anaerobic oxidation of methane coupled to sulphate reduction in sediment from a marine gas hydrate area. *Environmental Microbiology*, 4(5):296–305.

Nealson, K. H., Inagaki, F., and Takai, K. (2005). Hydrogen-driven subsurface lithoautotrophic microbial ecosystems (SLiMEs): Do they exist and why should we care? *Trends in Microbiology*, 13(9):405–410.

Nickel, J. C., di Primio, R., Mangelsdorf, K., Stoddart, D., and Kallmeyer, J. (2012). Characterization of microbial activity in pockmark fields of the SW-Barents Sea. *Marine Geology*, 332:152–162.

Noble, R. and Fuhrman, J. (1998). Use of SYBR Green I for rapid epifluorescence counts of marine viruses and bacteria. *Aquatic Microbial Ecology*, 14:113–118.

Nunoura, T., Soffientino, B., Blazejak, A., Kakuta, J., Oida, H., Schippers, A., and Takai, K. (2009). Subseafloor microbial communities associated with rapid turbidite deposition in the Gulf of Mexico continental slope (IODP Expedition 308). *FEMS Microbiology Ecology*, 69(3):410–424.

Odom, J. M. and Peck, H. D. (1984). Hydrogenase, electron-transfer proteins, and energy coupling in the sulfate-reducing bacteria desulfovibrio. *Annu. Rev. Microbiol*, 38:551–592.

Olson, J. W. and Maier, R. J. (2002). Molecular hydrogen as an energy source for Helicobacter pylori. *Science*, 298(5599):1788–1790.

Onstott, T. C., Phelps, T. J., Colwell, F. S., Ringelberg, D. B., White, D. C., and Boone, D. R. (1998). Observations pertaining to the origin and ecology of microorganisms recovered from the deep subsurface of Taylorsville Basin, Virginia. *Geomicrobiology*, 15:353–385.

Oremland, R. S., Culbertson, C., and Simoneit, B. R. T. (1982). Methanogenic activity in sediment from Leg 64, Gulf of California. In Curray, J. R. and Moore, D. G., editors, *Initial Reports of the Deep Sea Drilling Program*, volume 64, pages 759–762. Deep Sea Drilling Program, Washington, DC, USA.

Oremland, R. S., Dowdle, P. R., Hoeft, S., Sharp, J. O., Schaefer, J. K., Miller, L. G., Blum, J. S., Smith, R. L., Bloom, N. S., and Wallschlaeger, D. (2000). Bacterial dissimilatory reduction of arsenate and sulfate in meromictic Mono Lake, California. *Geochimica et Cosmochimica Acta*, 64(18):3073–3084.

Parkes, R. J., Cragg, B. A., Bale, S. J., Getliff, J. M., Goodman, K., Rochelle, P. A., Fry, J. C., Weightman, A. J., and Harvey, S. M. (1994). Deep bacterial biosphere in pacific-ocean sediments. *Nature*, 371(6496):410–413.

Parkes, R. J., Cragg, B. A., and Wellsbury, P. (2000). Recent studies on bacterial populations and processes in subseafloor sediments: A review. *Hydrogeology Journal*, 8:11–28.

Parkes, R. J., Webster, G., Cragg, B. A., Weightman, A. J., Newberry, C. J., Ferdelman, T. G., Kallmeyer, J., Jorgensen, B. B., Aiello, I. W., and Fry, J. C. (2005). Deep sub-seafloor prokaryotes stimulated at interfaces over geological time. *Nature*, 436(7049):390–394.

Paull, C., Matsumoto, R., and Wallace, P. (1996). Initial Reports. *Proceedings of the Ocean Drilling Program*, 164.

Pedersen, K. (2006). Exploration of deep intraterrestrial microbial life: Current perspectives. *FEMS Microbiology Letters*, 185(1):9–16.

Phelps, T. J., Murphy, E. M., Pfiffner, S. M., and White, D. C. (1994). Comparison between geochemical and biological estimates of subsurface microbial activities. *Microbial Ecology*, 28:335–349.

Phillips, G. N., Myers, R. E., and Palmer, J. A. (1987). Problems with the placer model for Witwatersrand gold. *Geology*, 15:1027–1030.

Pruesse, E., Quast, C., Knittel, K., Fuchs, B., Ludwig, W., Peplies, J., and Glöckner, F. (2007). SILVA: A comprehensive online resource for quality checked and aligned ribosomal RNA sequence data compatible with ARB. *Nucleic acids research*, 35(21):7188–7196.

Raghoebarsing, A. A., Pol, A., van de Pas-Schoonen, K. T., Smolders, A. J. P., Ettwig, K. F., Rijpstra, W. I. C., Schouten, S., Damste, J. S. S., op den Camp, H. J. M., Jetten, M. S. M., and Strous, M. (2006). A microbial consortium couples anaerobic methane oxidation to denitrification. *Nature*, 440(7086):918–921.

Rasmussen, H. and Jørgensen, B. B. (1992). Microelectrode studies of seasonal oxygen uptake in a coastal sediment: Role of molecular diffusion. *Marine Ecology Progress Series*, 81(3):289–303.

Ravenschlag, K., Sahm, K., Knoblauch, C., Jørgensen, B. B., and Amann, R. (2000). Community structure, cellular rRNA content, and activity of sulfate-reducing bacteria in marine Arctic sediments. *Applied and Environmental Microbiology*, 66(8):3592–3602.

Reimer, A., Landmann, G., and Kempe, S. (2009). Lake Van, eastern Anatolia, hydrochemistry and history. *Aquatic Geochemistry*, 15(1-2):195–222.

Riedinger, N., Kasten, S., Groger, J., Franke, C., and Pfeifer, K. (2006). Active and buried authigenic barite fronts in sediments from the Eastern Cape Basin. *Earth and Planetary Science Letters*, 241:876–887.

Romanova, N. D. and Sazhin, A. F. (2010). Relationships between the cell volume and the carbon content of bacteria. *Oceanology*, 50(4):522–530.

Rothman, D. H. and Forney, D. C. (2007). Physical model for the decay and preservation of marine organic carbon. *Science*, 316(5829):1325–1328.

Roussel, E. G., Bonavita, M.-A. C., Querellou, J., Cragg, B. A., Webster, G., Prieur, D., and Parkes, R. J. (2008). Extending the sub-sea-floor biosphere. *Science*, 320(5879):1046–1046.

Røy, H., Kallmeyer, J., Adhikari, R. R., Pockalny, R., Jorgensen, B. B., and D'Hondt, S. (2012). Aerobic microbial respiration in 86-million-year-old deep-sea red clay. *Science*, 336(6083):922–925.

Russell, J. B. and Cook, G. M. (1995). Energetics of bacterial growth: Balance of anabolic and catabolic reactions. *Microbiological reviews*, 59(1):48–62.

Sakaguchi, A., Chester, F., Curewitz, D., Fabbri, O., Goldsby, D., Gaku Kimura, C.-F. L., Masaki, Y., Screaton, E. J., Tsutsumi, A., Ujiie, K., and Yamaguchi, A. (2011). Seismic slip propagation to the updip end of plate boundary subduction interface faults: Vitrinite reflectance geothermometry on Integrated Ocean Drilling Program NanTro SEIZE cores. *Geology*, 39(4):395–398.

Sauer, P., Glombitza, C., and Kallmeyer, J. (2012). A system for incubations at high gas partial pressure. *Frontiers in Microbiology*, 3(25):1–9.

Schink, B., Lupton, F. S., and Zeikus, J. G. (1983). Radioassay for hydrogenase activity in viable cells and documentation of aerobic hydrogen-consuming bacteria living in extreme environments. *Appl. Environ. Microbiol.*, 45(5):1491–1500.

Schink, B. and Zeikus, J. G. (1984). Ecology of aerobic hydrogen-oxidizing bacteria in two freshwater lake ecosystems. *Canadian Journal of Microbiology*, 30:260–265.

Schippers, A. and Jørgensen, B. B. (2001). Oxidation of pyrite and iron sulfide by manganese dioxide in marine sediments. *Geochimica et Cosmochimica Acta*, 65(6):915–922.

Schippers, A., Neretin, L. N., Kallmeyer, J., Ferdelman, T. G., Cragg, B. A., Parkes, R. J., and Jørgensen, B. B. (2005). Procaryotic cells of the deep sub-seafloor biosphere identified as living bacteria. *Nature*, 433:861–864.

Schouten, S., Hopmans, E. C., Schefuss, E., and Damste, J. S. S. (2002). Distributional variations in marine crenarchaeotal membrane lipids: A new tool for reconstructing ancient sea water temperatures? *Earth and Planetary Science Letters*, 204(1-2):265–274.

Schouten, S., Middelburg, J. J., Hopmans, E. C., and Damste, J. S. S. S. S. (2010). Fossilization and degradation of intact polar lipids in deep subsurface sediments: A theoretical approach. *Geochimica et Cosmochimica Acta*, 74(13):3806–3814.

Schrum, H. N., Spivack, A. J., Kastner, M., and D'Hondt, S. (2009). Sulfate-reducing ammonium oxidation: A thermodynamically feasible metabolic pathway in subseafloor sediment. *Geology*, 37:939–942.

Schulz, H. N. and Jorgensen, B. B. (2001). Big bacteria. *Annual Review of Microbiology*, 55:105–137.

Seiter, K., Hensen, C., and Zabel, M. (2005). Benthic carbon mineralization on a global scale. *Global Biogeochemical Cycles*, 19(1):GB1010.

Sherwood Lollar, B., Voglesonger, K., Lin, L., Lacrampe-Couloume, G., Telling, J., Abrajano, T., Onstott, T., and Pratt, L. (2007). Hydrogeologic controls on episodic H_2 release from precambrian fractured rocks–Energy for deep subsurface life on Earth and Mars. *Astrobiology*, 7(6):971–986.

Shibata, A., Goto, Y., Saito, H., Kikuchi, T., Toda, T., and Taguchi, S. (2006). Comparison of SYBR Green I and SYBR Gold stains for enumerating bacteria and viruses by epifluorescence microscopy. *Aquatic Microbial Ecology*, 43(3):223–231.

Simon, M. and Azam, F. (1989). Protein-content and protein-synthesis rates of planktonic marine-bacteria. *Marine Ecology-Progress Series*, 51(3):201–213.

Sleep, N. and Zoback, M. (2007). Did earthquakes keep the early crust habitable? *Astrobiology*, 7(6):1023–1032.

Soffientino, B., Spivack, A., Smith, D., and D'Hondt, S. (2009). Hydrogenase activity in deeply buried sediments of the Arctic and North Atlantic Oceans. *Geomicrobiology Journal*, 26(7):537–545.

Soffientino, B., Spivack, A. J., Smith, D. C., Roggenstein, E. B., and D'Hondt, S. (2006). A versatile and sensitive tritium-based radioassay for measuring hydrogenase activity in aquatic sediments. *J Microbiol Methods*, 66(1):136–46.

Sogin, M., Morrison, H., Huber, J., Welch, D., Huse, S., Neal, P., Arrieta, J., and Herndl, G. (2006). Microbial diversity in the deep sea and the underexplored "rare biosphere". *Proceedings of the National Academy of Sciences*, 103(32):12115–12120.

Solheim, A. (1991). The depositional environment of surging sub-polar tidewater glaciers: A case study of the morphology, sedimentation and sediment properties in a surge affected marine basin outside Nordaustlandet, Northern Barents Sea. *Norsk Polarinstitutt Skrifter*, 194(97).

Staley, J. (1999). Bacteria, their smallest representatives and subcellular structures, and the purportet precambrian fossil "Metallogenium". *Size Limits of Very Small Microorganisms: Proceedings of a Workshop*, pages 62–67.

Stephenson, M. and Stickland, L. H. (1931). Hydrogenase: A bacterial enzymme activating molecular hydrogen. *Biochemical Laboratory*, pages 205–214.

Stevens, T. O. and McKinley, J. P. (1995). Lithoautotrophic microbial ecosystems in deep basalt aquifers. *Science*, 270(5235):450–455.

Stockner, J. G., Klut, M. E., and Cochlan, W. P. (1990). Leaky filters: A warning to aquatic ecologists. *Canadian journal of fisheries and aquatic sciences*, 47(16–23).

Strasser, M., Moore, G., Kimura, G., Kitamura, Y., Kopf, A., Lallemant, S., Park, J., Screaton, E., Su, X., Underwood, M., et al. (2009). Origin and evolution of a splay fault in the Nankai accretionary wedge. *Nature Geoscience*, 2(9):648–652.

Stripp, S. T., Goldet, G., Brandmayr, C., Sanganas, O., Vincent, K. A., Haumann, M., Armstrong, F. A., and Happe, T. (2009). How oxygen attacks [FeFe] hydrogenases from photosynthetic organisms. *Proceedings of the National Academy of Sciences*, 106(41):17331–17336.

Sturt, H., Summons, R., Smith, K., Elvert, M., and Hinrichs, K. (2004). Intact polar membrane lipids in prokaryotes and sediments deciphered by high-performance liquid chromatography/electrospray ionization multistage mass spectrometry–new biomarkers for biogeochemistry and microbial ecology. *Rapid Communications in Mass Spectrometry*, 18(6):617–628.

Takai, K., Nakamura, K., Toki, T., Tsunogai, U., Miyazaki, M., Miyazaki, J., Hirayama, H., Nakagawa, S., Nunoura, T., and Horikoshi, K. (2008). Cell proliferation at 122 degrees C and isotopically heavy CH_4 production by a hyperthermophilic methanogen under high-pressure cultivation. *Proceedings of the National Academy of Sciences of the United States of America*, 105(31):10949–10954.

Tan, T. L. and Rüger, H.-J. (1989). Benthic studies of the Northwest African upwelling region: Bacteria standing stock and ETS-activity, ATP-biomass and Adenylate Energy Charge. *Marine Ecology Progress Series*, 51:167–176.

Taylor, B., Huchon, P., and Klaus, A. (1999). Initial Reports. *Proceedings of the Ocean Drilling Program*, 180.

Teske, A. P. (2005). The deep subsurface biosphere is alive and well. *TRENDS in Microbiology*, 13(9):402–404.

Teske, A. P. (2012). Tracking microbial habitats in subseafloor sediments. *Proceedings of the National Academy of Sciences*, 109(42):16756–16757.

Thauer, R. K., Klein, A. R., and Hartmann, G. C. (1996). Reactions with molecular hydrogen in microorganisms: Evidence for a purely organic hydrogenation catalyst. *Chem. Rev.*, 96:3031–3042.

Treude, T., Boetius, A., Knittel, K., Wallmann, K., and Jørgensen, B. B. (2003). Anaerobic oxidation of methane above gas hydrates (Hydrate Ridge, NE Pacific Ocean). *Marine Ecology Progress Series*, 264:1–14.

Treude, T., Niggemann, J., Kallmeyer, J., Wintersteller, P., Schubert, C. J., Boetius, A., and Jørgensen, B. B. (2005). Anaerobic oxidation of methane and sulfate reduction along the Chilean continental margin. *Geochimica et Cosmochimica Acta*, 69(11):2767–2779.

van Bodegom, P. (2007). Microbial maintenance: A critical review on its quantification. *Microbial Ecology*, 53(4):513–523.

Velimirov, B. (2001). Nanobacteria, ultramicrobacteria and starvation forms: A search for the smallest metabolizing bacterium. *Microbes Environ*, 16:67–77.

Vignais, P. M. (2008). Hydrogenases and H^+-reduction in primary energy conservation. *Results Probl Cell Differ*, 45:223–52.

Vignais, P. M. and Billoud, B. (2007). Occurrence, classification, and biological function of hydrogenases: An overview. *Chemical reviews*, 107(10):4206.

Vignais, P. M., Billoud, B., and Mayer, J. (2001). Classification and phylogeny of hydrogenases. *FEMS Microbiological Reviews*, 25:455–501.

Vuillemin, A., Ariztegui, D., and the PASADO Science Team 1 (2013). Geomicrobiological investigations in subsaline maar lake sediments over the last 1500 years. *Quaternary Science Reviews*, 71:119–130.

Wagner, D., Görsch, J., and Kallmeyer, J. (2012). Tiefe Biosphäre: Leben im Untergrund. *System*, 2:2.

Wang, G., Spivack, A. J., Rutherford, S., Manor, U., and D'Hondt, S. (2008). Quantification of co-occurring reaction rates in deep subseafloor sediments. *Geochimica et Cosmochimica Acta*, 72(14):3479–3488.

Weinbauer, M. G., Beckmann, C., and Höfle, M. G. (1998). Utility of green fluorescent nucleic acid dyes and aluminum oxide membrane filters for rapid epifluorescence enumeration of soil and sediment bacteria. *Applied and Environmental Microbiology*, 64(12):5000–5003.

Wenzhöfer, F. and Glud, R. N. (2002). Benthic carbon mineralization in the Atlantic: A synthesis based on *in situ* data from the last decade. *Deep Sea Research Part I-Oceanographic Research Papers*, 49(7):1255–1279.

Wenzhöfer, F., Holby, O., and Kohls, O. (2001). Deep penetrating benthic oxygen profiles measured *in situ* by oxygen optodes. *Deep Sea Research Part I-Oceanographic Research Papers*, 48(7):1741–1755.

Wessel, P. and Smith, W. (1998). New improved version of generic mapping tools released. *Eos, Transactions, American Geophysical Union*, 79:579.

Westbrook, G., Carson, B., and Musgrave, R. (1994). Expedition Reports. *Proceedings of the Ocean Drilling Program–Initial Reports (Pt 1)*, 146.

Whelan, J. K., Oremland, R., Tarafa, M., Smith, R., Howarth, R., and Lee, C. (1985). Evidence for sulfate-reducing and methane producing microorganisms in sediments from sites 618, 619, and 622. *Ocean Drilling Project*, pages 767–775.

Whitman, W. B., Coleman, D. C., and Wiebe, W. J. (1998). Prokaryotes: The unseen majority. *Proceedings of the National Academy of Sciences of the United States of America*, 95(12):6578–6583.

Yamaguchi, A., Sakaguchi, A., Sakamoto, T., Iijima, K., Kameda, J., Kimura, G., Ujiie, K., Chester, F. M., Fabbri, O., Goldsby, D., Tsutsumi, A., Li, C.-F., and Curewitz, D. (2011). Progressive illitization in fault gouge caused by seismic slip propagation along a megasplay fault in the Nankai Trough. *Geology*, 39(11):995–998.

Yamamoto, M., Oba, T., Shimamume, J., and Ueshima, T. (2004). Orbital-scale anti-phase variation of sea surface temperature in mid-latitude North Pacific margins during the last 145,000 years. *Geophysical Research Letters*, 31(16):L16311.

Yamamoto, S., Alcauskas, J. B., and Crozier, T. E. (1976). Solubility of methane in distilled water and seawater. *Journal of Chemical and Engineering Data*, 21(1):78–80.

Zeikus, J. G. (1977). The biology of methanogenic bacteria. *Bacteriological Reviews*, 41(2):514–541.

ZoBell, C. E. and Johnson, F. H. (1949). The influence of hydrostatic pressure on the growth and viability of terrestrial and marine bacteria. *Journal of Bacteriology*, 57(2):179.